

AD-A092 814

ENERGY RESEARCH CORP DANBURY CONN

F/6 10/2

IMPROVEMENT OF PHOSPHORIC ACID FUEL CELL STACKS: (U)

JUL 80 S G ABENS, F J ASCENZO, B S BAKER

DAAK70-77-C-0174

UNCLASSIFIED

NL

1 104
41-
6/20/84

END
DATE
FILMED
181
DTIC

AD A092814

LEVEL II

(12)

IMPROVEMENT OF PHOSPHORIC ACID

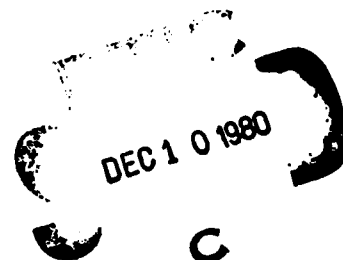
FUEL CELL STACKS

Final Technical Report

October 1980

Prepared By:

S. G. Abens
F. J. Ascenzo
B. S. Baker
G. Garretson
M. Lambrech

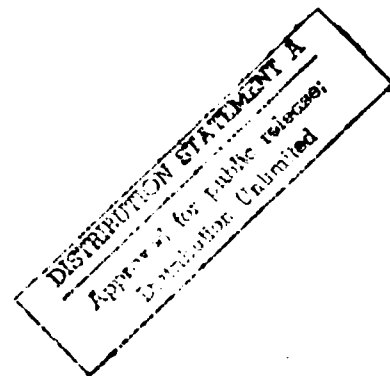


Prepared For:

U. S. Army Mobility Equipment
Research and Development Command
Fort Belvoir, VA 22060

Contract DAAK70-77-C-0174

ENERGY RESEARCH CORPORATION
3 Great Pasture Rd.
Danbury, Connecticut 06810



DDC FILE COPY

80 12 08 097

NOTICES

DISCLAIMERS

The citation of trade names and names of manufacturers in this report is not to be construed as official Government endorsement or approval of commercial products or services referenced herein.

DISPOSITION

Destroy this report when it is no longer needed. Do not return it to originator.

REPORT DOCUMENTATION PAGE		READ INSTRUCTIONS BEFORE COMPLETING FORM
1. REPORT NUMBER	2. GOVT ACCESSION NO.	3. RECIPIENT'S CATALOG NUMBER
	AD-A092824	
4. TITLE (and Subtitle)	5. TYPE OF REPORT & PERIOD COVERED	
(1) Improvement of Phosphoric Acid Fuel Cell Stacks	Final Technical Report, Aug 77 - June 80	
7. AUTHOR(s)	6. PERFORMING ORG. REPORT NUMBER	
10 S. G. Abens, F. J. Ascenzo, B. S. Baker G. Garretson, M. Lambrech		
9. PERFORMING ORGANIZATION NAME AND ADDRESS	8. CONTRACT OR GRANT NUMBER(s)	
Energy Research Corporation 3 Great Pasture Road Danbury, Connecticut 06810	(15) DAAK70-77-C-0174	
11. CONTROLLING OFFICE NAME AND ADDRESS	10. PROGRAM ELEMENT, PROJECT, TASK AREA & WORK UNIT NUMBERS	
US Army Mobility Equipment Research and Development Command, DRDME-EC Fort Belvoir, VA 22060	(16) 63702A, 1L263702DGL0 03, 012EF	
14. MONITORING AGENCY NAME & ADDRESS (if different from Controlling Office)	12. REPORT DATE	
Chief, DCASO US Courthouse - Fed. Bldg. 915 Lafayette Blvd. Bridgeport, CT 06603	(11) July 1980	
13. DISTRIBUTION STATEMENT (of this Report)	13. NUMBER OF PAGES	
This document has been approved for public release and sale. Its distribution is unlimited.		
15. SECURITY CLASS. (of this report)		
UNCLASSIFIED		
15a. DECLASSIFICATION/DOWNGRADING SCHEDULE		
17. DISTRIBUTION STATEMENT (of the abstract entered in Block 20, if different from Report)		
18. SUPPLEMENTARY NOTES		
19. KEY WORDS (Continue on reverse side if necessary and identify by block number)		
Fuel Cells Electrodes Phosphoric Acid Matrix Bipolar Plate Methanol		
20. ABSTRACT (Continue on reverse side if necessary and identify by block number)		
Phosphoric acid fuel cell components and stack assembly methods were evaluated. Electrodes with Pt loading between 0.3 and 0.9 g/ft ² were employed. Matrix materials were phenolic (Kynol) fibers and SiC. 7 new ERC proprietary matrix was used also. Graphite bipolar plates with 33% phenolic resin binder were used. Stacks were tested on hydrogen and simulated reformed methanol for up to 18,000 hours. Two 80-cell (2.1 kW) stacks and a methanol reformer were built and delivered to MERADCOM.		

Phosphoric acid fuel cell component designs and stack assembly methods were evaluated for gastightness, performance and endurance. All work was with 5 in. x 15 in. cell dimensions, a size employed for constructing 2 kW stacks for the 1.5 kW methanol fuel cell powerplant.

Component development covered electrodes, the matrix, and the bipolar plate. The electrodes employed platinum on carbon catalyst at loadings of 0.3 to 0.9 grams/ft². A coating technique for preparing SiC matrices was developed and a new ERC proprietary matrix (Mat-1) was evaluated. Bipolar plate mechanical and electrical characteristics were determined for a range of graphite-resin ratios.

The components were evaluated in multi-cell stacks. A total of 468 cells were assembled into 3, 10, and 80-cell stacks. Stack assembly techniques using both prefilled and dry matrices with wick filling were employed with equally good results. Phenolic fiber (Kynol) and SiC matrices were used in addition to the Mat-1 matrix.

Stack testing was conducted with hydrogen and with reformed methanol as fuel. Testing was also conducted for the effect of elevated temperature, low current density, unreformed methanol in the fuel, and thermal cycling of the stack.

Endurance testing of stacks was carried out for over 18,000 hours with the best cell performance above 600 mV at 100 ASF. Optimum cell performance during life testing with pure hydrogen was above 640 mV at 100 ASF. Two 80-cell stacks and a methanol reformer were assembled, tested and delivered to MERADCOM.

Accession For	THIS CASE	<input checked="" type="checkbox"/>	<input type="checkbox"/>	<input type="checkbox"/>
	CLASSIFIED			
	UNCLASSIFIED			
	DECLASSIFICATION			
37	Distribution/			
	Availability Codes			
	Avail and/or			
	Dist Special			
	A			

ENERGY RESEARCH CORPORATION

TABLE OF CONTENTS

<u>Section</u>		<u>Page No.</u>
	<u>SUMMARY</u>	i
1.0	<u>INTRODUCTION</u>	1
2.0	<u>COMPONENT DEVELOPMENT</u>	2
2.1	BIPOLAR PLATE	2
2.1.1	<u>Evaluation of PF Resin Content</u>	2
2.1.1.1	Specific Conductance	3
2.1.1.2	Voltage Drop Thru Plate	3
2.1.1.3	Density	7
2.1.1.4	Weight Loss in Air	9
2.1.1.5	Weight Loss in H ₃ PO ₄	9
2.1.2	Other Resins	11
2.1.3	Mechanical Properties	11
2.1.4	Endurance	11
2.1.5	Gas Distribution	12
2.1.6	DIGAS Cooling Plate	17
2.2	ELECTRODES	17
2.3	SiC MATRIX DEVELOPMENT	21
3.0	<u>STACK ASSEMBLY DEVELOPMENT</u>	23
3.1	HARDWARE	25
3.2	EDGE SEALS	26
3.3	MANIFOLD SEALS	26
3.4	ELECTROLYTE WICKING	30
3.5	ASSEMBLY WITH DIGAS PLATES	30
3.6	STACK TERMINALS	30

ENERGY RESEARCH CORPORATION

TABLE OF CONTENTS,
(concluded)

<u>Section</u>		<u>Page No.</u>
4.0	<u>STACK TESTING</u>	33
4.1	CONSTRUCTION	33
4.2	PROCEDURE	33
4.2.1	Oxygen Gain Measurement	35
4.2.2	Resistance Measurement	35
4.3	THREE-CELL STACKS	35
4.3.1	Initial Performance	37
4.3.2	Performance Stability	37
4.3.3	Performance with SRF	40
4.3.4	Carbon Monoxide Tolerance	41
4.3.5	Effect of CO ₂	41
4.3.6	Electrolyte Consumption	43
4.3.7	Overtemperature Testing	43
4.3.8	Low Current Testing	46
4.4	TEN-CELL STACKS	47
4.4.1	Cell Voltage Reproducibility	47
4.4.2	Thermal Profile	54
4.4.3	Thermal Cycling	57
4.4.4	Effect of Methanol in Fuel	60
4.5	EIGHTY-CELL STACKS	62
4.5.1	Construction	62
4.5.2	Performance with Hydrogen Fuel	68
4.5.3	Testing with Methanol Reformer	70
5.0	<u>CONCLUSIONS</u>	74

ENERGY RESEARCH CORPORATION

LIST OF FIGURES

<u>Figure No.</u>		<u>Page No.</u>
1.	Four Point Resistivity Measurement	4
2.	Bipolar Plate Material Resistivity	4
3.	Contact Resistance Set-up	6
4.	Bipolar Plate Contact Resistance	6
5.	Bipolar Plate Material Density	8
6.	Bipolar Plate Weight Change in Air	9
7.	Bipolar Plate Stability in H_3PO_4	10
8.	Bipolar Plate Weight Loss in H_3PO_4	10
9.	Bipolar Plate After 7000 hours of Service at 350°F	13
10.	Bipolar Plate Design	15
11.	Plate Pressing Dies	16
12.	Cutaway View of DIGAS Stack with Air Flow in 15 in. Direction	18
13.	DIGAS Cooling Plate, 5 in. x 15 in.	18
14.	Small Cell Performance	19
15.	Electrode Manufacturing Process	20
16.	Coating Machine	23
17.	Bubble Pressure Testing Set-up	24
18.	Tie Bar Deflection	25
19.	Cemented Area on Matrix	27
20.	Cemented Area on Plate	28
21.	Stack Cutaway	28
22.	Manifold Seals	29
23.	Kynol and Graphite Paper Areas in DIGAS Assembly	31
24.	O-Ring Seal for DIGAS Plate	31

ENERGY RESEARCH CORPORATION

LIST OF FIGURES

<u>Figure No.</u>		<u>Page No.</u>
25.	5 x 15 in. Fuel Cell Stack Assembly	32
26.	Test Set-up Schematic	34
27.	Stack Test Panel	34
28.	Stack Resistance Change During Wicking	36
29.	H ₂ /H ₂ Polarization for Stack 16	36
30.	Polarization Data	39
31.	Cell Voltage Stability	40
32.	Effect of Temperature on Load Voltage	42
33.	Effect of CO ₂ on Load Voltage	42
34.	Lifegraph of Stack 39	44
35.	High Temperature Test	45
36.	Stack Performance Before Low Current Testing	48
37.	Stack Performance After Low Current Testing	48
38.	Stack Polarization, Dry Assembly	52
39.	Stack Polarization, Wet Assembly	53
40.	Stack Performance Stability, Dry Assembly	55
41.	Stack Performance Stability, Wet Assembly	56
42.	Extended Life Testing, Stack 48	57
43.	Temperature Profile for Stack 50	58
44.	10-Cell Stack Warm-up	59
45.	Temperature Cycle for 10-Cell Stack	59
46.	Thermal Cycle Test	60
47.	Eighty-Cell Stack Assembly	65
48.	80-Cell Stack without and with Gas Manifolds Installed	66
49.	The Second 80-Cell Stack with DIGAS Cooling Plates	67

ENERGY RESEARCH CORPORATION

LIST OF FIGURES
(concluded)

<u>Figure No.</u>		<u>Page No.</u>
50.	80-Cell Stack Performance	69
51.	Methanol Reformer	71
52.	Temperature Profile of 1.5 kW Reformer	73
53.	Fuel Cell Test Set-up with Methanol Reformer	73

ENERGY RESEARCH CORPORATION

LIST OF TABLES

<u>Table No.</u>		<u>Page No.</u>
I.	Plate Material Resistivity	5
II.	Apparent Plate Resistance	7
III.	Plate Density Determination	8
IV.	Bipolar Plate Mechanical Properties	12
V.	Electrode Characteristics	21
VI.	SiC Matrix Composition	22
VII.	Three-Cell Stack Summary	38
VIII.	Performance Drop with SRF	41
IX.	Elevated Temperature Test	45
X.	Low Current Test	47
XI.	Ten-Cell Stack Summary	50
XII.	Cell No Load Potentials	51
XIII.	Cell Load Potentials	51
XIV.	Stack Performance with SRF	54
XV.	Methanol Concentration	61
XVI.	Methanol Flow	61
XVII.	Cell Load Voltage with Methanol in Fuel	62
XVIII.	Eighty-Cell Stack Components	63
XIX.	Stack Component Weights	64
XX.	Eighty-Cell Stack Performance	68
XXI.	Reformer Characteristics	70
XXII.	Reformer Gas Composition (Dry Basis)	72
XXIII.	Performance of Stack 61 with Reformed Methanol	72

ENERGY RESEARCH CORPORATION**1.0 INTRODUCTION**

The purpose of this project was to improve performance and reliability of phosphoric acid fuel cell stacks. The effort was focused on improving bipolar plates, electrodes, matrices, and gas seals.

Stack component manufacturing methods have been the subject of earlier work by Energy Research Corporation conducted under contract to USA MERADCOM. As a result of this effort, component manufacturing processes which are amenable to mass production methods were developed and evaluated in stack tests.*

The present project was conducted in two 15-month phases. During the first phase, 51 stacks were built and tested. Improved bipolar plate designs and a low loading platinum-on-carbon electrode catalyst were employed. Silicon carbide and Kynol fiber were evaluated as matrix materials; in addition, an ERC proprietary matrix (Mat-1) was tested. Simplified stack assembly methods with reliable gas seals were developed.

Extensive endurance testing was undertaken at 100 ASF and 350°F nominal stack temperature. Two stacks were tested with hydrogen fuel for more than 6000 hours, five additional stacks were tested for over 5000 hours, and another 15 stacks were tested beyond 2000 hours. Several thousand hours of testing with simulated reformer product gas were also conducted.

At the conclusion of this phase of the project, an 80-cell stack was constructed, tested, and delivered to MERADCOM.

* Contract DAAK02-74-C-0367, Final Report, 1977.

ENERGY RESEARCH CORPORATION

During the second phase (which commenced about four months after the completion of the first phase), additional stack testing was conducted to determine the short-term effects of over-temperature, high operating voltage and methanol in the gaseous fuel. Thermal cycling between 150 and 350°F was also evaluated, and endurance testing was extended to 18,000 hours.

At the conclusion of this phase of the project, another 80-cell stack and a 3 kW reformer were built, tested, and delivered to MERADCOM.

2.0 COMPONENT DEVELOPMENT

2.1 BIPOLAR PLATE

A molded bipolar gas distribution plate is the key component in a low cost, air-cooled stack. Its design has a major bearing on performance characteristics and manufacturing economics of the phosphoric acid fuel cell.

In an earlier effort,* techniques were developed for molding bipolar plates using phenol-formaldehyde (PF) resins as binders for graphite. In the current project, the task was to examine various properties of the plates, to evaluate new gas channel configurations, and to obtain further life and performance data, both under simulated and actual stack operating conditions.

2.1.1 Evaluation of PF Resin Content

A number of plate properties are determined by the carbon-resin ratio in the plate. Among those of immediate interest for phosphoric acid stacks are specific conductance, contact (skin) resistance, and the stability in air and in phosphoric acid. These properties were tested using PF resin in the

*Contract DAAK02-74-C-0367, Final Report, 1977.

ENERGY RESEARCH CORPORATION

composition range of 17 to 33% resin.

Test samples were molded in the 15 in. x 5 in. plate mold using flat mold faces from various mixtures of Colloid 8440 resin and graphite. The mixture of two graphites, employed for all samples, consisted of 11 parts by weight Asbury A99 synthetic (50 μ m average particle size) and 4 parts by weight Asbury 850 natural graphite (6 μ m average particle size). Molding conditions were the same as used for bipolar plate production, i.e., 4300 psi at 350°F for 5 minutes. Eleven samples were post-cured for 6 hours at 400°F and six samples were tested without post-curing.

2.1.1.1 Specific Conductance: Resistivity measurements for the molded material samples were obtained by the conventional 4-point method using the test circuit shown in Figure 1. The values plotted in Figure 2 show that conductance varies linearly with resin concentration up to about 30 wt% resin; above this resin concentration, a rapid increase in resistance occurs. The resistivity was found to range from 7 m Ω -cm at 17% resin to about 35 m Ω -cm at 33% resin as shown in Table I.

2.1.1.2 Voltage Drop Thru Plate: Contact resistance between the plate and electrode materials is of major interest since it contributes to stack resistance beyond the resistivity of the components themselves.

Voltage drop thru the molded plate material samples was determined with graphite paper (catalyst layer support) and Ag contacts as shown in Figure 3. The samples were compressed to 80 psi and tested with a constant current of 2.75 amperes. The data obtained is shown in Table II.

The apparent resistivity is shown in Figure 4 and has a value 5 to 10 times higher than the resistivity of the plate material. The difference between the two sets of figures may be taken as a measure of contact resistance between the electrode and the bipolar plate.

ENERGY RESEARCH CORPORATION

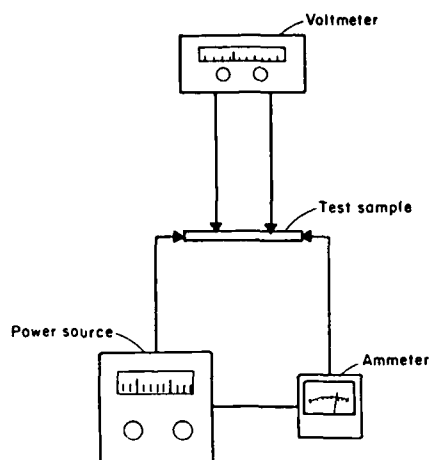
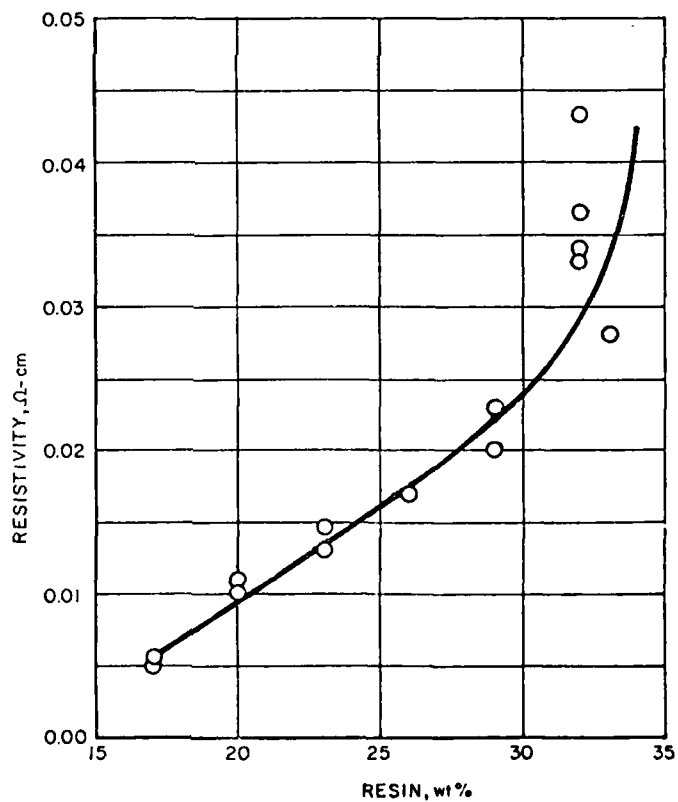


FIGURE 1
FOUR POINT RESISTIVITY MEASUREMENT

D0505



D0504

FIGURE 2. BIPOLAR PLATE MATERIAL RESISTIVITY

ENERGY RESEARCH CORPORATION

TABLE I
PLATE MATERIAL RESISTIVITY

- 4 point measurement
- 5 in. x 0.5 in. sample
- Voltage measured at 3 in. length
- 100 mA input current

SAMPLE NO.	RESIN, wt%	THICKNESS, in.	VOLTAGE, volts	RESISTANCE, Ω	RESISTIVITY, Ω -cm
4698	33	0.175	0.0376	0.376	0.0278
4686	32	0.148	0.0544	0.544	0.0341
4684	32	0.167	0.0537	0.537	0.0415
4683	32	0.142	0.0603	0.608	0.0365
4682	32	0.120	0.0649	0.649	0.0329
4690	29	0.151	0.0312	0.312	0.0199
4691	29	0.155	0.0354	0.354	0.0232
4683	26	0.151	0.0263	0.263	0.0168
4682	23	0.151	0.0201	0.201	0.0128
4693	23	0.149	0.0231	0.231	0.0146
4694	20	0.155	0.0150	0.150	0.0098
4695	20	0.152	0.0175	0.175	0.0113
4685	17	0.131	0.0033	0.033	0.0040
4697	17	0.155	0.0086	0.086	0.0056

Note that contact resistance rose proportionately with material resistivity as resin content is increased. Also, a lowering of contact resistance was observed with increased post-cure time. This result suggests that resin concentration on the plate surface may be reduced during post-cure; however this needs to be verified in view of the difficulty of reproducing contact resistance measurements.

These data also indicate that plate-electrode contact resistance voltage loss for cells with the higher resin content plates may be in the order of 30 to 40 mV at 100 ASF (the bipolar plate provides only about 40% of the surface area for

ENERGY RESEARCH CORPORATION

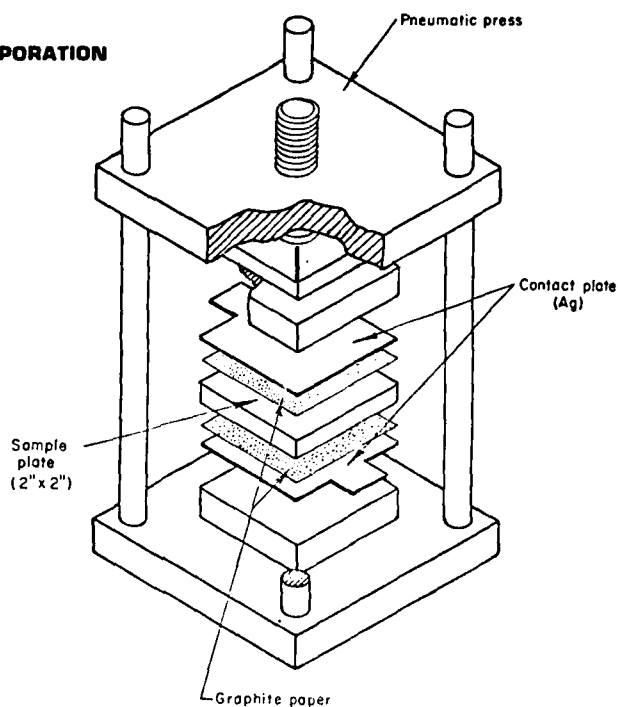


FIGURE 3.
CONTACT RESISTANCE SET-UP

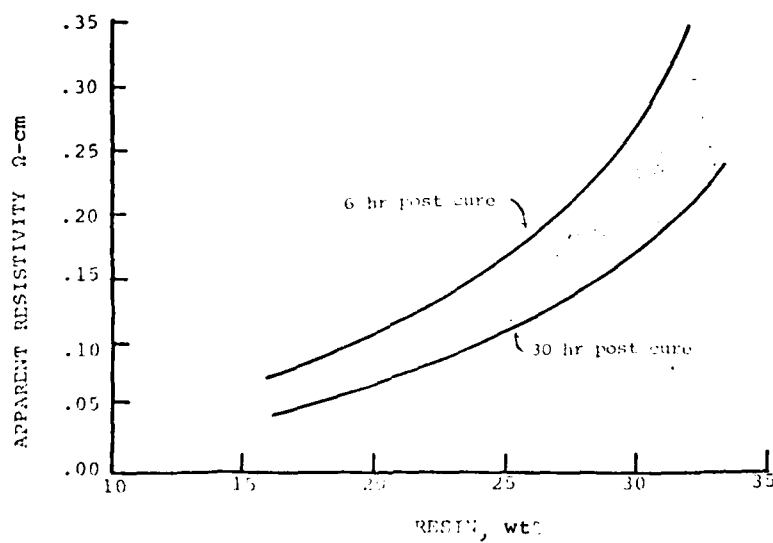


FIGURE 4
BIPOLAR PLATE CONTACT RESISTANCE

D0318

ENERGY RESEARCH CORPORATION

TABLE II.
APPARENT PLATE RESISTANCE

- 2 in. x 2 in. Sample
- 80 psi
- 70°F
- 2.75A (100 ASF)

SAMPLE NO.	RESIN, wt%	THICKNESS, in.	VOLTAGE, volts	RESISTANCE, Ω	RESISTIVITY, Ω -cm
4682*	32	0.113	0.0110	0.0040	0.359
4683*	32	0.152	0.0137	0.0050	0.334
4684	32	0.168	0.0165	0.0060	0.363
4685	17	0.116	0.0026	0.00095	0.083
4686	32	0.15 ^c	0.0123	0.0045	0.295
4687	32	0.164	0.0136	0.0049	0.314
4688	26	0.154	0.0094	0.0030	0.193
4689	26	0.152	0.0077	0.0028	0.187
4690	29	0.159	0.0121	0.0044	0.281
4691	29	0.161	0.0034	0.0030	0.199
4692	23	0.155	0.0048	0.0017	0.111
4693	23	0.142	0.0053	0.0019	0.136
4694	20	0.155	0.0043	0.0016	0.103
4695	20	0.147	0.0044	0.0016	0.111
4696	17	0.153	0.0025	0.00091	0.060
4697	17	0.157	0.0035	0.00127	0.082
4698	33	0.181	0.0135	0.0049	0.275

* Horizontal hairline crack in sample.

contact). This represents about one-half of total cell resistance loss (compare cell resistivity data in Section 4.2). Use of low resin content (17%), more conductive plates could reduce this loss by a factor of 3; however at present these plates do not show adequate acid resistance.

2.1.1.3 Density: Density of the molded samples was determined by the water immersion method. Densities ranged from 1.92 g/cc for 17% resin to 1.76 g/cc for 33% resin as shown in Figure 5. These data were taken on samples with a 6 hour, 400°F post-cure. Results obtained for the individual test samples are shown in Table III.

ENERGY RESEARCH CORPORATION

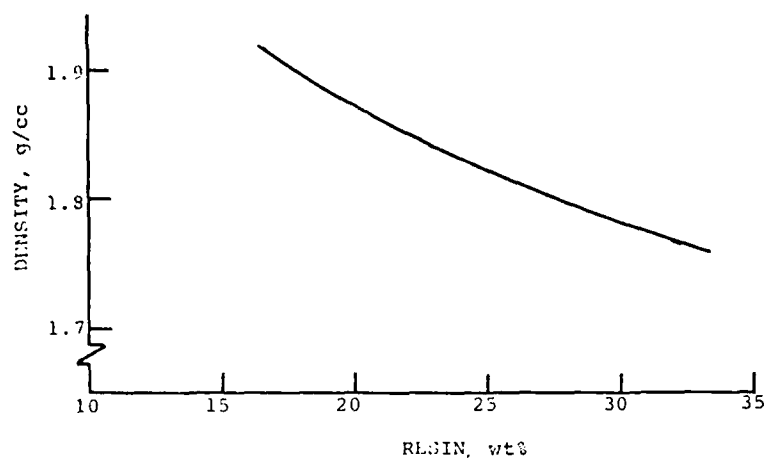


FIGURE 5.

D0319

BIPOLAR PLATE MATERIAL DENSITY

TABLE III
 PLATE DENSITY DETERMINATION
 (Water Displacement Method)
 2 in. x 2 in. x 0.2 in.

SAMPLE NO.	RESIN, wt%	WT. IN AIR, g	WT. IN H ₂ O, g	DENSITY, g/cc
4682	32	12.7823	5.4103	1.73
4683	32	17.0091	7.0642	1.71
4684	32	19.4252	8.3563	1.75
4685	17	14.9926	7.2387	1.93
4686	32	18.3036	8.0178	1.78
4687	32	19.1111	8.2726	1.76
4688	26	18.8922	8.6934	1.85
4689	26	18.4688	8.4009	1.83
4690	29	19.0590	8.5904	1.82
4691	29	19.2300	8.5655	1.80
4692	23	19.1265	8.8838	1.86
4693	23	17.3511	8.1682	1.84
4694	20	19.4801	9.2213	1.90
4695	20	18.3103	8.4802	1.86
4696	17	19.7990	9.6325	1.96
4697	17	19.6788	9.3786	1.91
4698	33	21.1692	9.2198	1.77

ENERGY RESEARCH CORPORATION

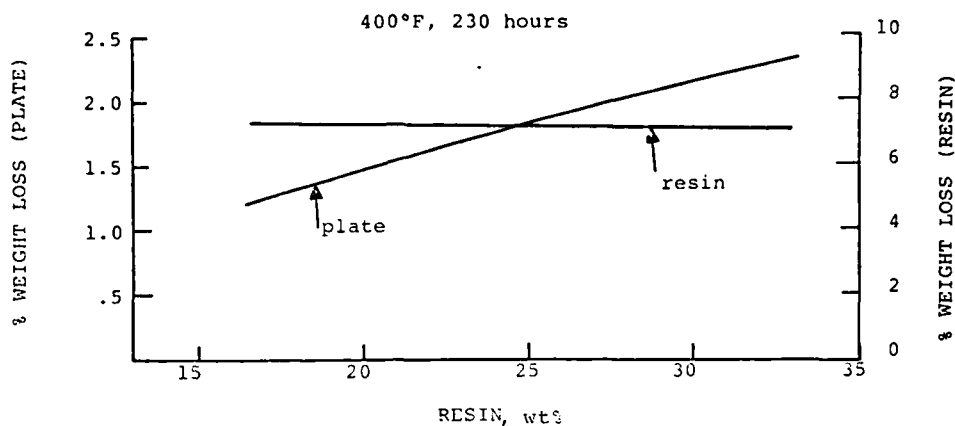


FIGURE 6

D0320

BIPOLAR PLATE WEIGHT CHANGE IN AIR

2.1.1.4 Weight Loss in Air: The bipolar plate material samples were exposed to air in an oven at 400°F, and weight changes were monitored periodically. The data plotted in Figure 6 show a small weight loss proportional to the resin concentration. When the same data is normalized with respect to the weight of resin in the plate, the weight loss can be seen to be independent of resin concentration.

2.1.1.5 Weight Loss in H₃PO₄: The test samples were maintained in H₃PO₄ at 350°F for over 5000 hours. The samples were periodically removed from the acid and washed in boiling water until a neutral condition had been achieved (pH=7). The samples were then oven dried at 250 to 275°F for a period of 12 hours and weighed on an analytical balance. As seen in Figure 7, weight loss is again proportional to the concentration of resin in the plate. The total weight loss over a period of 5000 hours was 1%, indicating increasing stability of the material with time as shown in Figure 8. No evidence of extensive attack of the samples by the acid was observed.

ENERGY RESEARCH CORPORATION

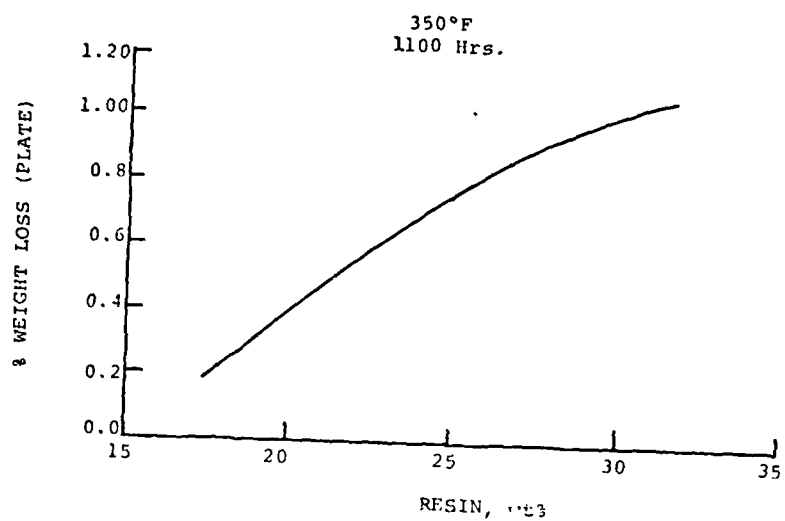
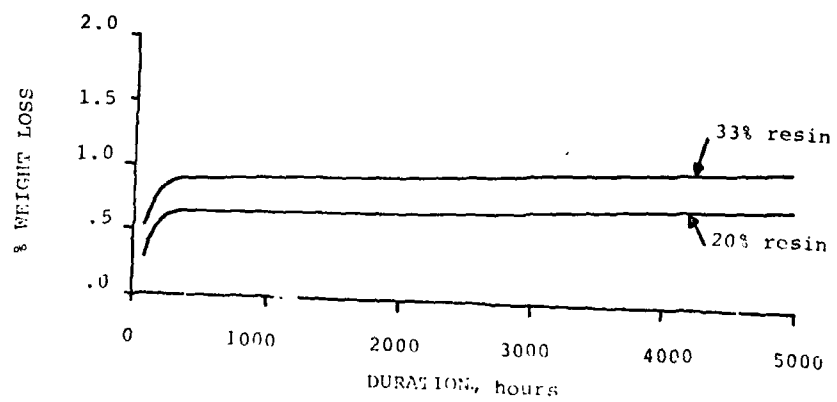


FIGURE 7

D0321

BIPOLAR PLATE STABILITY IN H_3PO_4 

D0322

FIGURE 8
BIPOLAR PLATE WEIGHT LOSS IN H_3PO_4

ENERGY RESEARCH CORPORATION

2.1.2 Other Resins

Several new potential plate molding resins were examined during this phase of the project. This work was limited to preliminary compatibility tests of small samples in H_3PO_4 .

Flat plates measuring 4 in. x 4 in. were molded with Kinel 5505 resin from Rhodia, Inc. The test samples molded at 460°F using 33% resin with the current graphite mix showed surface cracks after overnight immersion in H_3PO_4 at 350°F.

An experimental Arofene resin from Ashland Oil Co. appeared resistant to H_3PO_4 at 390°F, but needs to be tested in the full size molding process. The current resins of choice for bipolar plates remain Arofene 890 and Colloid 8440. Most of the work on the project utilized the Colloid resin because of somewhat better molding characteristics.

2.1.3 Mechanical Properties

Mechanical testing of a bipolar plate sample was performed at Bridgeport Testing Laboratory, Inc. The sample was molded in the 5 in. x 15 in. bipolar plate mold using flat mold faces and was composed of 32% Colloid 8440 resin, 50% Asbury A99 graphite, and 18% Asbury 850 graphite. Molding conditions were 4300 psi at 340°F. The thickness of the plate from which the test samples were randomly cut was 0.165 in. Results of the mechanical tests are presented in Table IV.

The results of these tests indicate that fairly uniform mechanical properties are obtained over the entire molded plate area.

2.1.4 Endurance

Endurance of the bipolar plates produced on this project was evaluated as part of numerous extended stack performance tests. During these tests, 52 plates were in cells that operated over 5000 hours at 350°F; 101 plates accumulated more than 3000 hours, and 161 plates were in stacks which were tested for over 2000 hours. The appearance of the plates following endurance

ENERGY RESEARCH CORPORATION

TABLE IV.

BIPOLAR PLATE MECHANICAL PROPERTIES

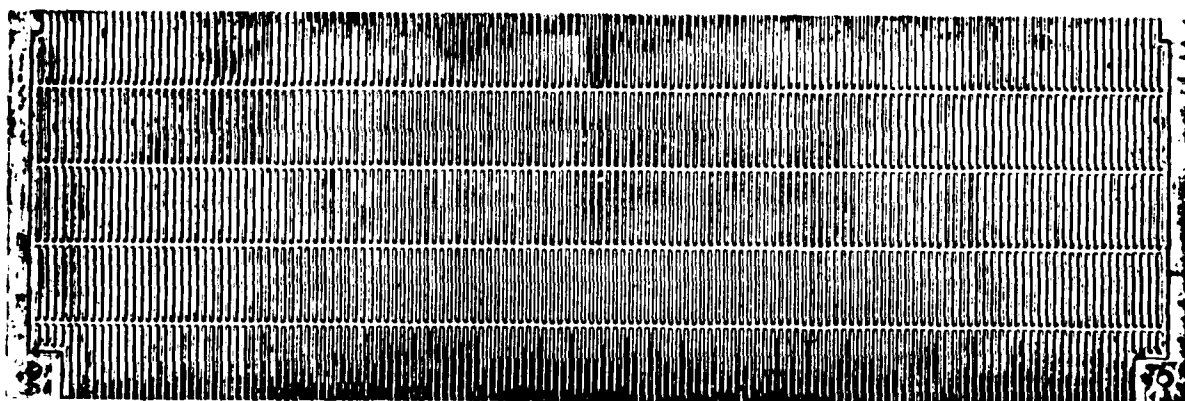
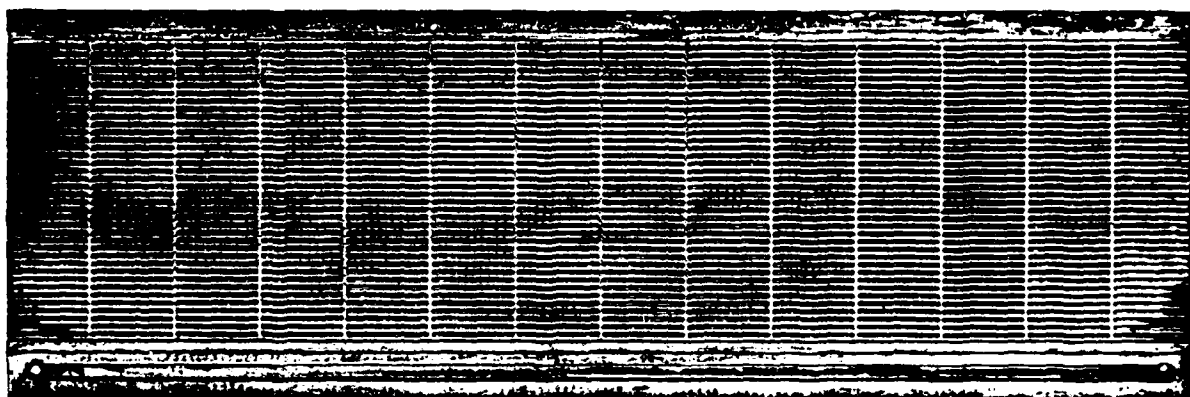
<u>Tensile Strength</u>	(ASTM-D-638)
#1	6,850 psi
#2	6,460 psi
#3	7,080 psi
<u>Flexural Strength</u>	(ASTM-D-638)
#1	10,700 psi
#2	9,870 psi
#3	9,130 psi
#4	9,140 psi
#5	10,440 psi
<u>Shear Strength</u>	(ASTM-D-732)
#1	4,030 psi
#2	4,020 psi
#3	3,800 psi
<u>Hardness</u>	(ASTM-D-785)
#1	112
#2	112
#3	113
#4	113
#5	112

testing was generally similar to unused plates, with no apparent systematic deterioration during the test, as seen from the photograph of a plate after 7000 hours of stack testing, (Figure 9).

Soft areas were observed on some plates during post-test analysis. This condition was generally limited to a single manufacturing run of about 20 plates which were molded at modified conditions (20 seconds vs 5 to 10 seconds of preheat in the mold before compression). The softening can be attributed to incompletely densified plate sections (porosity of the plate) which allows acid to be wicked into the plate, causing structural deterioration.

2.1.5 Gas Distribution

Two modifications to the gas distribution pattern on the bipolar plate were evaluated on this project. The objectives for undertaking these modifications were:



P0094

FIGURE 9
BIPOLAR PLATE AFTER 7000 HOURS OF SERVICE
AT 350°F

ENERGY RESEARCH CORPORATION

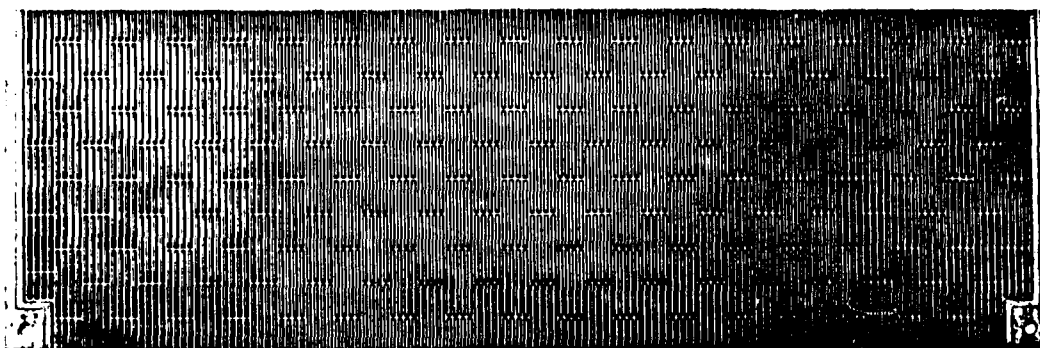
- increased plate strength
- improved moldability
- larger cell active area
- deeper electrode recess
- lower tooling costs

The modified bipolar plate designs are evident in the bipolar plate photograph (Figure 10). The Type B plate has a staggered cross-flow channel pattern, eliminating extended thin plate sections for greater plate strength. On the Type C plate, the perpendicular gas channels are eliminated, which greatly reduces tooling costs. Photographs of the plate pressing dies for these two designs are shown in Figure 11.

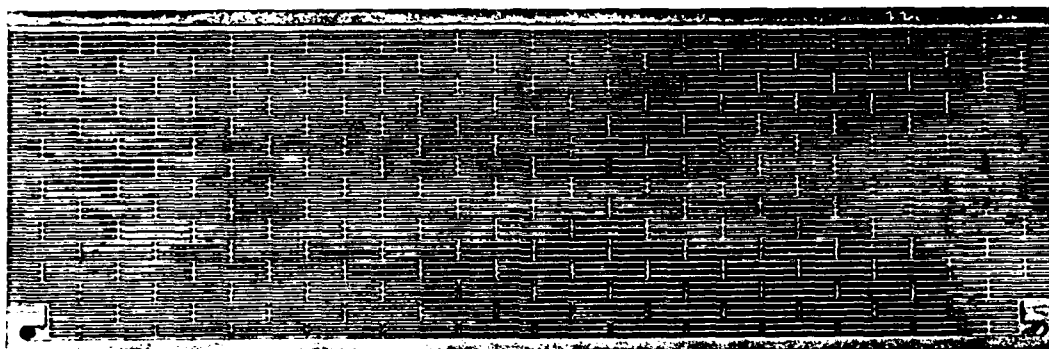
Type B and C plates were designed with an electrode recess depth of 0.014 in. for the anode and 0.018 in. for the cathode compared to 0.012 in. for both anode and cathode on the earlier (Type A) plate. This change was made to accommodate the increased electrode thickness resulting from the use of supported catalyst instead of platinum black on this project.

The presently available tooling in the 5 in. x 15 in. size can produce the following plate configurations:

- A. Mold A: Present standard mold in use since the commencement of the MM&T program. This mold produces an enclosed electrolyte channel, electrode recesses 0.012 in. deep, and straight line grooves perpendicular to the direction of the gas flow.
- B. Mold B: Modification of Mold A as follows:
 - Electrolyte channel not closed on top
 - Electrode recessed 0.18 in. (air side) and 0.14 in. deep (fuel side)
 - Staggered grooves perpendicular to direction of gas flow for increased strength.
- C. Mold C: Modification of Mold A as follows:
 - No electrolyte channel - mold is symmetrical on both air and fuel sides.
 - Electrode recesses are same as for Mold B.
 - There are no grooves in the plate perpendicular to direction of gas flow.

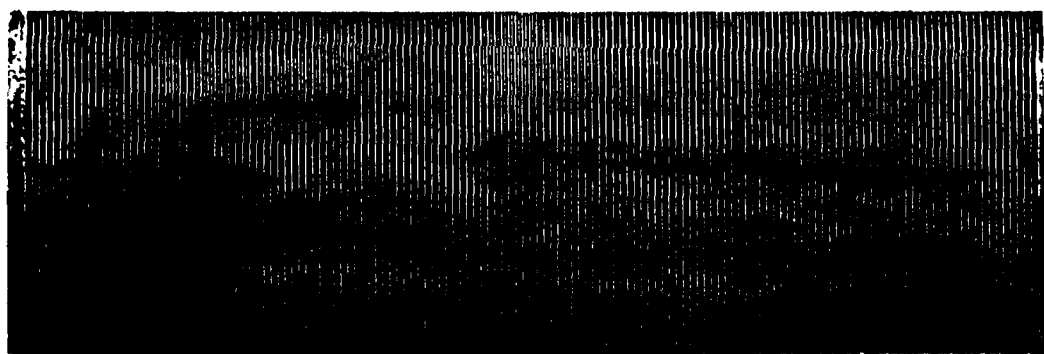


Air Side

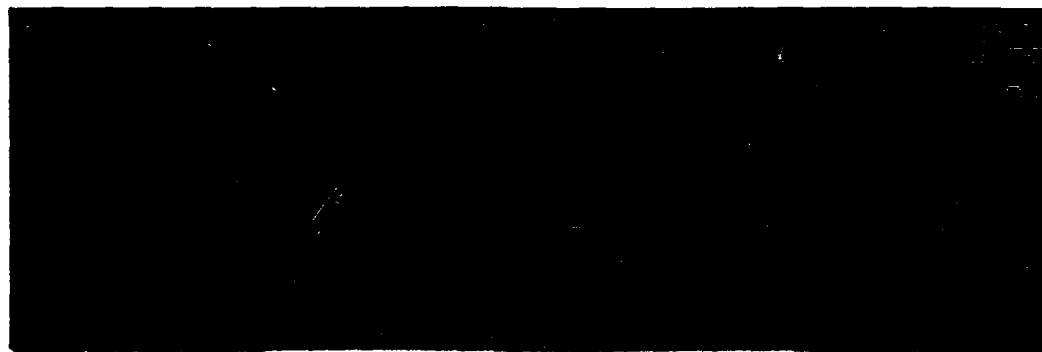


Fuel Side

Type "B" Bipolar Plate



Air Side

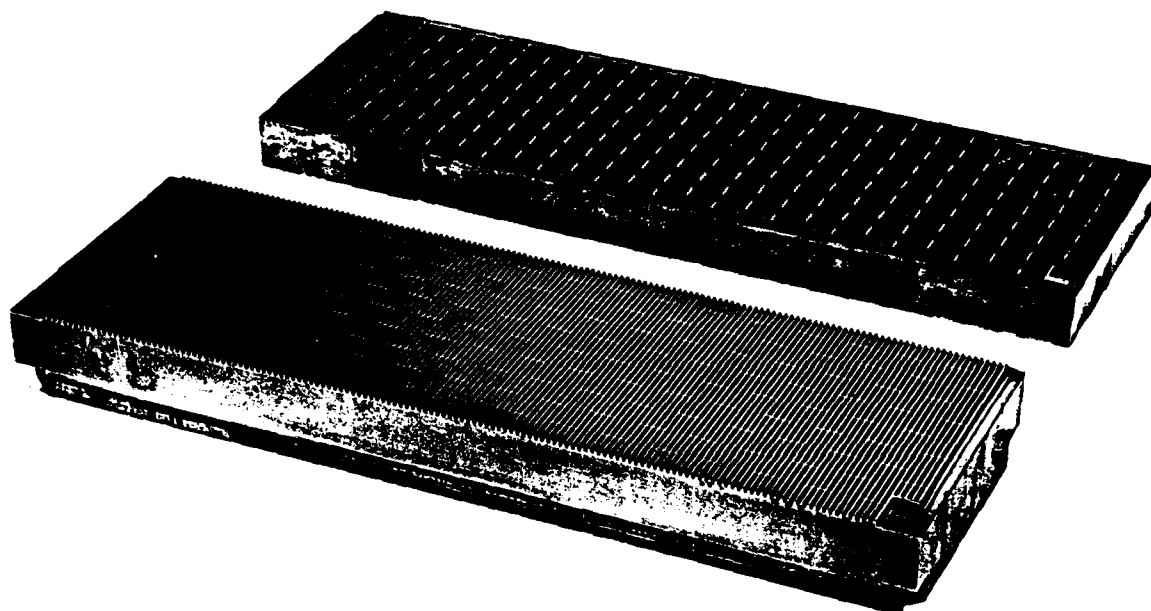


Fuel Side

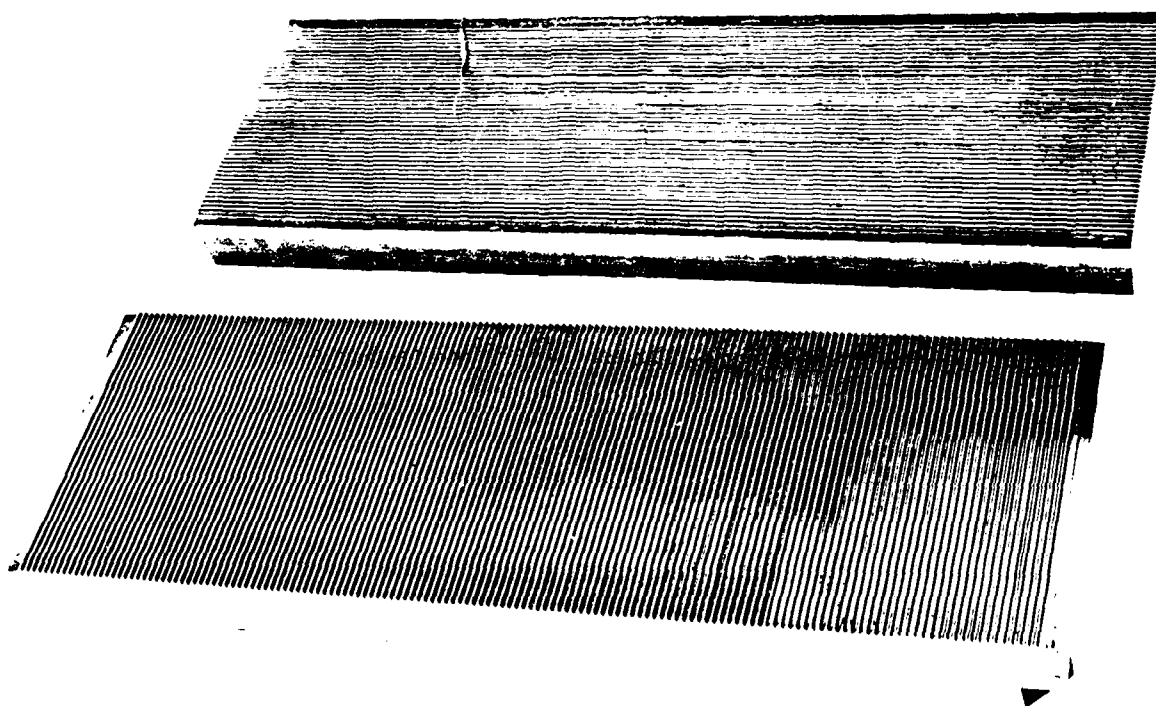
Type "C" Bipolar Plate

FIGURE 10

BIPOLAR PLATE DESIGN



Type "B" Plate Mold



Type "C" Plate Mold

FIGURE 11
PLATE PRESSING DIES

ENERGY RESEARCH CORPORATION

Initial stack performance was not affected by gas distribution pattern design. This had been expected since both fuel and air field depths as well as overall plate thickness remained unchanged. However the deeper electrode recesses in B and C plates have improved the edge seal gastightness of the stacks.

Since the 5 x 15 in. tooling components are interchangeable, combinations of rib patterns on the same plate are possible. Most of the plates used on this project were molded with the "A" fuel side pattern combined with the "B" air pattern. Also some plates were molded with no rib pattern on one side for use as the first or last plate in the stack.

Dimensional tolerances for the plates were monitored continuously. Plates not conforming to a ± 0.002 in. thickness tolerance were rejected. For standard molding procedures, the rejection rate was 20 to 30%. All plates were also checked for gastightness with 2 psig hydrogen as the test gas. The rejection rate on this test was less than 4%.

2.1.6 DIGAS Cooling Plate

The second 80-cell stack built on this project utilized distributed gas (DIGAS) cooling plates. This air cooling plate concept provides additional cooling channels thru the stack in the air flow direction as seen in the stack cutaway drawing (Figure 12).

The cooling plates were fabricated by molding half plates (plates with one ribbed and one flat side) and machining the cooling channels as needed. The DIGAS cooling plate design used for this project is shown in Figure 13.

2.2 ELECTRODES

As part of an earlier effort toward development of a stack manufacturing process,* ERC evolved a technique for

*Contract DAAK02-74-C-0367, Final Report, 1977.

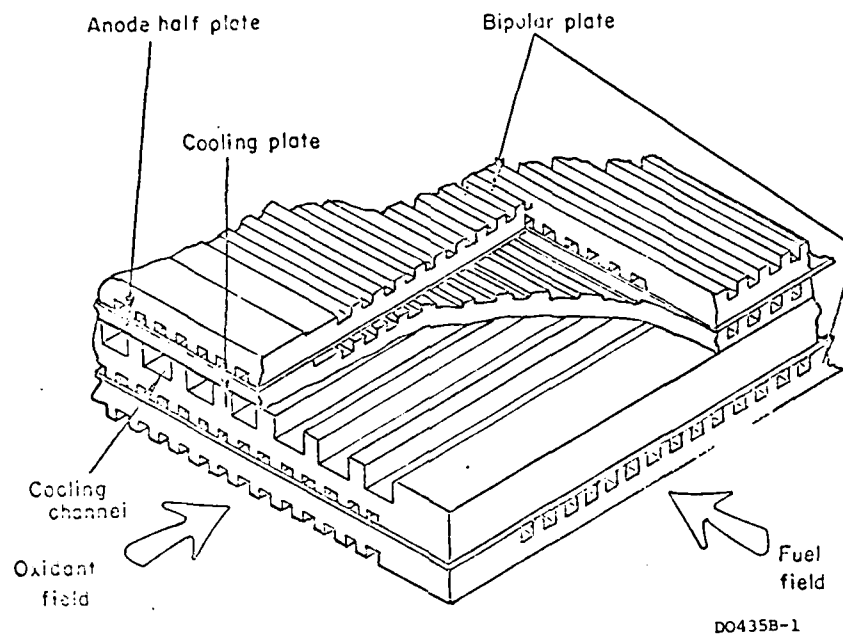


FIGURE 12 CUTAWAY VIEW OF DIGAS STACK WITH
AIR FLOW IN 15 in. DIRECTION

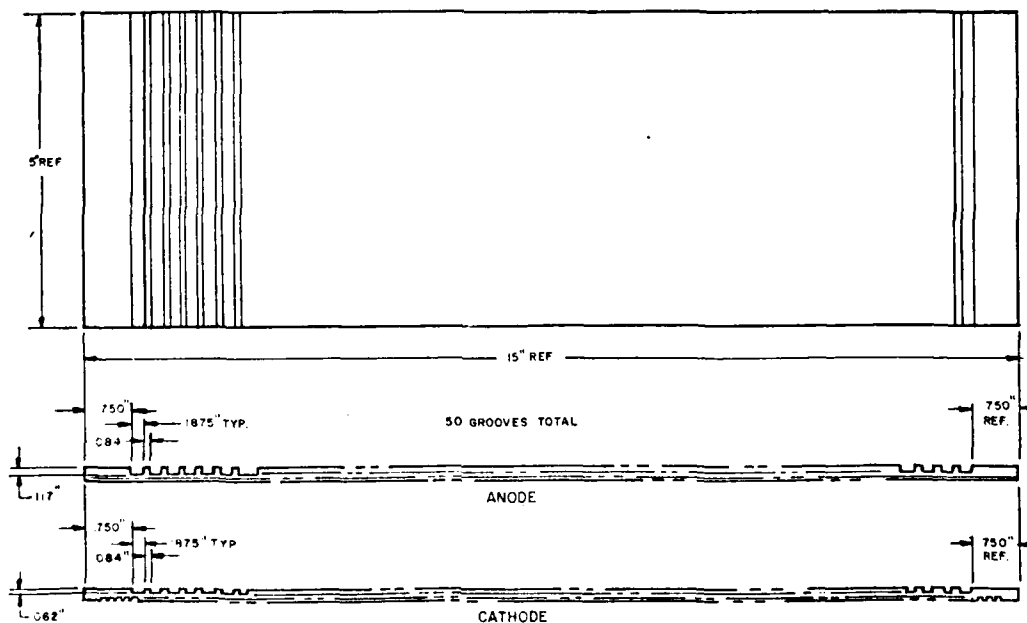


FIGURE 13 DIGAS COOLING PLATE, 5 in. x 15 in.

D1288

ENERGY RESEARCH CORPORATION

production of fuel cell electrodes using platinum black or rhodium-platinum catalyst for portable powerplant stacks (5 in. x 15 in. electrode size). Other work at ERC with small (2 in. x 2 in.) cells demonstrated performance gains and catalyst cost reduction potential of platinum-on-carbon compared to platinum black as the cathode catalyst, as seen from the polarization curves of Figure 14. On the present project, manufacturing techniques for platinum-on-carbon supported catalyst electrodes were established for the 5 in. x 15 in. stack size.

The electrode manufacturing process used for this project is summarized in Figure 15. This process was employed to produce electrodes with platinum loadings ranging from about 0.2 to 1.0 grams/ft². Physical characteristics of electrodes having 0.6 and 0.9 grams Pt/ft² are listed in Table V.

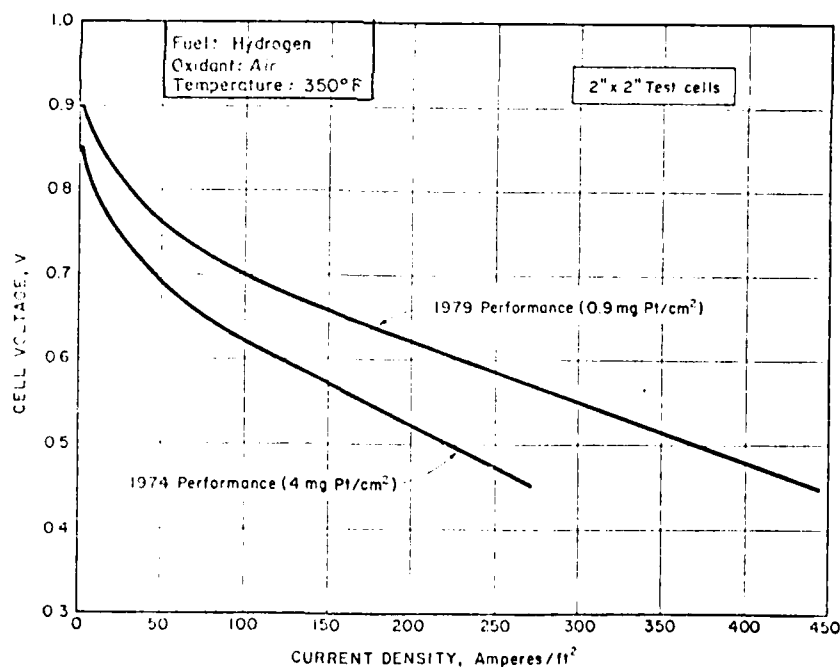
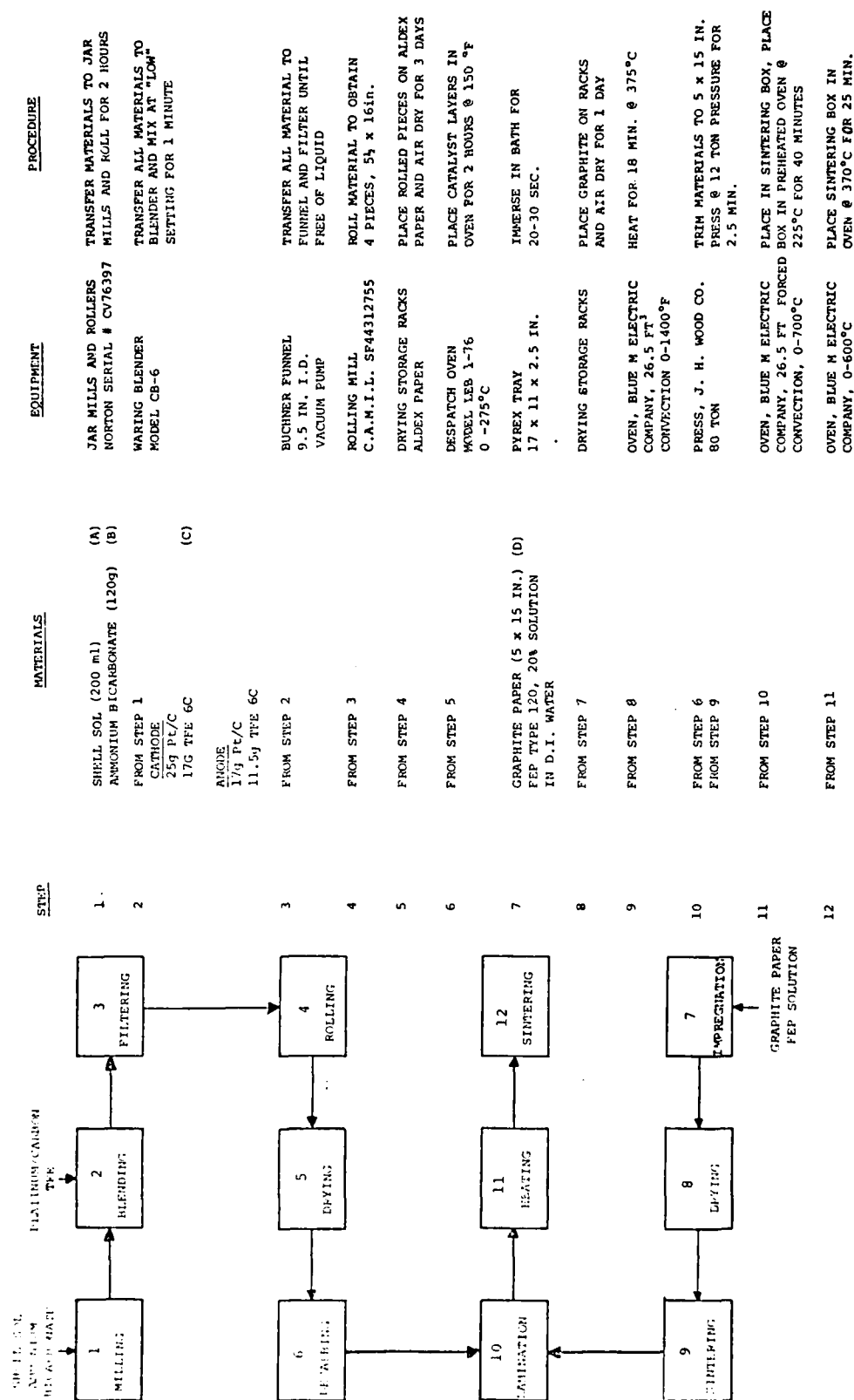


Figure 14

SMALL CELL PERFORMANCE

D0503R



NOTES:

- (A) SHELL SOL - GUARD ALL CO.
 (B) AMMONIUM BICARBONATE - ANALYTICAL REAGENT, FISHER SCIENTIFIC CO.
 (C) TFE - DUPONT
 (D) FEP - DUPONT

FIGURE 15 ELECTRODE MANUFACTURING PROCESS

ENERGY RESEARCH CORPORATION

TABLE V.

ELECTRODE CHARACTERISTICS

ELECTRODE :	Cathode	Anode
Catalyst-Layer		
Catalyst	10% Platinum on Carbon	
Loading, g Pt/ft ²	0.9	0.6
TFE, wt%	40	40
Support layer		
Material*	Graphite paper, 83% porous	
Thickness, in.	0.017	± .001
Weight, g/ft ²	13.0	± .13
FEP, wt%	20	
Electrode		
Thickness, in.	0.023	± .002
Weight, grams	18	± 2
		13
		± 2

* Supplied by Stackpole Carbon Co.

Electrodes with these catalyst loadings (0.6 anode, 0.9 cathode) were used in most stacks in the last phase of the project. The second 80-cell stack, however, was built with cathode and anode loadings of 0.5 and 0.25g Pt/ft², respectively.

Performance of 5 in. x 15 in. cell stacks built with the supported platinum catalyst electrodes was higher than with platinum black catalyst. Individual cell voltages in some stacks were 0.65 to 0.67V at 100 ASF compared to 0.61 to 0.62 obtained with the best Pt black electrodes with a 2g Pt/ft² catalyst loading.

Stacks built with anodes having a 0.3 to 0.6g Pt/ft² were tolerant to 1% CO in the fuel. Performance data with various fuels for stacks built with the supported catalyst electrodes are shown in the stack test section of this report (Section 4.0).

2.3 SiC MATRIX DEVELOPMENT

Silicon carbide is among the few materials which appear to be completely inert to phosphoric acid at fuel cell operating temperatures. Fuel cell matrices made from fine grit SiC powder as well as from SiC whiskers have been evaluated at ERC in small cell (2 in. x 2 in.) test rigs. As a separate task of this project, matrix manufacturing and stack assembly techniques

ENERGY RESEARCH CORPORATION

were developed to adapt the SiC matrix process to the 5 in x 15 in. stack hardware.

Although SiC matrices have been successfully prepared in the past by the papermaking process,* the unavailability of a consistent quality SiC whisker material (obtained previously from Exxon Enterprises, Inc.) limited the material choice to SiC powder. Throughout this project, 1000-grit SiC powder from Carborundum Corp. was employed.

The matrices were prepared by applying an aqueous SiC slurry (formulated as shown in Table VI) directly onto the electrode by means of the coating machine shown in Figure 16.

TABLE VI.
SiC MATRIX COMPOSITION

Material	wt%, dry basis
Silicon Carbide (1000 grit)	96 - 98
Polyethylene Oxide	0.3
Polytetrafluoroethylene (TFE 30)	2 - 4

The electrode is placed on the bed of the machine and a uniform layer of the slurry is spread onto the electrode by a wire-bound bar mounted in a yoke driven by a variable speed motor. The thickness of the matrix is controlled by the gauge of the wire on the casting bar and also by the clearance between the bar and the electrode surface. After casting, the matrix is air dried and sintered at 275°C. The resulting matrix typically has a thickness of 0.007 in. and porosity in the 50 to 60% range. Bubble pressure for the SiC matrix prepared by this process was somewhat higher than bubble pressure measured for Kynol matrices (15 to 20 psi vs ~ 10 psi).

Matrix bubble pressure was measured with the testing apparatus shown in Figure 17. The prewet, coated electrode was placed matrix down in the appropriate area of the bottom stainless steel plate. The top plate was then properly secured over the sample. Water was placed in the water retention area and H₂ pressure was slowly increased. The pressure was constantly monitored by the pressure gauge and by the manometer. Thus the

* Contract DAAK02-75-C-0045, Final Report, June 1977.

ENERGY RESEARCH CORPORATION

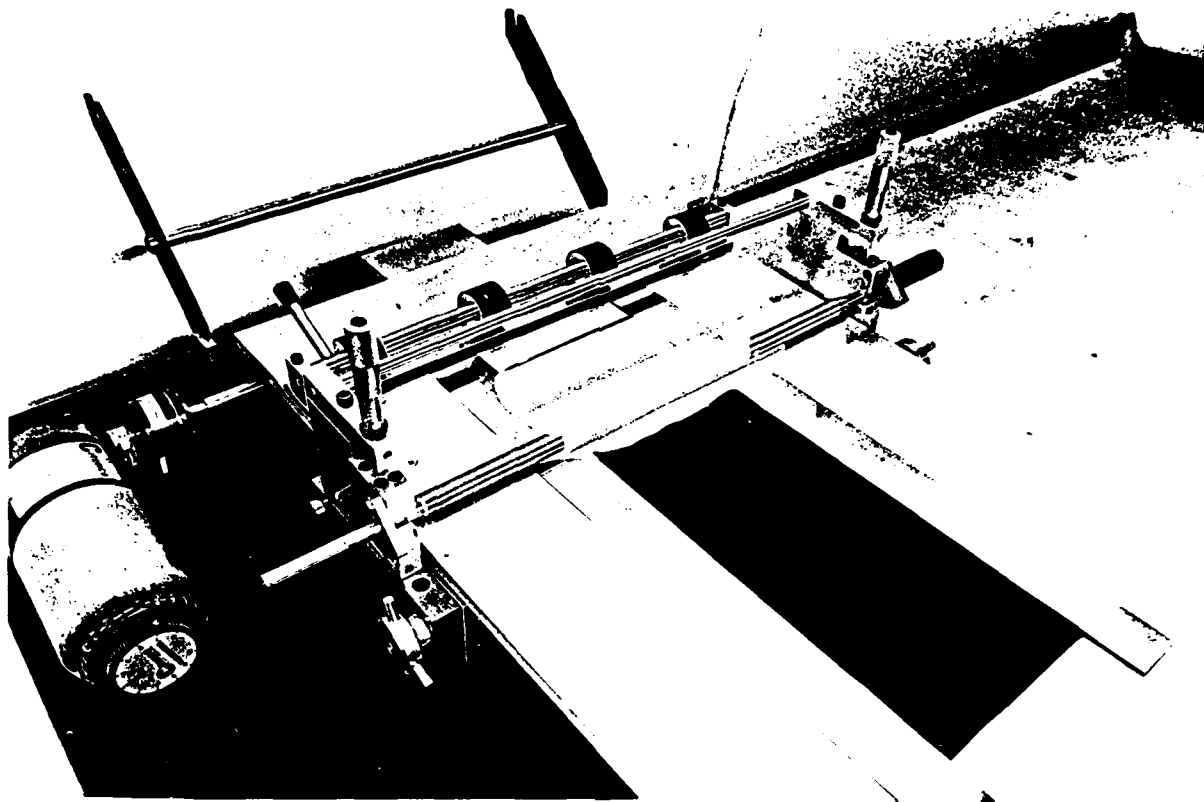


FIGURE 16
COATING MACHINE

P0095

pressure point (when bubbles were observed through the water layer on top of the matrix) was determined.

Several stacks utilizing the SiC matrix were constructed and tested. Performance of these stacks was generally comparable to that obtained with stacks having Kynol matrices, except for open circuit voltage which was somewhat lower for the SiC stacks. This may have been due to a modified stack assembly technique used with the SiC matrix. Stack construction details and stack test results are presented elsewhere in this report (Sections 3.0 and 4.0, respectively).

3.0 STACK ASSEMBLY DEVELOPMENT

Effective separation of the gases in the stack and gas-tight manifolding of the fuel are essential for good stack performance and fuel utilization. Various methods for achieving gastight assemblies were studied on this project.

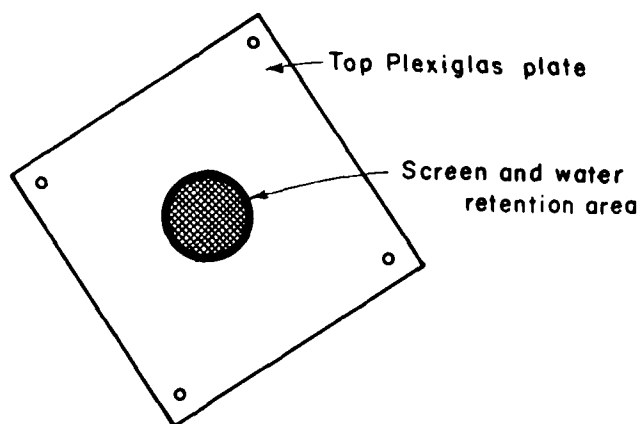
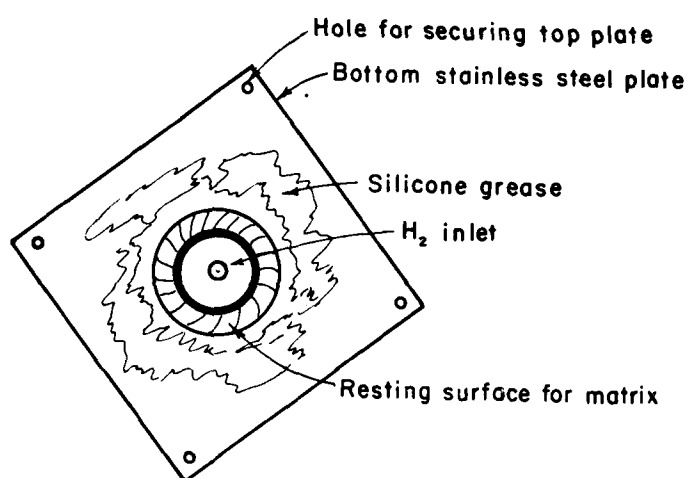
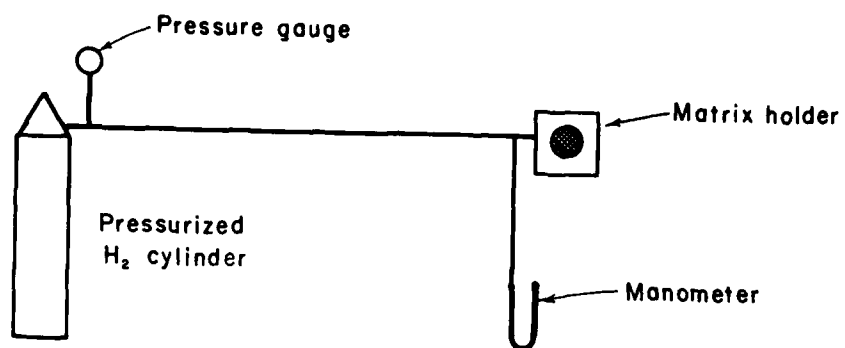


FIGURE 17
BUBBLE PRESSURE TESTING SET-UP

ENERGY RESEARCH CORPORATION

3.1 HARDWARE

The stacks were assembled with hardware described in reports on earlier stack development programs.* The end support plates were 1 in. thick solid aluminum with 1/4 in. thick fiberglass-epoxy insulators and electric blanket heaters for temperature control. Phenolic manifolds with 1/2 in. deep plenums were used on both fuel and air sides of the stack.

Stack compression was maintained at approximately 5400 lbs (72 psi). This value was determined by measuring the deflection of previously calibrated compression bars as shown in Figure 18. (The compression bars are made from AISI tool steel hardened to a Rockwell hardness of 46 to 48.)

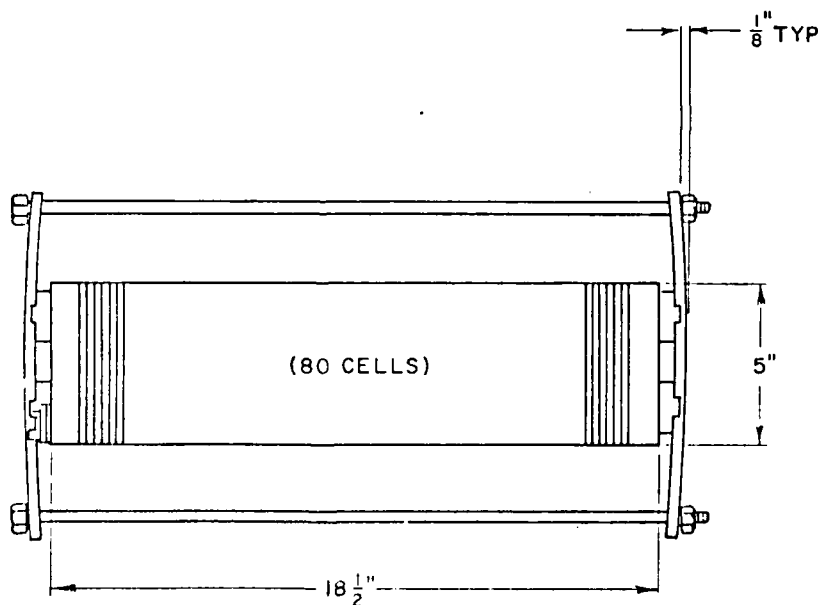


FIGURE 18
TIE BAR DEFLECTION

D0528

* Contract DMAK02-74-C-0367, Final Report, June 1977.

ENERGY RESEARCH CORPORATION

3.2 EDGE SEALS

Two basic methods for obtaining cell edge seals were evaluated. The first utilizes a fluoroelastomer cement* around the edges of the matrix, applied as shown in Figure 19. The cement penetrates the porous matrix and also forms a bond to the bipolar plate as shown in Figure 20. The stack is assembled with dry components, the electrolyte being allowed to wick into the matrix from the electrolyte fill channel. The electrolyte fill channel can be seen in the cutaway stack section drawing, shown in Figure 21.

The second method depends entirely on the acid filled matrix to provide edge sealing, with no cement being used (except to position the electrodes on the bipolar plate). The stack is assembled with prefilled matrices, reducing the time required for wicking the stack via the electrolyte fill channel from 4-5 days to 1-2 days. A 98% acid concentration is used in the wet assembly technique. Prior to use, the acid is heated to 170°F. Next, 16 to 20 ml of acid is applied by syringe uniformly over the 5 in. x 15 in. matrix; the stack is then assembled in normal fashion.

Testing of 3- and 10-cell stacks assembled by both methods did not indicate superior performance or endurance for either method. Fuel utilization over 90% could be achieved consistently with both assembly techniques. Initial stack performance and endurance under load also appeared to be similar.

3.3 MANIFOLD SEALS

Viton rubber gaskets were used in all stacks to achieve tight fuel manifold gas seals. This rubber undergoes some residual flow when compressed at stack operating temperatures (250 to 350°F), producing a tight fit between the manifold and the plate stack. Figure 22 shows the area of the manifold over which gasket material is used.

* C-328 Viton RTV Cement, The Connecticut Hard Rubber Co.

ENERGY RESEARCH CORPORATION

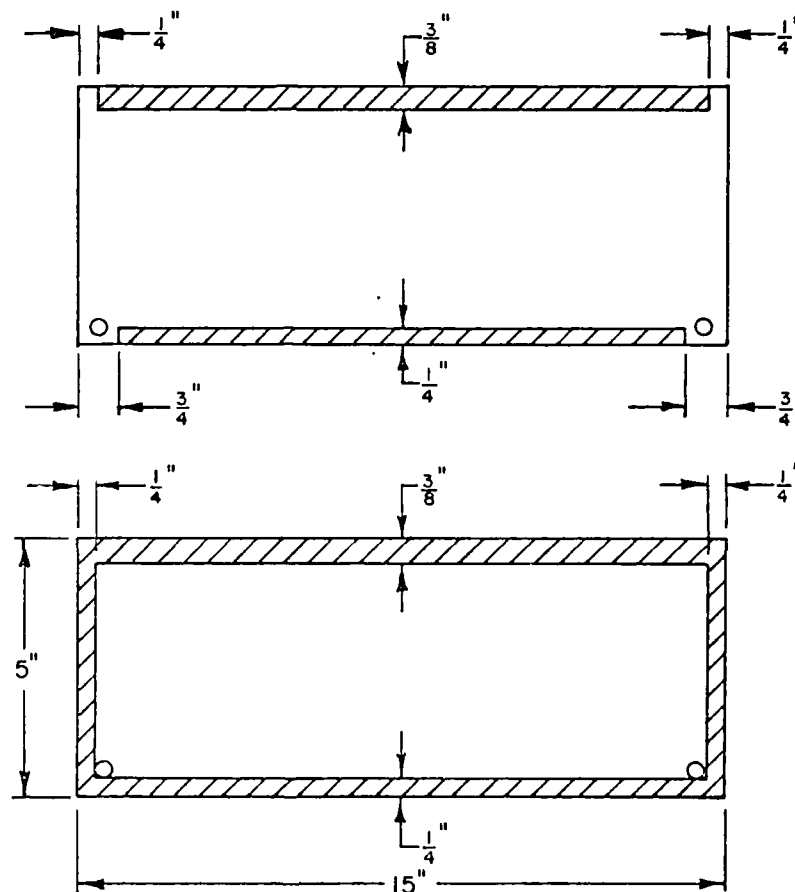


FIGURE 19
CEMENTED AREA ON MATRIX

D050H

ENERGY RESEARCH CORPORATION

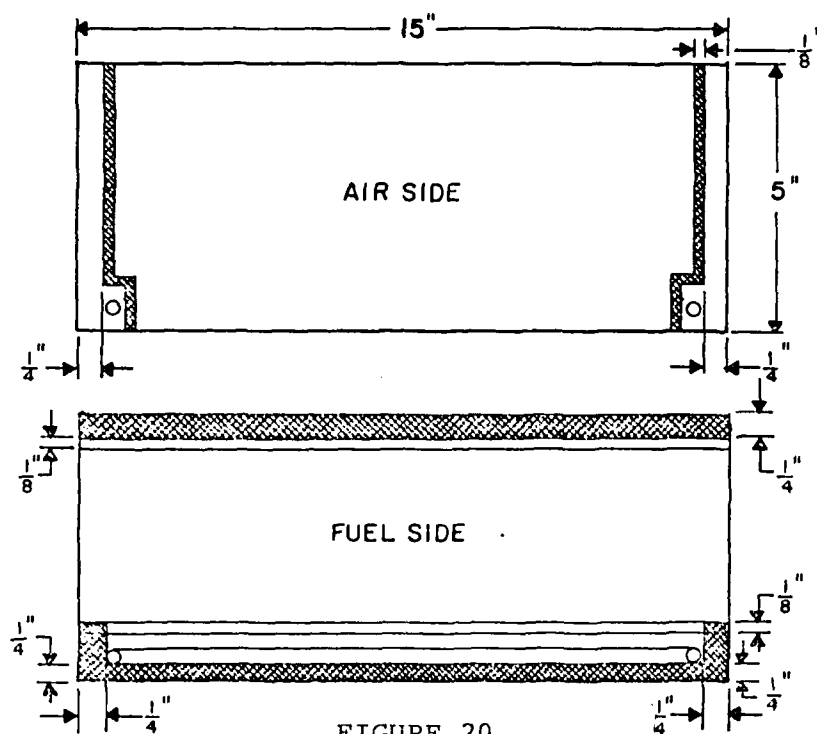


FIGURE 20

CEMENTED AREA ON PLATE

D0509

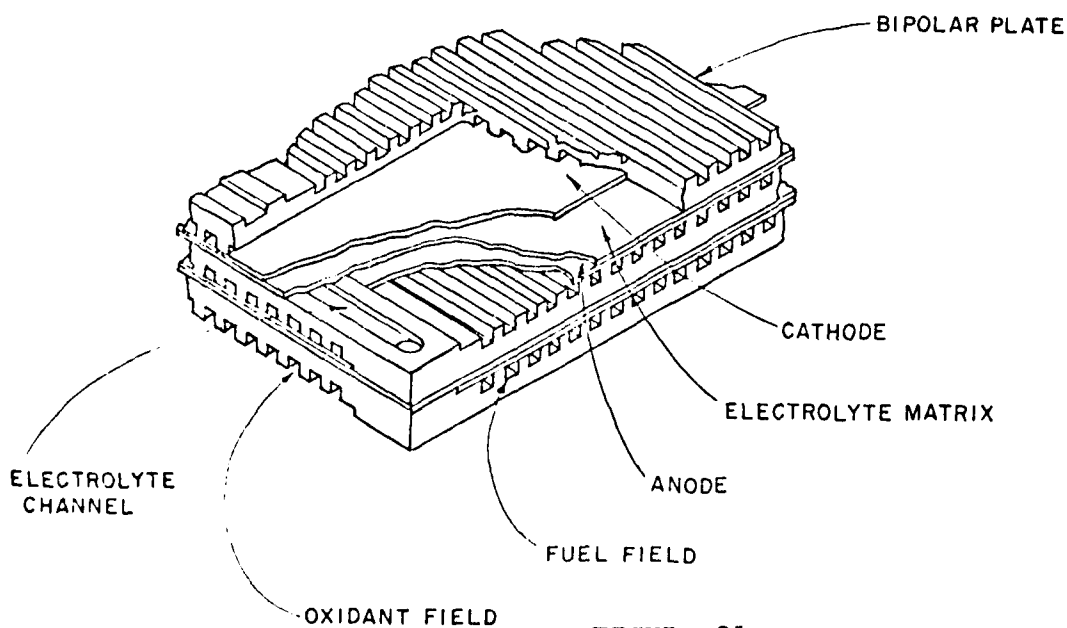


FIGURE 21

STACK CUTAWAY

D0510

ENERGY RESEARCH CORPORATION

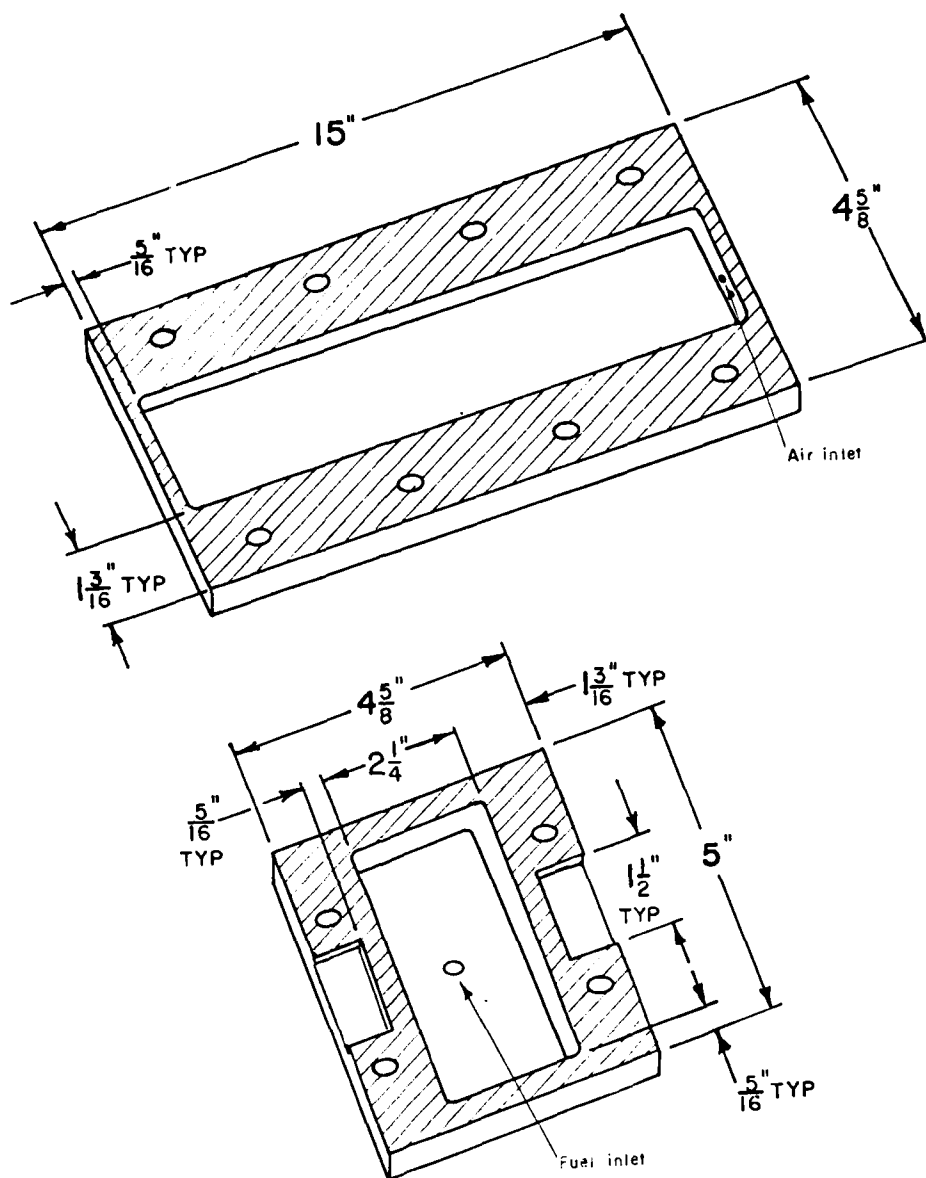


FIGURE 22
MANIFOLD SEALS

D0507

ENERGY RESEARCH CORPORATION

Results of stack testing for evaluation of gastightness are presented in the stack performance evaluation section of this report.

3.4 ELECTROLYTE WICKING

Both the wet and dry-assembled stacks received additional acid filling after assembly. The electrolyte was 98 to 102% H_3PO_4 , prepared by heating reagent grade material (J.T. Baker, 85% H_3PO_4) to the desired concentration (determined by specific gravity measurement). A head of 1/2 to 3/4 in. acid was maintained above the acid channels in the plates to assure adequate flow from the acid container to the stack. During wicking, stack temperature was maintained at 230 to 270°F. For wet assembled stacks, wicking time was usually 2 days, while dry assembled stacks were wicked for one to two weeks, with Kynol stacks requiring the shortest time and Mat-1 stacks the longest. Gastightness and internal resistance were used as criteria for completion of the wicking process.

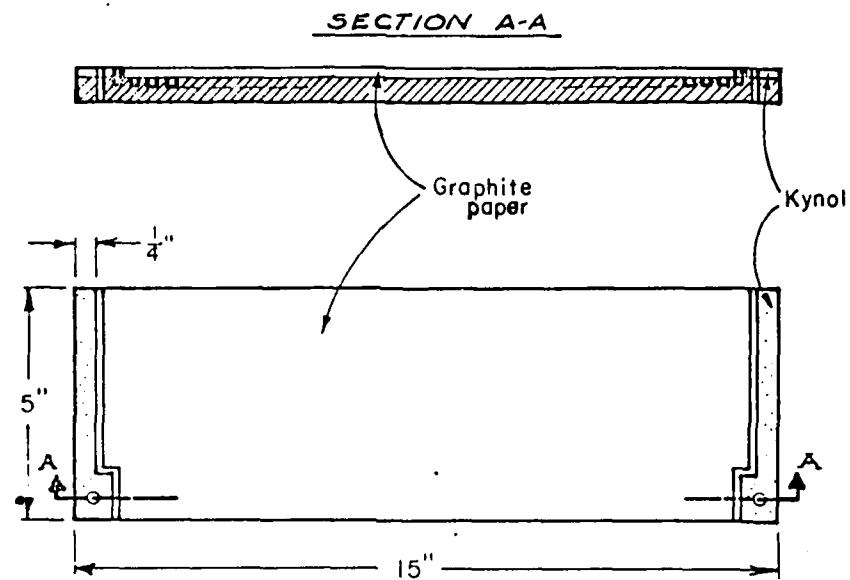
3.5 ASSEMBLY WITH DIGAS PLATES

To obtain sufficient electrical conductivity between the two half plates, graphite paper (catalyst layer support) was employed. Gas seals between the fuel manifold and the DIGAS channels were obtained by placing the acid-filled Kynol matrix on the edges of DIGAS half plates, as shown in Figure 23. A 10-cell stack was also built with an O-ring seal (Figure 24), but this approach was abandoned because the Kynol wet seal proved to be effective and simpler to construct.

3.6 STACK TERMINALS

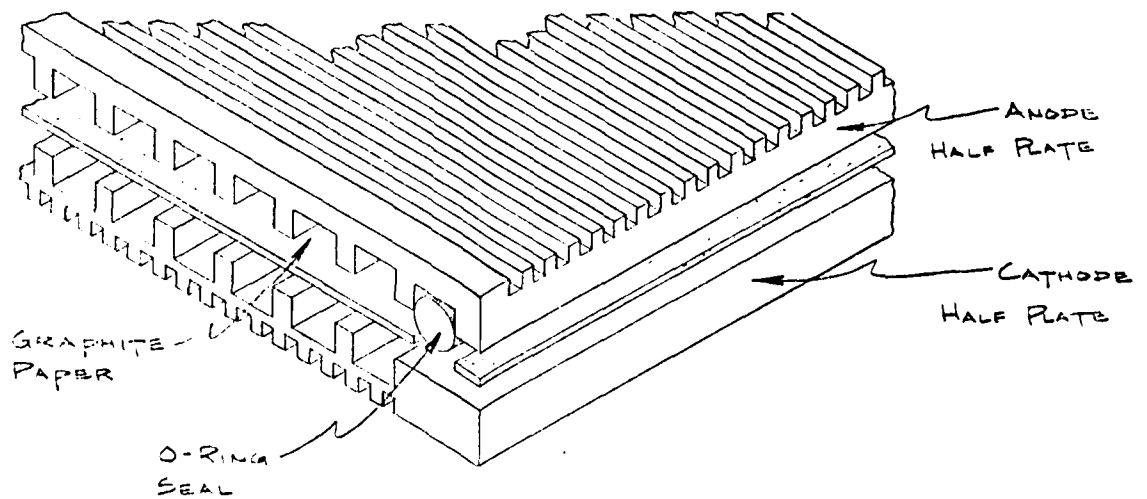
Short stack terminals were usually formed by extending a 1-1/2 in. wide tab from the current collectors beyond the fuel manifold seal. For the tall (80-cell) stacks and some 10-cell stacks, an insulated lug terminal was provided, as shown in the stack assembly drawing (Figure 25). To improve the corrosion

ENERGY RESEARCH CORPORATION



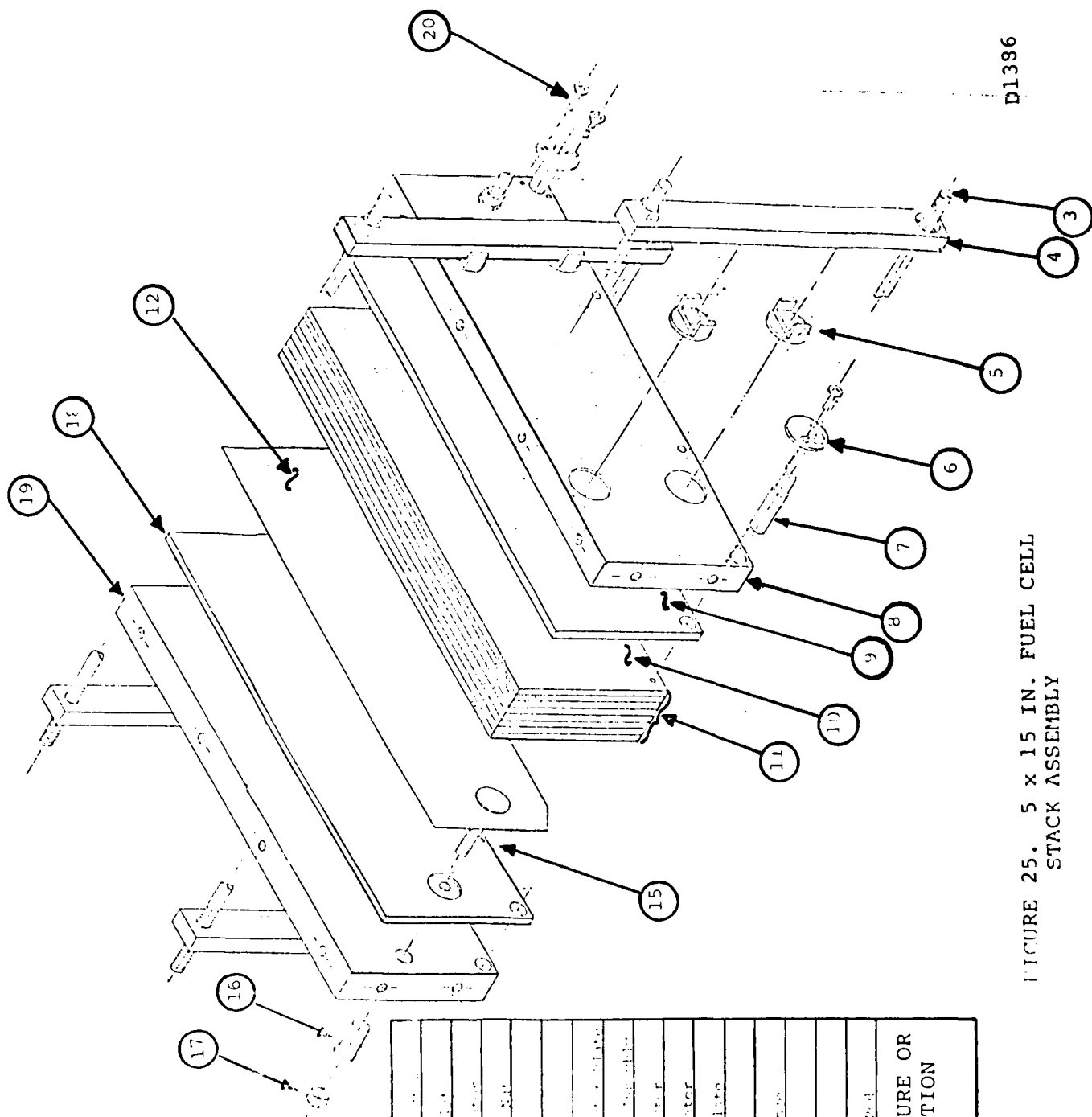
D1289

FIGURE 23 KYNOL AND GRAPHITE PAPER AREAS
IN DIGAS ASSEMBLY



D1290

FIGURE 24 O-RING SEAL FOR DIGAS PLATE



D1396

FIGURE 25. 5 x 15 IN. FUEL CELL
STACK ASSEMBLY

ITEM NO.	NOMENCLATURE OR DESCRIPTION
1	3/4 x 16 inch bar
2	1/2 inch thick plate
3	1/2 inch thick plate
4	1/2 inch thick plate
5	1/2 inch thick plate
6	1/2 inch thick plate
7	1/2 inch thick plate
8	1/2 inch thick plate
9	1/2 inch thick plate
10	1/2 inch thick plate
11	1/2 inch thick plate
12	1/2 inch thick plate
13	1/2 inch thick plate
14	1/2 inch thick plate
15	1/2 inch thick plate
16	1/2 inch thick plate
17	1/2 inch thick plate
18	1/2 inch thick plate
19	1/2 inch thick plate
20	1/2 inch thick plate

ENERGY RESEARCH CORPORATION

4.2.1 Oxygen Gain Measurement

Operation on pure oxygen cathode gas was conducted periodically for most stacks to diagnose the change in performance due to electrode wetting. The oxygen performance tests were generally of short duration (under 5 minutes) with oxygen flow in the range of 2 to 3 stoich. Typical oxygen gains were in the 60 to 80 mV range at 100 ASF.

4.2.2 Resistance Measurement

Stack resistance was measured using a Hewlett Packard Model 4328A milliohmmeter. The major purpose for these measurements was to ascertain that acid wicking has been completed and that stack terminals are in good contact with the outermost graphite plates. An example of a series of resistance measurements taken on a 10-cell stack during electrolyte wicking is shown in Figure 28.

A disadvantage of the milliohmmeter is that only total stack resistance (not individual cell resistances) can be measured directly. To obtain cell resistance values, an indirect method was employed. The stack was operated with an external power supply and hydrogen flowing to the anode as well as the cathode; i.e., the cathode was evolving hydrogen. Since the polarization of both the hydrogen anode and the hydrogen cathode is relatively small (under 5mV/100 ASF), the slope of the voltage-current plot corresponds closely to cell resistance. Cell polarization data obtained in this manner for Stack 16 are shown in Figure 29. The cell resistance values of 1.5, 1.7 and 1.8 m Ω agreed well with the milliohmmeter reading of 5 m Ω across the stack terminals.

4.3 THREE-CELL STACKS

Three-cell stacks were assembled to test both component performance and assembly endurance. These stacks were also used to evaluate the effect of several operating parameters on cell performance since, unlike 10-cell stacks, these stacks showed relatively small temperature variation cell to cell and inlet to

ENERGY RESEARCH CORPORATION

resistance of the 0.005 in. thick Cu collector, a gold flash (under 0.1 mil thick) was applied.

4.0 STACK TESTING

A total of fifty-six 3- and 10-cell stacks were tested on this project for initial characteristics and endurance. Two 80-cell stacks were also tested using hydrogen and steam reformed methanol as fuel.

4.1 CONSTRUCTION

Construction variables evaluated in the stack tests included bipolar plates (gas diffusion pattern), matrix (Kynol, SiC and Mat-1) and an electrode catalyst loading in the range of 0.3 to 0.9g Pt/ft² of electrode. A number of electrolyte filling procedures were also evaluated.

4.2 PROCEDURE

Stacks were evaluated for initial performance under a number of operating conditions and for performance stability under continuous load conditions. Most of the testing was performed with hydrogen fuel, but some tests were also conducted with simulated reformed fuel (SRF). Air rates thru the stacks were maintained at 6 to 10 times the stoichiometric reaction requirements. Diagnostic tests with oxygen as the cathode gas were conducted to periodically monitor cathode performance. A test set-up schematic is shown in Figure 26.

Stack temperatures were controlled by the end plate heater blankets and by air temperature and flow rate. All operating parameters (temperature, current, voltage, flow rates) were monitored on the test panels shown in Figure 27. A facility for simultaneous performance testing of twelve stacks was assembled for the purposes of this project. A separate test stand was built for testing the 80-cell stacks.

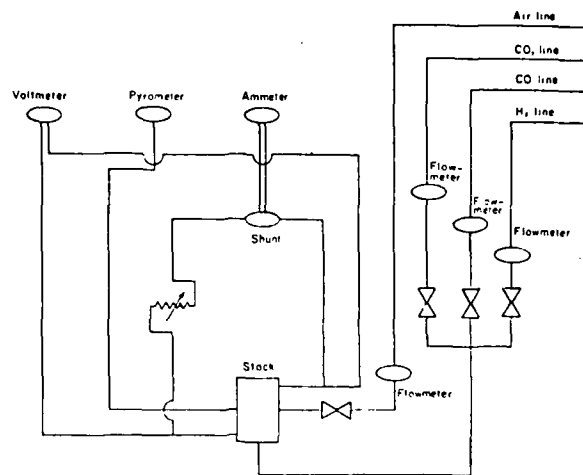


FIGURE 26. TEST SET-UP SCHEMATIC

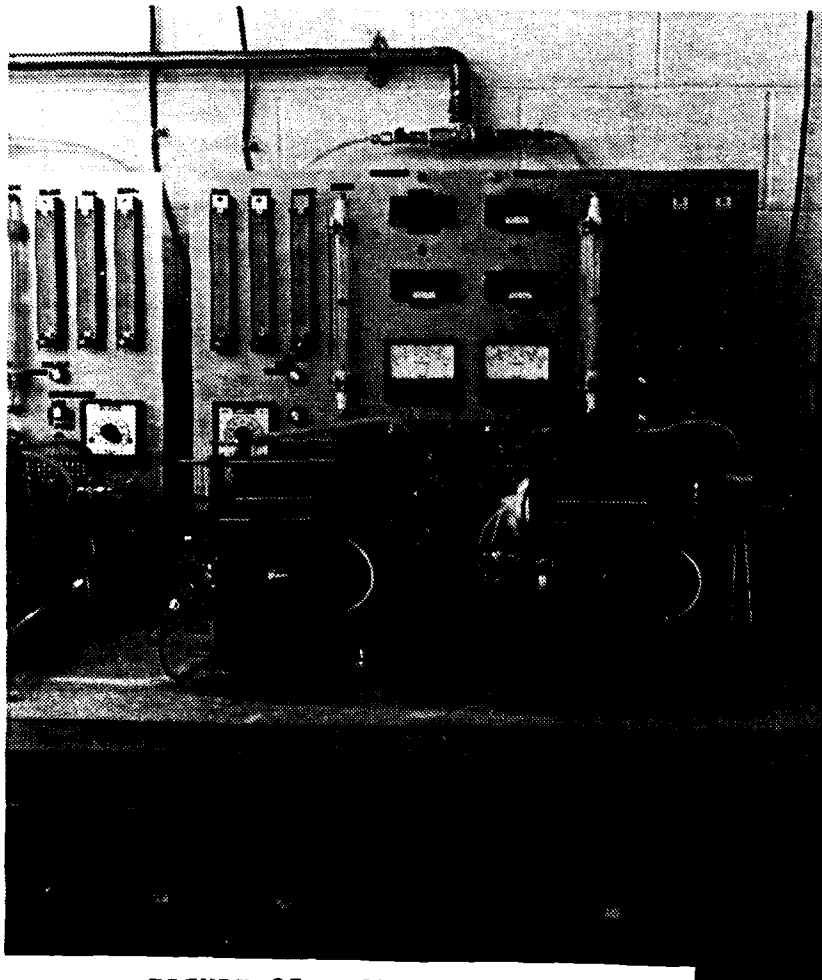


FIGURE 27. STACK TEST PANEL

ENERGY RESEARCH CORPORATION

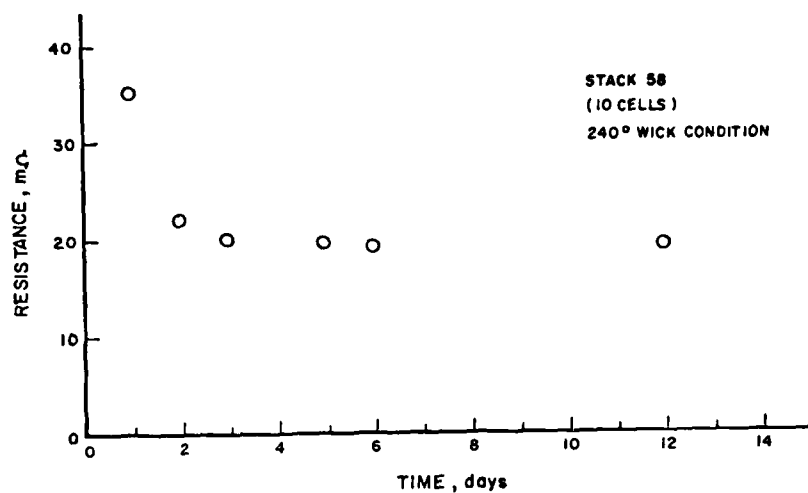
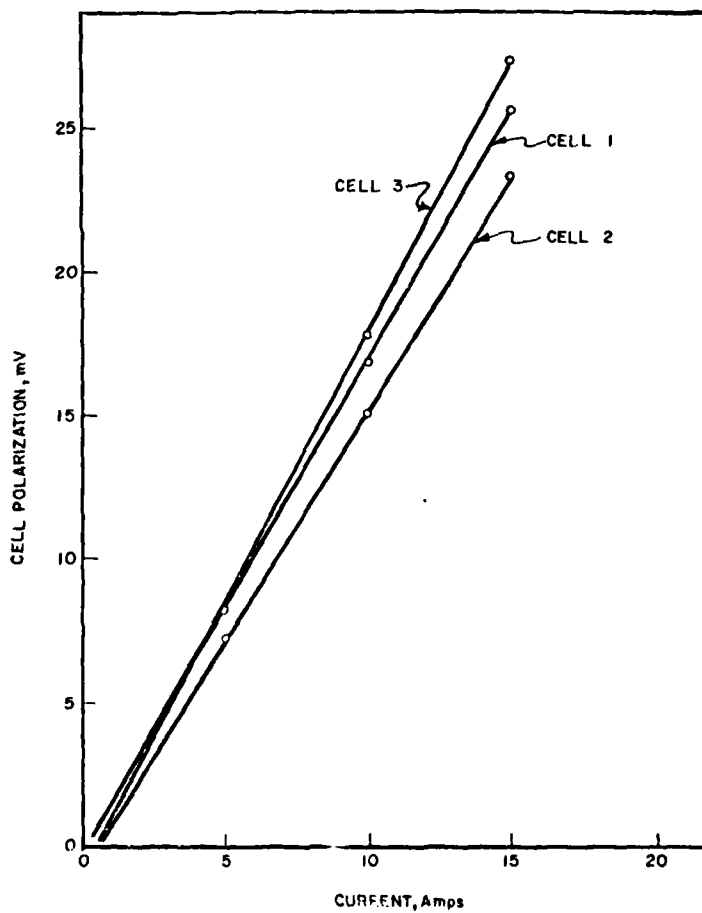


FIGURE 28. STACK RESISTANCE CHANGE DURING WICKING

D1376

FIGURE 29. H_2/H_2 POLARIZATION FOR STACK 16 (320°F)

D1377

ENERGY RESEARCH CORPORATION

outlet due to the proximity of end plate heaters to all cells. The major construction variables and test results for these stacks are summarized in Table VII.

4.3.1 Initial Performance

In general, peak cell voltages were observed within a few days after placing the stack on test. However a few stacks did show an increase of 30 to 40 mV/cell after they had operated at 40A and 350°F for 1000 to 1500 hours. All of these stacks had supported catalyst cathodes, and the operating voltage increase probably indicates continued wetting of the catalyst with the electrolyte.

The highest operating potentials in this series of stacks were obtained with Kynol matrices and supported catalyst electrodes with anode and cathode loadings around 0.6 and 0.9 Pt/ft², respectively. There was no apparent difference in performance between stacks assembled with wet and dry matrices. There was also no significant difference between stacks built with the various plate groove patterns. Polarization data for representative stacks are shown in Figure 30.

4.3.2 Performance Stability

Selected stacks were continued on test at 100 ASF and 350°F to observe performance stability. Seven stacks were tested for more than 5000 hours; another 15 stacks were tested beyond 2000 hours. Electrolyte was added periodically to all stacks during life testing in 1000 to 5000-hour intervals.

Oxygen gain was determined periodically on stacks undergoing endurance testing. In general, oxygen gains remained in the 60 to 80 mV range at 100 ASF, indicating cathode catalyst layer stability. This is also apparent from the voltage-time curves plotted in Figure 31.

Some of these stacks were terminated voluntarily at the end of the first phase of the project. Other stacks were terminated because of poor fuel utilization or low operating voltage. As

ENERGY RESEARCH CORPORATION

TABLE VII THREE-CELL STACK SUMMARY

STACK NO.	PLATE TYPE	MATRIX	ANODE CATALYST		CATHODE CATALYST		ASS'Y	CELL VOLTAGE, mv @ 40A, 350°F					HOURS TESTED	TERMINATION	REMARKS	
			TYPE	g/ft ²	TYPE	g/ft ²		INITIAL AVERAGE								
								1	2	3	1	2				3
03	AA	K	PB	4.2	PB	0.36	D	540	540	520	440	440	460	70	Crossover	100 hrs on SRF 700 hrs on SRF
04	AA	K	Pt/C	3.4	Pt/C	0.63	D	500	510	530	440	500	475	10	Crossover	
05	AA	K	PB	3.2	Pt/C	0.96	D	570	570	570	525	545	530	1180	Gasket leak	
06	AA	K	PB	3.3	Pt/C	0.85	D	620	630	630	570	580	580	2820	Soft plate	
07	AA	K	PB	3.0	PB	2.9	W	620	630	620	570	590	580	2700	Bad Terminal	100 hrs on SRF 300 hrs on SRF
08	AA	K	PB	3.4	PB	2.8	D	570	590	580	535	550	525	40	Dry Matrix	
09	AA	SIC	PB	3.0	Pt/C	0.67	D	520	560	570	465	485	485	1130	Dry Matrix	100 hrs on SRF 300 hrs on SRF
11	AA	K	PB	3.5	PB	3.0	W	630	610	620	575	570	575	2630	Voluntary	
12	AA	K	Pt/C	0.84	Pt/C	0.84	D	620	620	620	575	580	580	6850	Voluntary	Low voltage Low voltage Crossover Gasket leak Crossover
13	AA	K	Pt/C	0.98	Pt/C	0.99	D	490	530	440	465	500	420	330	Low voltage	
14	AA	K	Pt/C	1.0	Pt/C	0.99	D	490	530	520	420	475	460	260	Low voltage	
15	AA	K	Pt/C	0.99	Pt/C	1.0	D	540	550	490	465	505	450	260	Crossover	
16	AA	K	Pt/C	1.0	Pt/C	0.95	W	450	540	470	425	520	450	270	Gasket leak	Internal short Gasket leak Voluntary Dry Matrix
17	AA	K	Pt/C	0.85	Pt/C	0.91	D	610	630	490	570	570	420	1080	Crossover	
18	CC	K	Pt/C	0.65	Pt/C	0.80	W	-	-	-	-	-	-	0	Internal short	
19	AB	K	PB	2.4	Pt/C	0.35	W	630	640	620	580	590	540	1900	Gasket leak	
20	AA	K	PB	2.8	Pt/C	0.30	D	620	660	630	605	615	595	510	Voluntary	(MERADCOM)
21	AA	K	PB	2.6	Pt/C	0.87	D	550	600	600	515	585	585	835	Dry Matrix	
22	AB	K	PB	3.2	Pt/C	0.72	W	600	670	620	580	605	575	40	Plate crack	
23	BB	K	Pt/C	0.23	Pt/C	0.51	D	510	600	590	465	575	575	255	Gasket leak	
24	BB	K	Pt/C	0.30	Pt/C	0.58	W	550	390	490	550	390	490	60	Low voltage	Insuf. Electrolyte (MERADCOM)
25	BB	K	Pt/C	0.38	Pt/C	0.62	W	620	630	630	595	585	595	5220	Soft plate	
26	CC	K	Pt/C	0.68	Pt/C	0.77	W	620	620	620	610	600	610	10	Crossover	
27	AB	K	Pt/C	0.67	Pt/C	0.81	D	620	640	640	615	625	620	1100	Voluntary	
28	AB	K	Pt/C	0.61	Pt/C	0.82	W	660	660	640	640	650	640	1350	Soft plate	408 hrs on SRF 2165 hrs on SRF
30	CC	K	Pt/C	0.94	Pt/C	0.88	W	630	600	630	610	510	585	250	Dry matrix	
31	BB	K	Pt/C	0.59	Pt/C	0.84	D	630	670	650	595	630	630	4490	Voluntary	
32	AB	K	Pt/C	0.62	Pt/C	0.81	D	660	650	650	620	610	605	4010	Soft plate	
34	AB	K	Pt/C	0.57	Pt/C	0.77	W	640	650	620	610	625	575	4270	Voluntary	2-cell stacks high-temp. test. High Voltage test (3760 hr. @ 150ASF)
37	AB	K	Pt/C	0.62	Pt/C	0.87	D	640	660	660	615	635	625	3720	Voluntary	
38	AB	K	Pt/C	0.69	Pt/C	0.69	W	350	400	390	350	400	370	150	Low voltage	
39	AA	M	Pt/C	0.90	Pt/C	0.90	D	640	620	-	610	605	-	18187	Voluntary	
52	AB	SIC	Pt/C	0.58	Pt/C	0.90	D	600	640	620	570	640	620	2787	Voluntary	High Voltage test (3760 hr. @ 150ASF)
53	AB	SIC	Pt/C	0.54	Pt/C	0.55	D	630	640	610	630	610	640	5139	Voluntary	
54	AB	SIC	Pt/C	0.53	Pt/C	0.63	D	620	630	620	505	625	515	5446	Voluntary	
56	AB	M	Pt/C	0.30	Pt/C	0.52	D	610	620	620	580	585	590	1016	Voluntary	

Plate: AA - (A) Fuel Side, (B) Air Side
 AB - (A) Fuel Side, (B) Air Side
 BB - (A) Fuel Side, (B) Air Side
 CC - (C) Fuel Side, (C) Air Side
 Matrix K - Kynol
 Matrix K - Silicon Carbide
 Ass'y D - Dry Assembly
 M - MAT-1 Assembly with H₂PO₄
 SRF - Simulated Reformed Fuel
 74% H₂, 25% CO, 1% CO

ENERGY RESEARCH CORPORATION

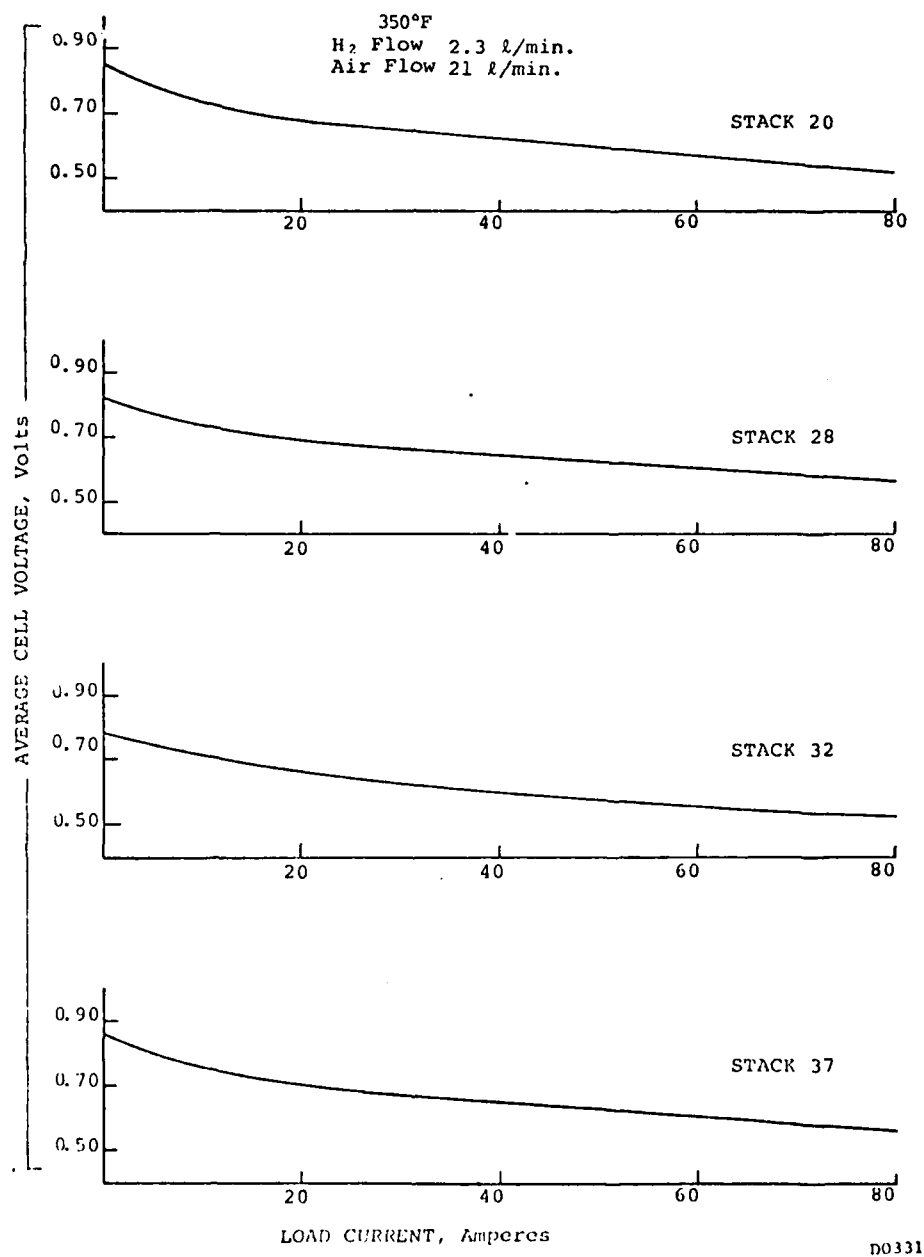


FIGURE 30 POLARIZATION DATA

ENERGY RESEARCH CORPORATION

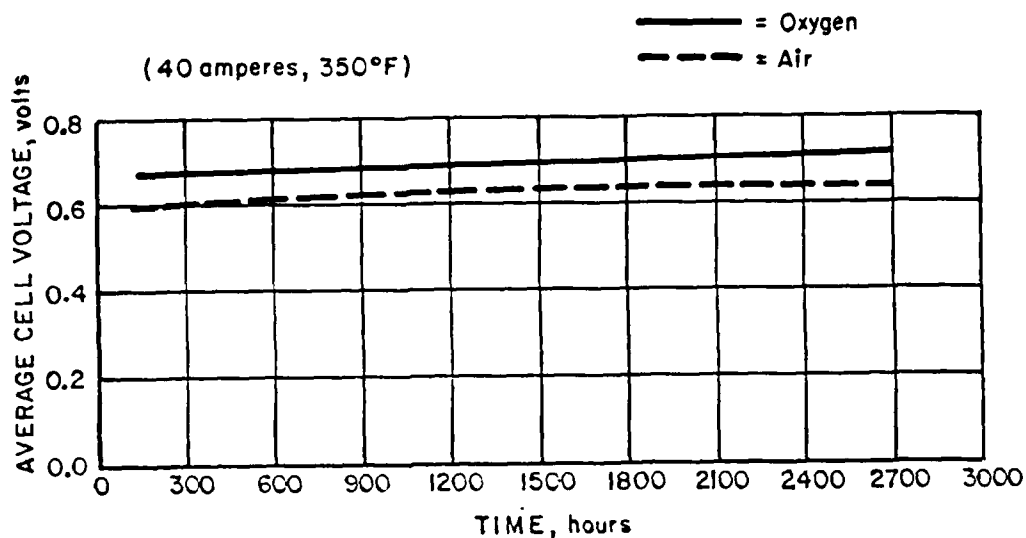


FIGURE 31
CELL VOLTAGE STABILITY

D0515

shown in Table VII, early stack failures could often be traced to gas crossover as indicated by the sensitivity of no-load cell potentials to gas flow rates. This condition was usually caused by insufficient electrolyte, particularly in some of the experimental wet assembly builds, or by inadequate edge gas seals. As discussed in Section 2.1, some stacks also dropped in performance after a few thousand hours of testing because of plate deterioration.

4.3.3 Performance with SRF

Several stacks were operated continuously on simulated reformed fuel (SRF) containing 72% H_2 , 24% CO_2 , 1% CO , and 3% H_2O . Cell operating voltages were recorded periodically for the operating condition of 100 ASF at 350°F while operating on SRF and pure hydrogen. Test results are shown in Table VIII for Stack 34. The hydrogen gain for this stack remained typically around 15 to 20 mV/cell throughout the duration of the test (over 2000 hours).

ENERGY RESEARCH CORPORATION

TABLE VIII
 PERFORMANCE DROP WITH SRF*
 40A, 340 to 360°F
 Stack 34
 80% Fuel Utilization

TIME, hours	3-CELL STACK VOLTAGE, volts	
	H ₂	SRF
2118	1.85	1.80
2259	1.86	1.82
2403	1.86	1.82
2595	1.87	1.82
2787	1.87	1.82
3027	1.87	1.84
3219	1.86	1.83
3411	1.88	1.85
3721	1.88	1.84
3933	1.88	1.83
4125	1.88	1.85
4270	1.88	1.82

* 72% - H₂, 24% - CO₂, 1% - CO, 3% - H₂O

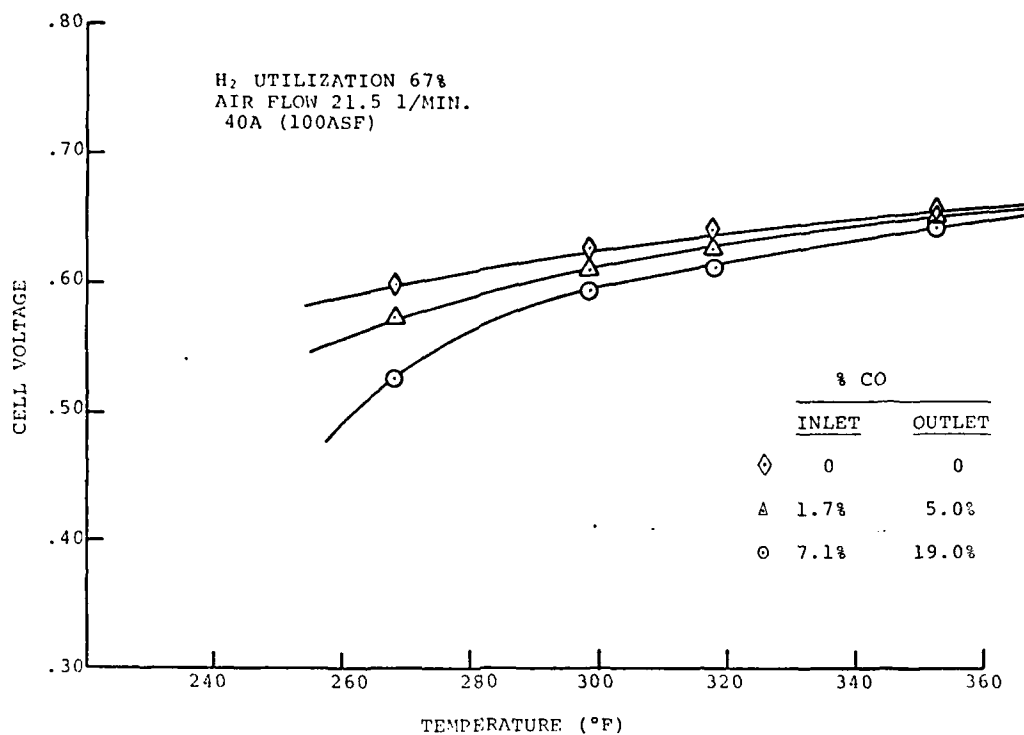
4.3.4 Carbon Monoxide Tolerance

The effect of CO in the fuel was evaluated for Stack 37 over the temperature range of 265 to 355°F. Hydrogen utilization for these tests was 80%. As seen from the data plotted in Figure 32, the anodes become progressively more CO tolerant with increasing temperature. At 315 to 320°F, the effect of 1.7% CO in the inlet is less than 10 mV at a current density of 100 ASF and about 5 mV at 350 to 355°F, the projected operating temperature for this stack design.

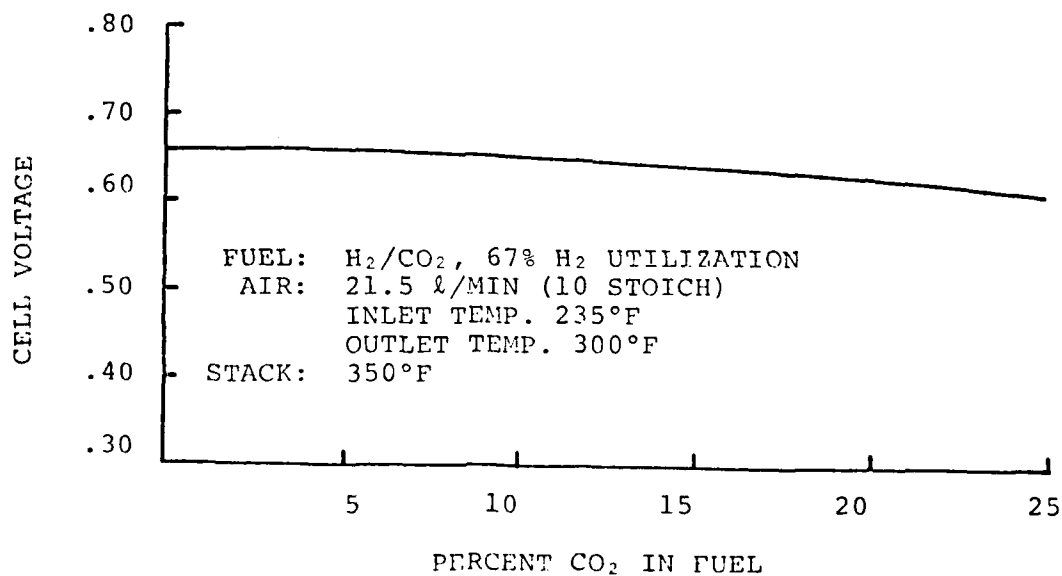
4.3.5 Effect of CO₂

The effect on cell voltage of CO₂ addition to the fuel can be seen in Figure 33. The results are consistent with the voltage effect observed with SRF.

ENERGY RESEARCH CORPORATION



D0332

FIGURE 32. EFFECT OF TEMPERATURE ON
LOAD VOLTAGE

D0333

FIGURE 33. EFFECT OF CO₂ ON LOAD VOLTAGE

ENERGY RESEARCH CORPORATION

4.3.6 Electrolyte Consumption

Replenishment of electrolyte in the stacks is possible thru the filling tubes at any time during operation or storage (with plates in the vertical position). During the extended testing of stacks in this project, acid was added at irregular intervals by wicking for 2 to 4 days, usually after a reduction of open circuit or load voltage was observed. The actual interval for needed electrolyte additions was not determined on this project, but frequency of acid additions usually varied between 1000 and 3000 hours of stack operation. However, one stack (No. 39) operated for over 5000 hours without electrolyte addition.

This procedure was modified for Stack 39 to determine the approximate rate of electrolyte loss at the operating conditions selected (350°F, 100 ASF). After an initial fill period of ~200 hours, the acid bottle was disconnected from this stack and all subsequent additions of electrolyte were accomplished by injecting a measured volume of acid directly thru the fill tubes. The frequency of acid addition and the volume added each time are shown on the stack lifegraph (Figure 34).

The average rate of acid loss during the 18,000 hours of testing this stack can be inferred from this data to be 1.09 ml/cell/1000 hours.

4.3.7 Overtemperature Testing

This test was performed to observe the effect of operating temperature above the normal operating temperature of 350 to 360°F for short periods of time.

The stack used for the elevated temperature test had anode and cathode catalyst loadings of 0.6 and 0.9g Pt/ft², respectively, and was built with a SiC matrix. Before commencing the high temperature test, this stack had undergone 2100 hours of testing at 350°F with hydrogen fuel.

ENERGY RESEARCH CORPORATION

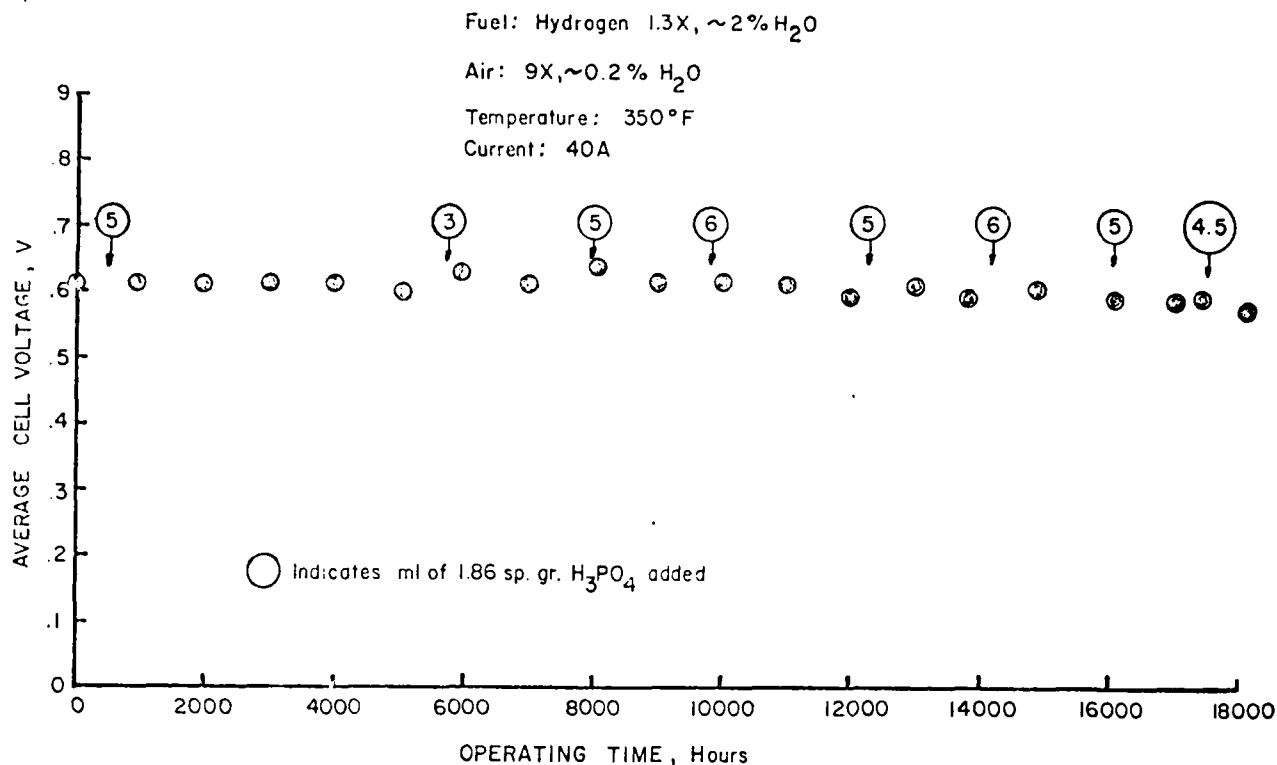


FIGURE 34 LIFEGRAPH OF STACK 39

D1291

The stack was operated with hydrogen fuel, humidified to $\sim 2\%$ moisture and air humidified to $\sim 5\%$. Stack temperature was adjusted by a thermostat which controlled the heating rate of the end plate heater blankets. Stack temperature increases of $10^\circ F$ were produced by manually adjusting the thermostat settings at about 50-hour intervals. The stoichiometric ratio of reactant flow was 1.3 for hydrogen and 9 for air. Fuel entered the stack at room temperature, and the air entered at 200 to $250^\circ F$.

Table IX shows the stack and cell voltage measurements obtained during elevated temperature testing. A voltage-time plot showing the temperatures used in this test is presented in Figure 35.

ENERGY RESEARCH CORPORATION

TABLE IX.

ELEVATED TEMPERATURE TEST

STACK 52

Load: 40A

Fuel: Hydrogen, 1.3X, 2% H₂O

Air : 9X, 5% H₂O

TEMPERATURE, °F	STACK VOLTAGE, V	CELL VOLTAGE, V			HOURS TESTED	REMARKS
		CELL 1	CELL 2	CELL 3		
350	1.86	0.59	0.66	0.61	2091	
360	1.87	0.59	0.66	0.62	48	
370	1.90	0.60	0.67	0.63	47	
380	1.84	0.60	0.64	0.60	50	Fuel line ruptured.
390	1.95	0.60	0.65	0.60	49	
400	1.89	0.61	0.66	0.62	48	
410	1.91	0.62	0.67	0.62	49	Shut down and cooled to room temp. (4 hrs.)
420	1.76	0.53	0.59	0.54	25	

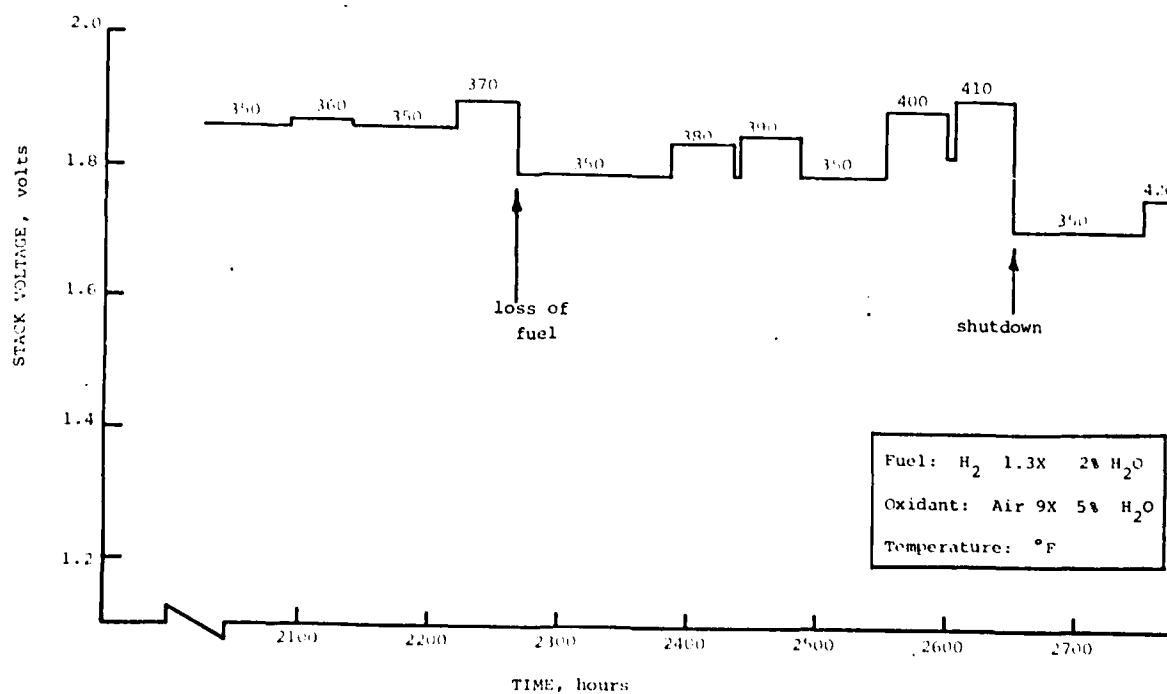


FIGURE 35 HIGH TEMPERATURE TEST

D1281R

ENERGY RESEARCH CORPORATION

After the 370°F test, a rupture in the fuel line occurred causing some dilution and redistribution of the phosphoric acid in the stack. As a result, the stack suffered a performance drop of about 70 mV. The stack was given 6 ml of acid and again stabilized at 350°F before the high temperature tests were resumed.

After the 410°F test the stack was shut down, and some loss of load voltage was noticed when the stack was restarted. However stack performance was stable and testing was resumed. The stack voltage dropped to below 1 volt during the 420°F testing phase, after operating for 25 to 41 hours at this temperature.

4.3.8 Low Current Testing

This test was performed to observe the short-term effects of operating the stack at low current density (high operating voltage).

The stack used for the elevated load potential testing was built with a SiC matrix. The average anode and cathode catalyst loadings were 0.5 and 0.6 grams Pt/ft², respectively.

The stack was operated with hydrogen fuel humidified to 2% moisture and compressed air at an estimated RH of 10 to 20% (room temperature). The fuel was not preheated, but air was maintained at 200 to 250°F by a heated tube preheater.

Testing of this stack was initiated at 40A (106 ASF). At the completion of 620 hours of stable operation, the load current was reduced, and the stack was operated for 50 to 70 hours at the reduced current. This procedure was repeated until the stack current was reduced to 5A and the corresponding average cell voltage had increased to 730 mV.

Table X provides the increased voltage test data. The polarization curves for this stack before and after operation at elevated potential are shown in Figures 36 and 37.

The performance data at the end of the test was identical to the initial performance data. The O₂ gain remained at \sim 75 mV at 40A throughout the testing. It appears, therefore, that

ENERGY RESEARCH CORPORATION

TABLE X.
LOW CURRENT TEST

Stack 54
Hydrogen 1.3X
Air 9X
350°F

STACK VOLTAGE, Volts	STACK CURRENT, amps	CELL VOLTAGE, volts			HOURS TESTED
		CELL 1	CELL 2	CELL 3	
1.36	40.0	0.60	0.65	0.62	622
1.92	32.5	0.62	0.67	0.64	49
1.98	24.3	0.64	0.69	0.66	66
2.04	17.6	0.66	0.71	0.68	50
2.10	12.4	0.68	0.73	0.70	50
2.16	8.2	0.69	0.76	0.72	66
2.22	5.2	0.71	0.78	0.74	49

operation at reduced load (elevated cell potential) does not result in significant cell performance decay over the relatively short operating times employed in these tests.

4.4 TEN-CELL STACKS

4.4.1 Cell Voltage Reproducibility

Twenty 10-cell stacks were assembled as described in Section 4.1. Ten builds were used to verify design and assembly procedures developed as part of the 3-cell stack construction task.

ENERGY RESEARCH CORPORATION

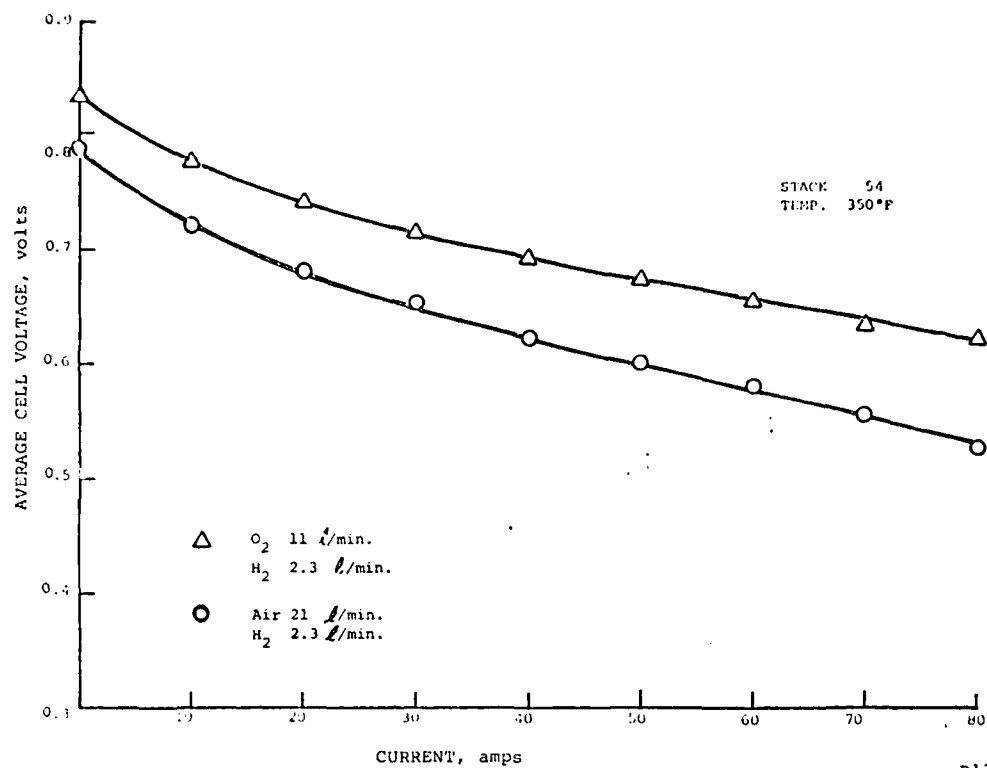


FIGURE 36 STACK PERFORMANCE BEFORE LOW CURRENT TESTING

D1282 R

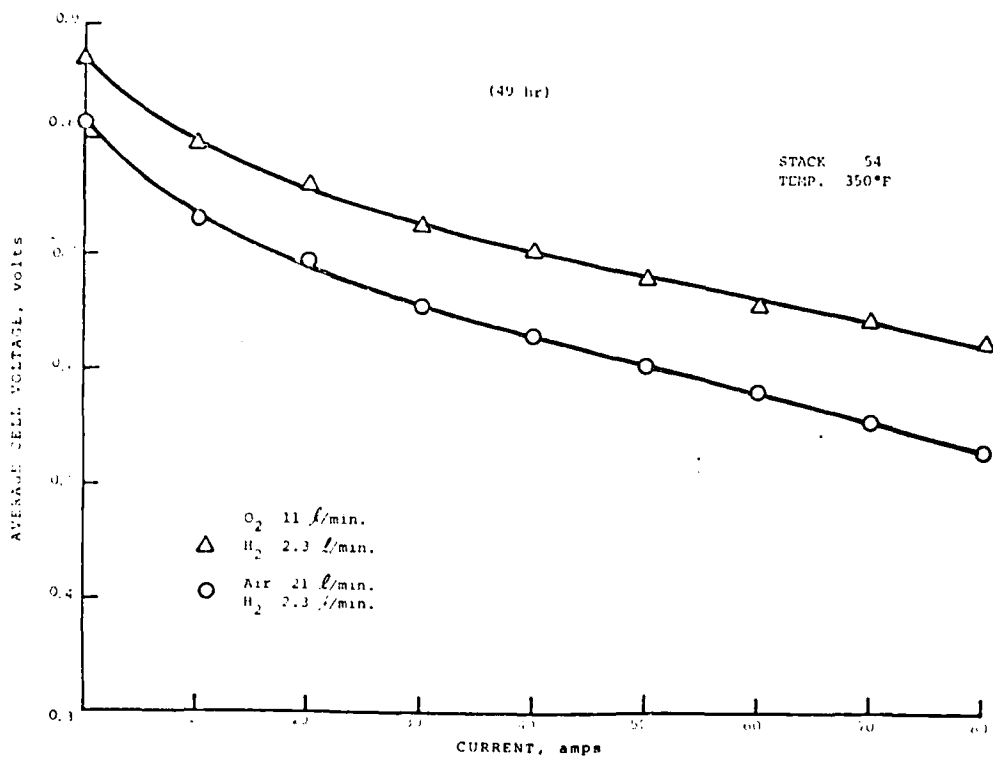


FIGURE 37 STACK PERFORMANCE AFTER LOW CURRENT TESTING

D1233R

ENERGY RESEARCH CORPORATION

Ten additional 10-cell stacks were dedicated to evaluation of reliability of the two assembly procedures, i.e., the "dry" assembly using Viton rubber cement and the "wet" assembly using prefilled Kynol matrices. The stacks were assembled with electrodes utilizing 10% Pt on carbon catalyst, 0.85g Pt/ft^2 for the cathode, and 0.6 g Pt/ft^2 for the anode. The standard Kynol matrices were employed, and bipolar plates had the "A" pattern on the fuel side and the "B" pattern on the air side. Five of the ten stacks were built by the "dry" assembly method, and the remaining five by the "wet" method.

Testing of these stacks was conducted in the usual fashion, i.e., measurements were made of the open circuit voltage, load voltage at 25 to 200 ASF, fuel utilization, performance on hydrogen and SRF, and performance stability under continuous load at 100 ASF.

All of the 10-cell stack construction and test data are summarized in Table XI. For the last 10 ten-cell stacks built during this phase of the project, cell open circuit and load potentials (100 ASF) are listed in Tables XII and XIII, respectively. The data show uniform performance for individual cells in a stack as well as between stacks. (The somewhat lower cell potentials at the ends of the stack are associated with lower cell temperatures.) Polarization curves for these stacks are plotted in Figures 38 and 39. Two stacks were operated on SRF; results of these tests are shown in Table XIV. The above results indicate no difference in initial performance between the two methods of stack assembly.

Endurance testing of all stacks was conducted at 100 ASF and 350°F on hydrogen fuel. No stack failures were encountered during 500 hours of operation, the duration of initial stack qualification according to the test plan. Voltage-time plots for these tests are shown in Figures 40 and 41.

ENERGY RESEARCH CORPORATION

TABLE XI. TEN-CELL STACK SUMMARY

STACK NO.	PLATE TYPE	ANODE CATALYST g/Ft.	CATHODE CATALYST g/Ft.	ASS'Y	AVERAGE CELL VOLTAGE mV @ 40A, 350°F		HOURS TESTED	REASON FOR TERMINATION	REMARKS
					INITIAL	AVERAGE			
10	AA	0.80	0.80	D	630	590	3220	Voluntary	
29	AB	0.39	0.95	D	610	605	5572	Voluntary	
33	AB	0.65	0.86	W	630	600	365	Voluntary	
35	BB	0.61	0.81	W	620	600	1535	Voluntary	
36	BB	0.62	0.81	W	630	620	60	Low Voltage	Undersintered Electr.
40	AB	0.61	0.88	W	605	585	550	Crossover	Dry Matrix
41	AB	0.58	0.89	W	595	590	1185	Voluntary	
42	AB	0.61	0.80	W	600	595	5154	Voluntary	< Submitted to MERADCOM SRF Testing (38 hours) +CH ₃ OH Testing
43	AB	0.63	0.85	W	595	580	2795	Voluntary	
44	AB	0.60	0.84	W	590	575	1385	Voluntary	
46	AB	0.60	0.89	D	600	595	670	Voluntary	<Delivered to MERADCOM SRF Testing (5 hours) Temp. Cyc. (121 ON-OFF CYCLES)
47	AB	0.61	0.89	D	595	575	2020	Voluntary	
48	AB	0.58	0.87	D	610	595	5035	Voluntary	
49	AR	0.60	0.89	D	610	580	3470	Voluntary	
50	AB	0.55	0.84	D	595	575	2220	Voluntary	Horiz. Oper. for 1800 hours Temp. Cycle testing (348 on-off cyc.)
55	AB	0.90	0.90	W	590	570	3909	Voluntary	
57	AB	0.50	0.90	D	585	575	2016	Voluntary	
58	AB	0.29	0.59	D	600	580	1015	Voluntary	
59	AB	0.60	0.90	W	605	610	773	Voluntary	
60	AB	0.23	0.52	W	603	577	186	Crossover	(No acid filler tubes)

Plate AA - (A) Fuel Side, (A) Air Side
 AB - (A) Fuel Side, (B) Air Side
 BB - (R) Fuel Side, (B) Air Side

Ass'y D - Dry Assembly
 W - Wet Assembly with H₃PO₄

SRF - Simulated Reformed Fuel
 74% H₂, 25% CO₂, 1% CO

Several 10-cell stacks were continued on test beyond the initial 500-hour test period, operating on hydrogen at 350°F and 100 ASF. Performance remained stable for up to 5000 hours of testing under these conditions as seen from the lifegraph for Stack 48 shown in Figure 42.

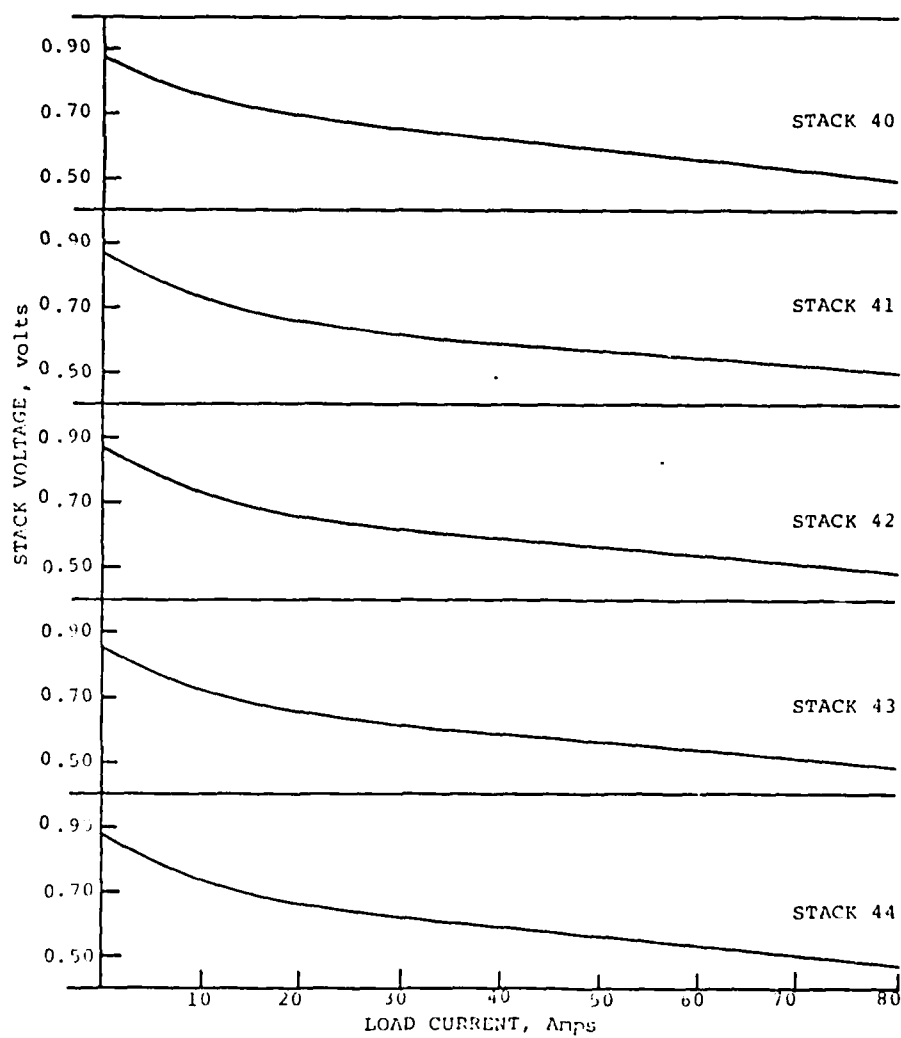
TABLE XII
CELL NO LOAD POTENTIALS
350°F

STACK	ASS'Y	CELL NO.									
		1	2	3	4	5	6	7	8	9	10
40	Dry	.84	.84	.84	.85	.85	.85	.86	.86	.86	.86
41	Dry	.88	.88	.82	.89	.87	.87	.87	.87	.98	.86
42	Dry	.88	.88	.93	.88	.86	.93	.87	.88	.88	.87
43	Dry	.89	.87	.87	.87	.87	.87	.88	.88	.89	.87
44	Dry	.85	.87	.83	.87	.85	.85	.94	.86	.85	.84
46	Wet	.35	.36	.87	.88	.87	.87	.87	.87	.87	.84
47	Wet	.90	.84	.87	.86	.90	.87	.92	.92	.90	.90
48	Wet	.86	.86	.86	.87	.87	.87	.88	.88	.88	.83
49	Wet	.85	.86	.85	.86	.84	.87	.87	.86	.87	.85
50	Wet	.35	.85	.35	.85	.85	.82	.95	.36	.86	.85

TABLE XIII
CELL LOAD POTENTIALS
330-350°F
40A

STACK	ASS'Y	CELL NO.									
		1	2	3	4	5	6	7	8	9	10
40	Wet	.53	.59	.60	.60	.59	.59	.60	.59	.59	.58
41	Wet	.59	.61	.60	.62	.61	.60	.61	.60	.60	.59
42	Wet	.58	.59	.60	.59	.60	.59	.59	.59	.58	.57
43	Wet	.60	.60	.60	.60	.60	.62	.60	.61	.60	.59
44	Wet	.57	.59	.59	.60	.60	.60	.59	.60	.57	.57
46	Dry	.59	.61	.61	.62	.61	.61	.61	.61	.62	.60
47	Dry	.58	.59	.61	.60	.61	.60	.60	.61	.60	.59
48	Dry	.59	.59	.60	.60	.60	.60	.60	.60	.61	.60
49	Dry	.60	.61	.61	.61	.59	.61	.61	.61	.61	.58
50	Dry	.58	.59	.59	.60	.59	.60	.61	.59	.59	.59

ENERGY RESEARCH CORPORATION

 H_2/AIR , 350°F

D0335

FIGURE 38
STACK POLARIZATION, DRY ASSEMBLY

ENERGY RESEARCH CORPORATION

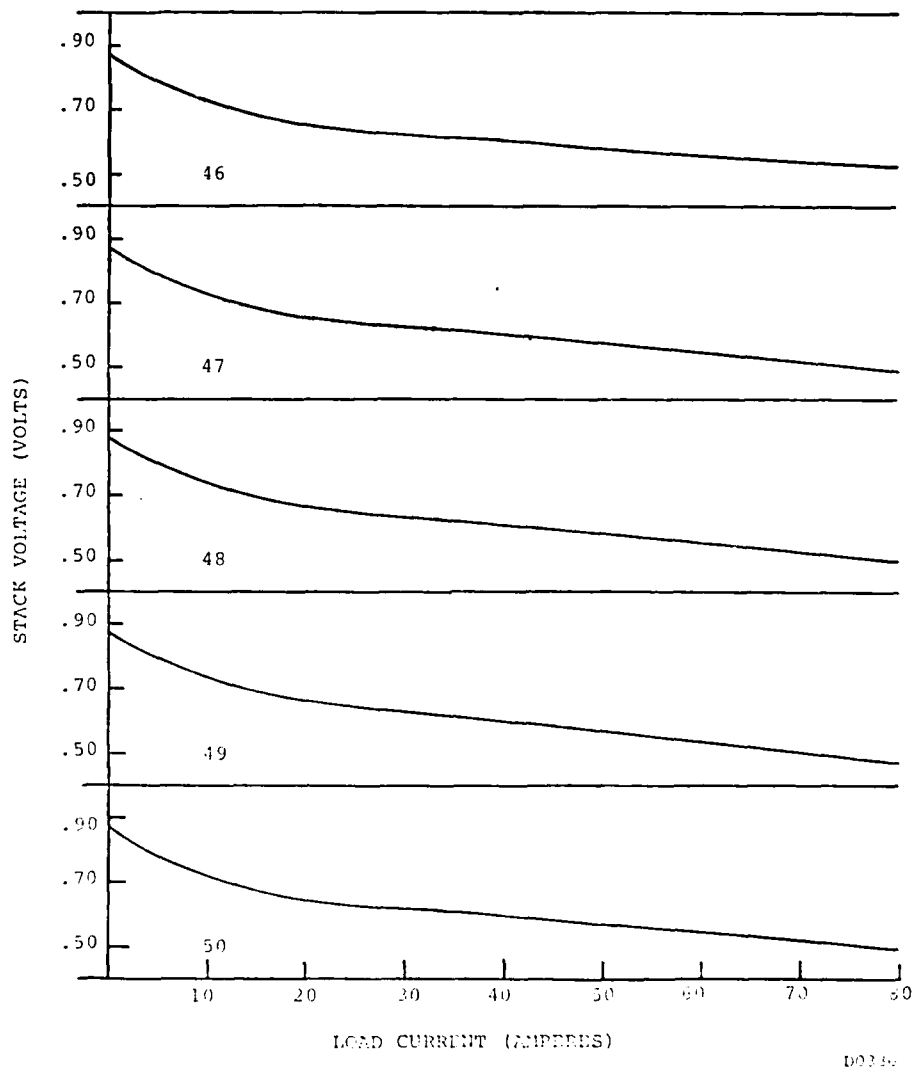
 H_2/AIR , 350°F

FIGURE 39
STACK POLARIZATION, WET ASSEMBLY

ENERGY RESEARCH CORPORATION

TABLE XIV.
STACK PERFORMANCE WITH SRF

Current: 40A (100 ASF)

Temperature: 350°F

SRF: 74% H₂, 25% CO₂, 1% CO

CELL NO.	STACK 42		STACK 46	
	H ₂	SRF	H ₂	SRF
1	0.54	0.52	0.56	0.54
2	0.60	0.58	0.58	0.57
3	0.60	0.53	0.59	0.53
4	0.60	0.53	0.59	0.53
5	0.60	0.53	0.59	0.58
6	0.59	0.57	0.60	0.59
7	0.59	0.57	0.61	0.59
8	0.59	0.57	0.60	0.59
9	0.58	0.56	0.59	0.53
10	0.54	0.52	0.59	0.58

4.4.2 Thermal Profile

The temperature profile of one ten-cell stack, No. 50, was investigated by inserting thermocouples into the air channels at 1 inch intervals. The air inlet temperature was 250°F and the H₂ inlet temperature was 75°F. The air supplied to the stack was a constant 58 liters/minute and the H₂ was a steady 3.4 liters/minute while operating at 40A.

As expected, the temperature was found to be lower near the air and fuel inlets. In all instances the hottest point in the long direction of the stack was found to be near the center. In the vertical direction the hottest point was approximately 2 inches from the air outlet. The first and last two cells also operate slightly cooler than the center cells. Temperature profiles for the first, third, sixth, eighth, and tenth cells from Stack 50 are shown in Figure 43.

ENERGY RESEARCH CORPORATION

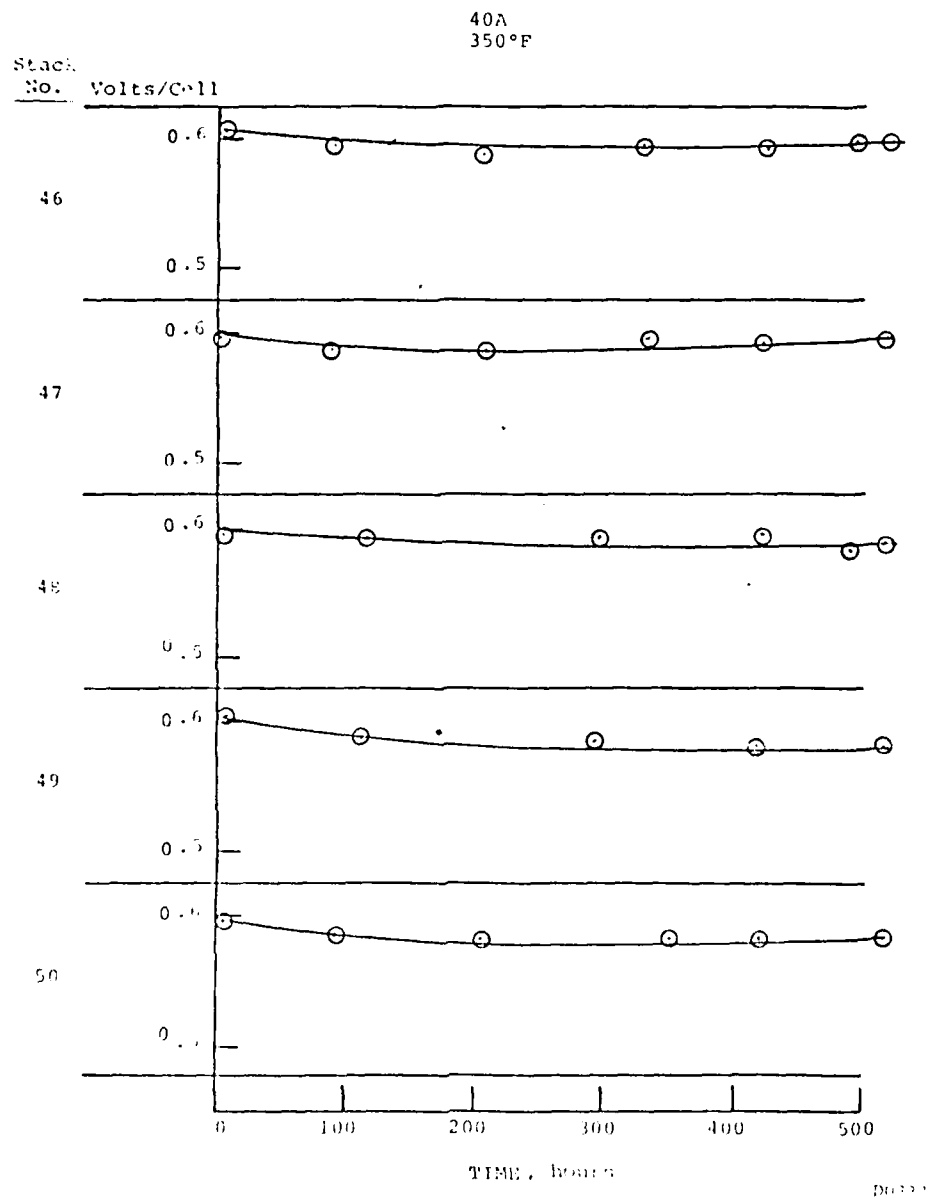


FIGURE 40
STACK PERFORMANCE STABILITY,
DRY ASSEMBLY

ENERGY RESEARCH CORPORATION

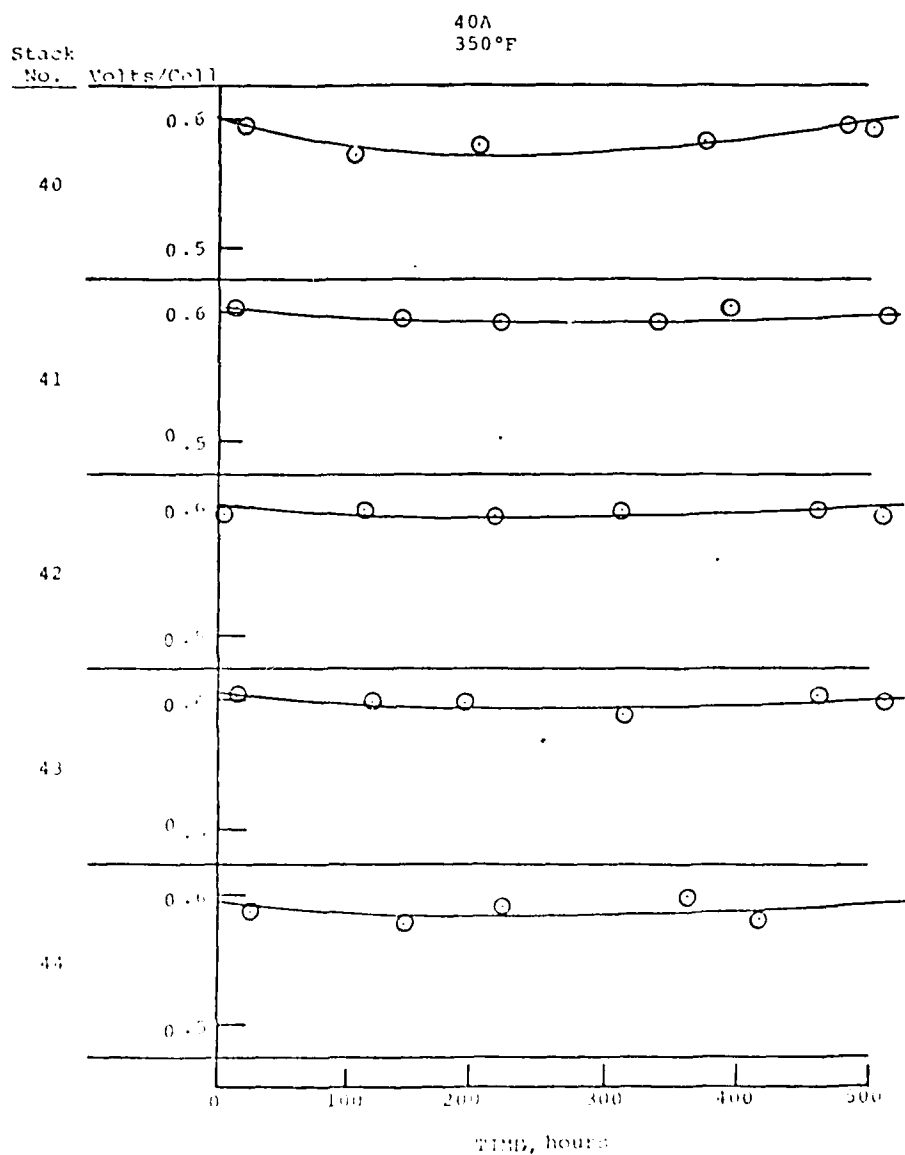
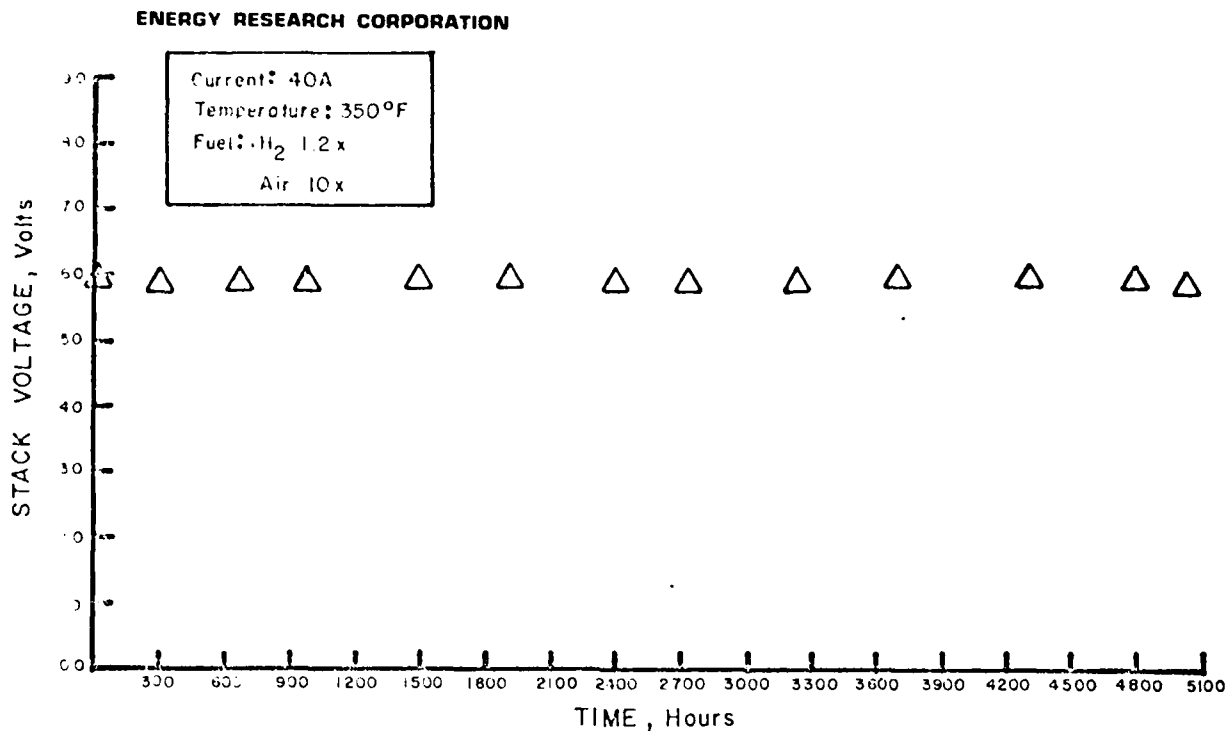


FIGURE 41
STACK PERFORMANCE STABILITY,
WET ASSEMBLY



D1292

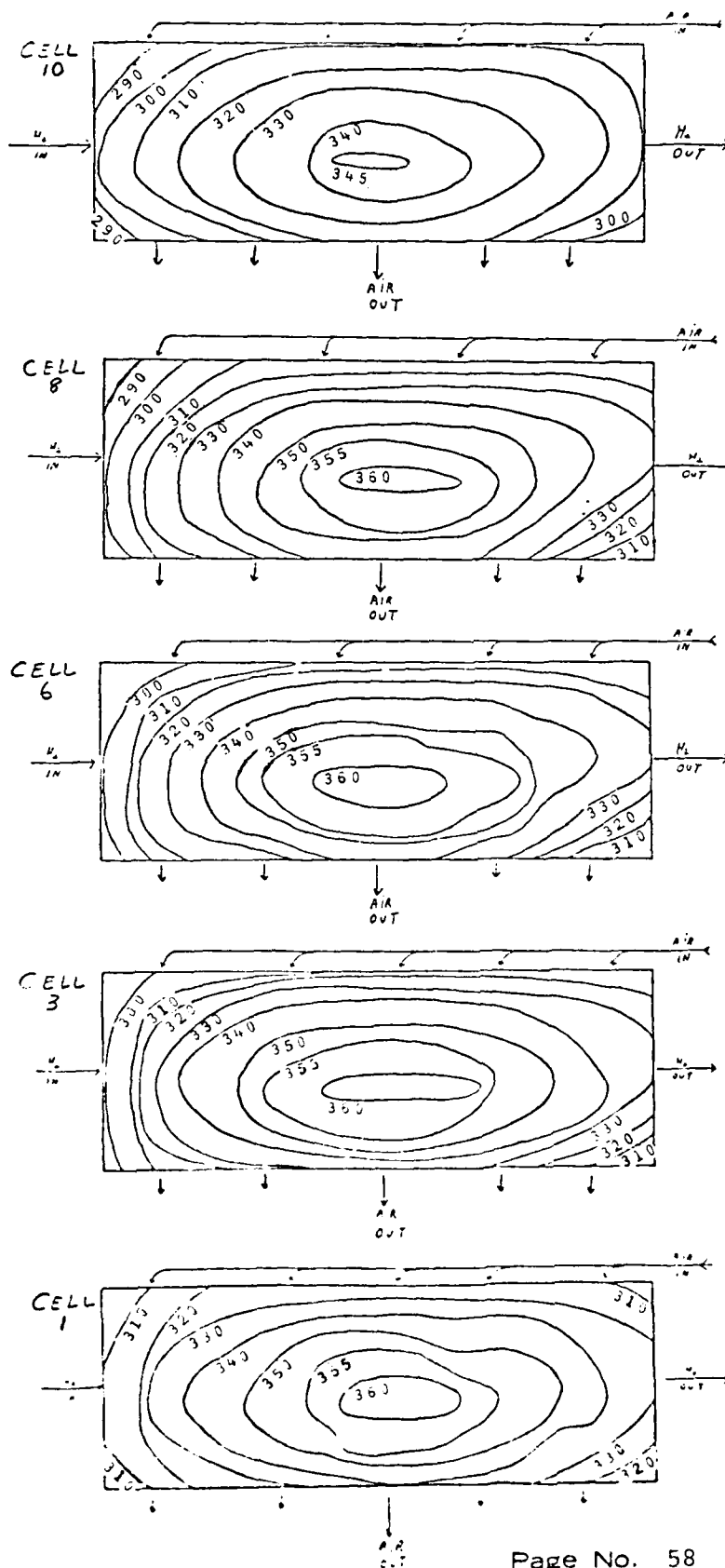
FIGURE 42. EXTENDED LIFE TESTING, STACK 48

4.4.3 Thermal Cycling

Temperature cycling was performed with two stacks. The cycle for the first stack consisted of a 2 hour shutdown and 6 hours of operation. During shutdown, the stack cooled to 140-150°F. At this point the stack and fuel heaters were activated, the fuel turned on, and the load bank connected. The warmup curve for the stack obtained with this arrangement is shown in Figure 44.

Under these test conditions, 120 temperature cycles were completed. The load voltage remained stable but there was a slight decline in the open circuit voltage over the cycling period. Some acid loss was observed in the form of drops of acid on the bottom of the stack. This acid loss was probably caused by the low start temperature of the stack and the long operating time below 250°F (10 min.). This test was terminated voluntarily at the conclusion of the first phase of the project.

ENERGY RESEARCH CORPORATION



AIR: 58.2 l/min.

H₂: 3.4 l/min.

Current: 40A

AIR TEMP: 250° F.

H₂ TEMP: 75° F

All temperatures in °F.

D1364

FIGURE 43.
TEMPERATURE PROFILE
FOR STACK 50

ENERGY RESEARCH CORPORATION

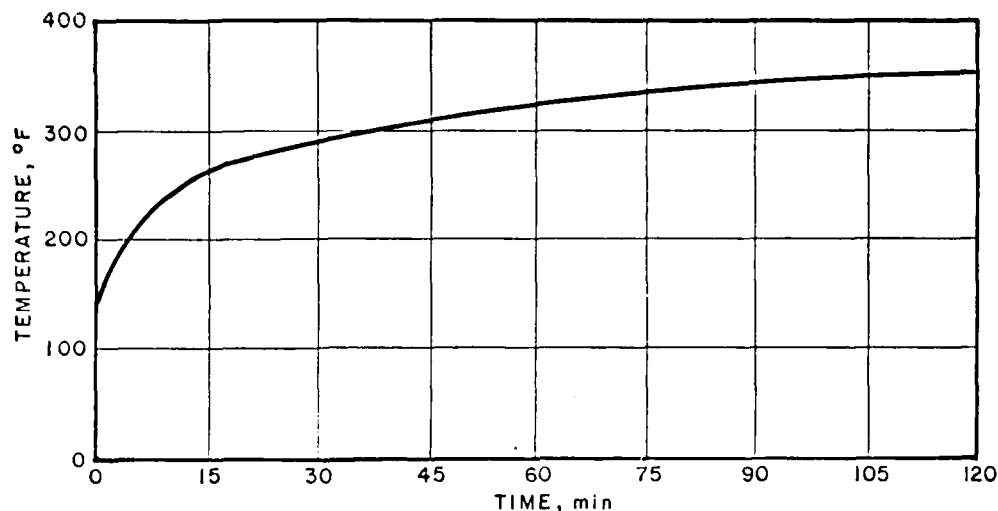


FIGURE 44
10-CELL STACK WARM-UP

D0516

A second thermal cycling experiment was conducted during the second phase of the project. As in the first cycling experiment, the stack was allowed to cool to 150°F following a shut-down; however, the bootstrap load was applied only after the stack had been reheated to 250°F with end plate heaters. The 8-hour temperature cycle obtained by this procedure is shown in Figure 45.

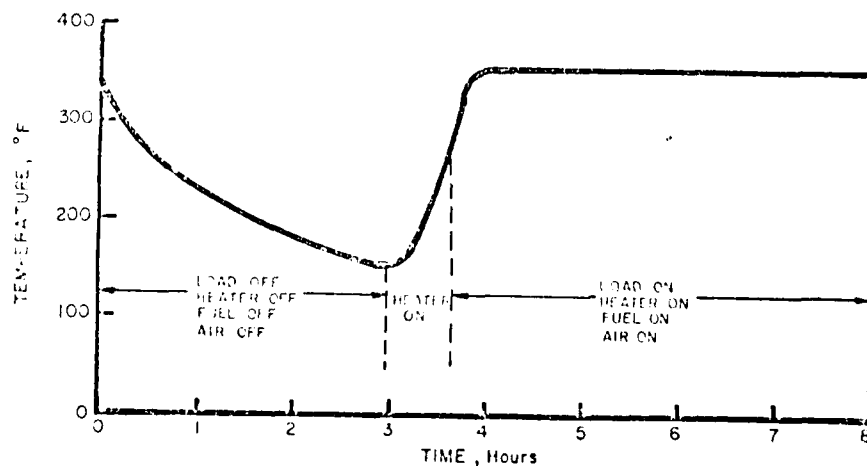
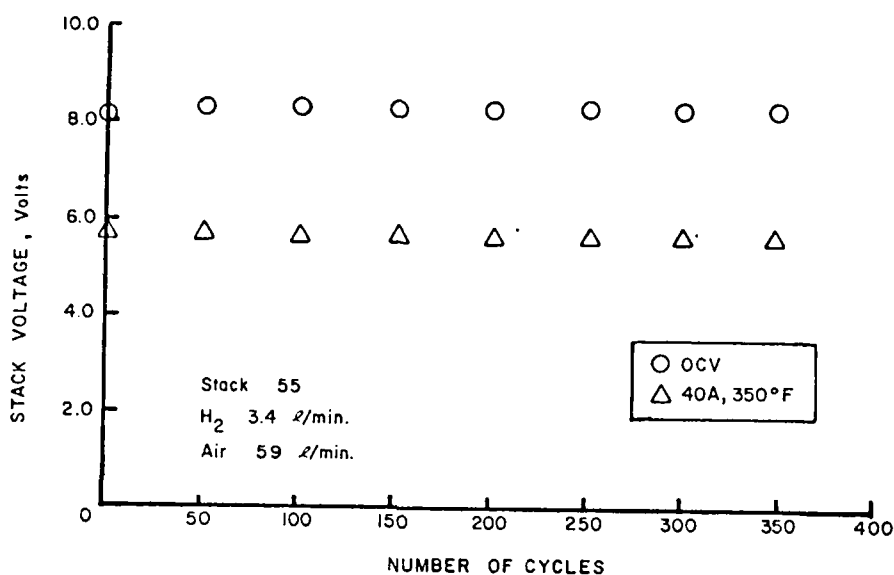


FIGURE 45 TEMPERATURE CYCLE FOR 10-CELL STACK
Page No. 59

D1292

ENERGY RESEARCH CORPORATION

This temperature cycle resulted in stable stack performance as seen from the life plot in Figure 46. There was no visible evidence of electrolyte loss, indicating that 250°F is a sufficiently high temperature for application of load to the stack during warmup.



D1294

FIGURE 46 THERMAL CYCLE TEST

4.4.4 Effect of Methanol in Fuel

Since methanol is the fuel of choice for small portable fuel cell powerplants, tolerance to methanol in the fuel entering the stack was evaluated.

Various methanol concentrations were produced in the fuel entering the stack by passing hydrogen gas thru an aqueous solution of methanol. A gas diffusion tube was used to assure adequate saturation of the gas with water and methanol vapor.

The partial pressure of methanol over the solution was calculated using Raoult's Law with methanol and water pressures taken as 124 and 23.7 mm Hg, respectively. (These vapor pressures correspond to 25°C). The methanol concentrations obtained by this method are shown in Table XV.

ENERGY RESEARCH CORPORATION

TABLE XV METHANOL CONCENTRATION

RUN NO.	SOLUTION		VAPOR	
	Wt%	Mol%	Vol%	Wt%
1	0.61	0.34	0.05	0.71
2	1.23	0.68	0.11	1.39
3	3.07	1.73	0.28	3.49
4	6.13	3.55	0.58	7.01
5	12.27	7.28	1.18	13.40
6	30.67	19.92	3.24	30.76
7	61.34	47.16	7.68	53.73

Because of the higher volatility of methanol compared to water, a reduction of methanol concentration occurs during the 50-hour test run, and the end-of-run concentration of methanol was found to be under 1% by weight for all runs as determined by specific gravity measurements. The average and total flows of methanol calculation for each run are shown in Table XVI.

TABLE XVI METHANOL FLOW

Run No.	% MeOH in Sol'n	Wt. MeOH, g	MeOH Flow, g/hour
1	0.61	5.18	0.10
2	1.23	10.43	0.21
3	3.07	26.13	0.52
4	6.13	52.13	1.04
5	12.27	104.33	2.08
6	30.67	260.73	5.21
7	61.34	521.4	10.43

Weight of starting solution: 850 grams

Run duration: 50 hrs. ± 2 hrs.

A 10-cell stack (No. 42) was used to obtain response to methanol in fuel. Cell voltage readings were recorded for the stack operating first on humidified hydrogen. The methanol-containing fuel was then switched on, voltage was allowed to stabilize for 2 hours, and readings were recorded. Results of these tests are shown in Table XVII.

ENERGY RESEARCH CORPORATION

TABLE XVII

CELL LOAD VOLTAGE WITH METHANOL IN FUEL

Stack No. 42, 40A, 350°F

50 hours \pm 2 hours

CELL No.	METHANOL IN FUEL, vol%				
	0	0.60	1.2	3.2	7.7
2	.591	.590	.590	.585	.571
3	.598	.597	.597	.593	.579
4	.600	.600	.598	.594	.582
5	.605	.605	.608	.598	.583
6	.595	.594	.593	.588	.577
7	.592	.592	.589	.584	.570
8	.600	.601	.599	.594	.581
9	.577	.578	.581	.572	.560

When the methanol concentration in the fuel exceeded 1.2%, a temperature rise was observed in the stack, possible because of diffusion of methanol thru the electrolyte and reaction with air on the cathode catalyst. This effect precluded use of a methanol concentration above 7.7%. The slight operating voltage depression caused by methanol in the fuel was found to be reversible.

4.5 EIGHTY-CELL STACKS

4.5.1 Construction

Two 80-cell stacks, nominally rated at 2.1 kW, were constructed and tested. The first stack was built at the conclusion of Phase I of the project with Kynol matrices. The second stack was built with Mat-1 matrices at the end of the second phase.

Both stacks were assembled dry and were filled with electrolyte by the conventional wicking method described earlier. Wicking time was about 10 days for Stack 51 (Kynol matrix) and 3 weeks for Stack 61 (Mat-1 matrix).

ENERGY RESEARCH CORPORATION

During the initial testing of Stack 61, a gas crossover condition was indicated in Cells 26 thru 30. The stack was opened and these cells were replaced, using the wet assembly technique. After the stack had been reassembled, it was given an additional 3 days of electrolyte wicking.

Specifications for the fuel cell components used for the two stacks and approximate component weights are listed in Tables XVIII and XIX, respectively.

TABLE XVIII
EIGHTY-CELL STACK COMPONENTS

<u>Cathode</u>	<u>Stack 51</u> <u>(Standard)</u>	<u>Stack 61</u> <u>(DIGAS)</u>
Catalyst Type	10% Pt on Carbon	
Platinum loading, g/ft ²	0.85 ± .5	0.52 ± .05
Support layer	Stackpole graphite paper	
Thickness, in.	.023 ± .002	.021 ± .002
Weight, g	17.8 ± .8	14.5 ± .5
<u>Anode</u>		
Catalyst type	10% Pt on Carbon	
Platinum loading, g/ft ²	0.60 ± .05	0.24 ± .03
Support layer	Stackpole graphite paper	
Thickness, in.	.021 ± .002	.019 ± .002
Weight, g	13.0 ± .7	9.8 ± .5
<u>Matrix</u>		
Material	Kynol	Mat-1
Thickness	0.018 ± .001	0.020 ± .002
Weight, g	7.7 ± .4	16.0 ± .5
<u>Bipolar Plate</u>		
Material	33% Colloid 8440	67% graphite
Design	"A" fuel side	"P" air side
Thickness, in.	0.165 ± 0.005	
Weight, g	192 ± 3	

ENERGY RESEARCH CORPORATION

TABLE XIX
STACK COMPONENT WEIGHTS

COMPONENT	STACK 51 (Standard)			STACK 61 (DIGAS)			
	Unit wt., g	No. used	Total wt., kg	Unit wt., g	No. used	Total wt., kg	Description
Bipolar Plates	192	81	15.55	190	66	12.54	
DIGAS Plate				310	15	4.65	
Anodes	13	80	1.04	9.8	80	0.78	(0.3g Pt/ft ²)
Cathodes	18	80	1.44	14.5	80	1.16	(0.5g Pt/ft ²)
Matrices	8	80	0.64	16.0	80	1.28	---
Ta Inserts	2	160	0.32	--	--	---	---
Cement	2.5	80	0.20	1.5/cell	80	0.12	---
Electrolyte	29	80	2.32	36/cell	80	2.88	---
Wt. of All Cell Components, kg			21.51			23.41	
Current Collectors	47	2	0.10	45	2	0.09	
Insulators	675	2	1.35	800	2	1.60	
End plates	3319	2	6.64	3000	2	6.00	
Air Manifolds	550	2	1.10	550	2	1.10	
Fuel Manifolds	403	2	0.81	400	2	0.80	
Fill Ports	72	4	0.29	70	4	0.28	
Tie Bars	773	4	3.09	770	4	3.08	
Tie Rods	252	4	1.01	250	4	1.00	
TOTAL wt., kg:			35.9 (79 lbs)			37.36 (82 lbs)	

Gas manifolds, blower, and recirculating ducts of the type employed on previous projects* for 2 kW stacks were fabricated and installed. A 2 kW nichrome wire electric heater installed in the air recirculation duct was used to provide startup heat for the stack. A schematic drawing of this arrangement is shown in Figure 47.

* Contract DAA-53-76-C-0113, Final Report, Apr. 1978.

ENERGY RESEARCH CORPORATION

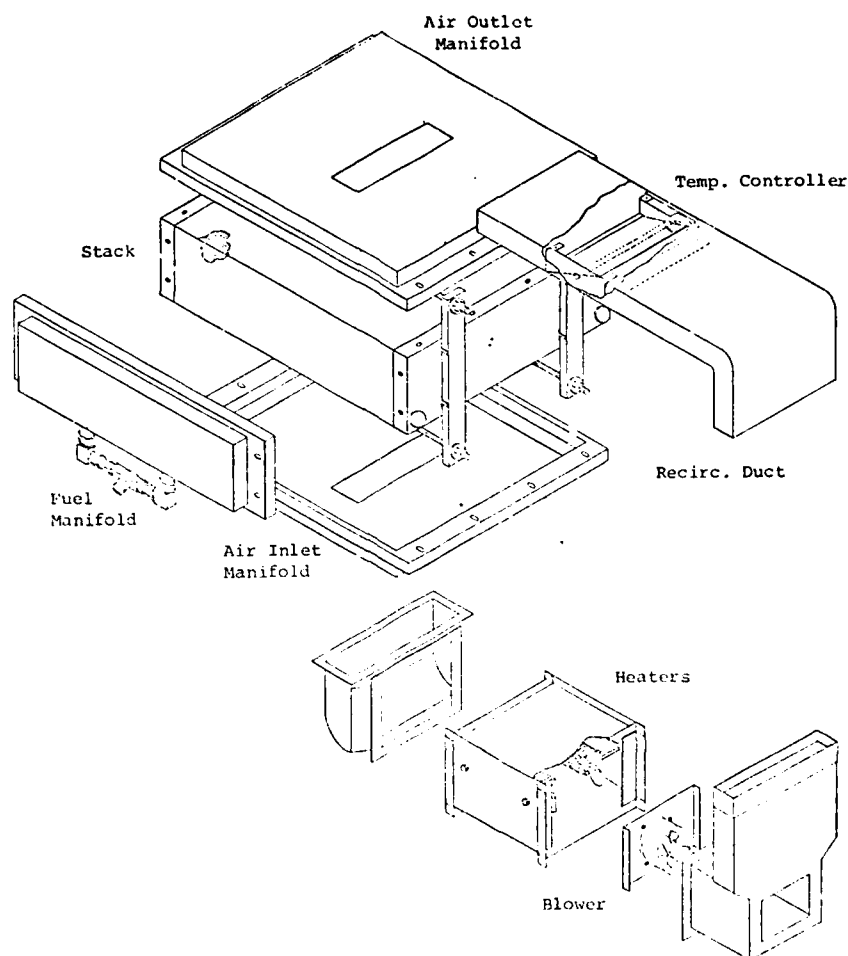


FIGURE 47 EIGHTY-CELL STACK ASSEMBLY

D1363

The 80-cell stack constructed at the end of the first phase of the project did not utilize DIGAS cooling plates. Photographs of this stack before and after installation of gas manifolds are shown in Figure 48.

The second 80-cell stack was constructed with DIGAS cooling plates spaced at 5-cell intervals. The spacing and design of the cooling plates used in this stack were based on results from an earlier ERC fuel cell development project.*

A photograph of this stack before installation of manifolds is shown in Figure 49.

* Contract EC-77-C-03-1404, Final Report, 1978.

FR-0174

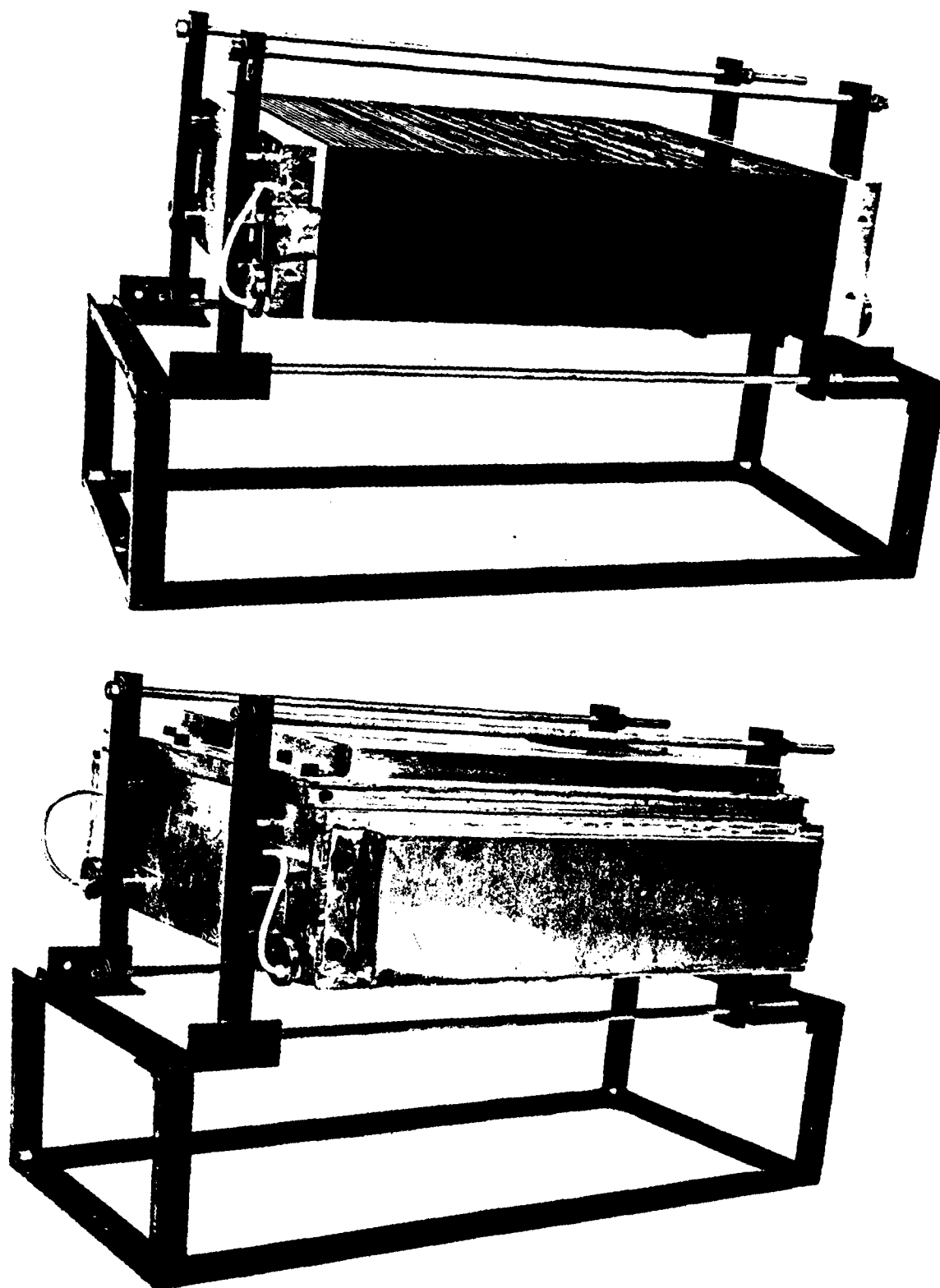
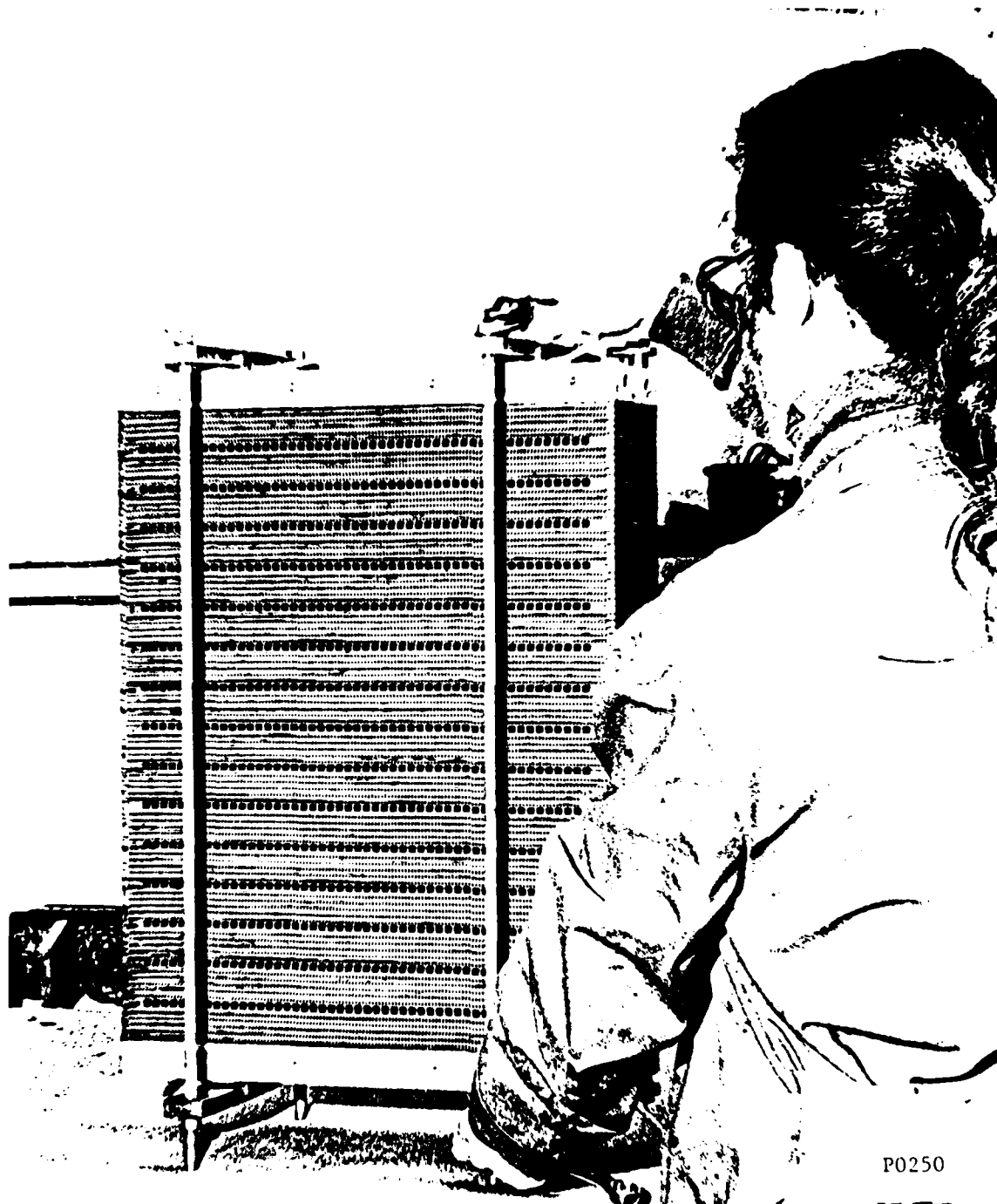


FIGURE 48
80-CELL STACK WITHOUT AND WITH GAS MANIFOLDS INSTALLED
Page No. 66

P0097

ENERGY RESEARCH CORPORATION



P0250

FIGURE 49
THE SECOND 80-CELL STACK WITH DIGAS COOLING PLATES

ENERGY RESEARCH CORPORATION

4.5.2 Performance with Hydrogen Fuel

Polarization data for the two 80-cell stacks were obtained with hydrogen diluted with CO₂ (80% H₂, 20% CO₂). Although Stack 61 (DIGAS Cooling) had only about 40% of the total catalyst loading of Stack 51 (0.76 vs 1.8g Pt/ft²), performance of the two stacks was remarkably similar as seen from the polarization curves, Figure 50. This is due, to a large extent, to the improved air circulation rate thru the DIGAS stack as evidenced by the higher inlet air temperature (280 vs 230°F). Both stacks employed the same air blower* and air side ducting.

Voltage measurements for the 10-cell groups at 40A load current are shown in Table XX. The fuel utilization employed for these tests was higher (80 to 90%) than the stack fuel utilization goals for the small powerplant design (~75%).

TABLE XX
EIGHTY-CELL STACK PERFORMANCE

Fuel: Hydrogen
Load Current: 40A
Temperature : 350°F

CELL GROUP	LOAD VOLTAGE, V	
	Stack 51	Stack 61
1 - 10	5.50	5.66
11 - 20	5.58	5.42
21 - 30	5.48	5.69
31 - 40	5.59	5.49
41 - 50	5.58	5.54
51 - 60	5.61	5.54
61 - 70	5.54	5.64
71 - 80	5.68	5.71

* Eaton Propimax AB, 70 CFM at 1.2 in. H₂O.

ENERGY RESEARCH CORPORATION

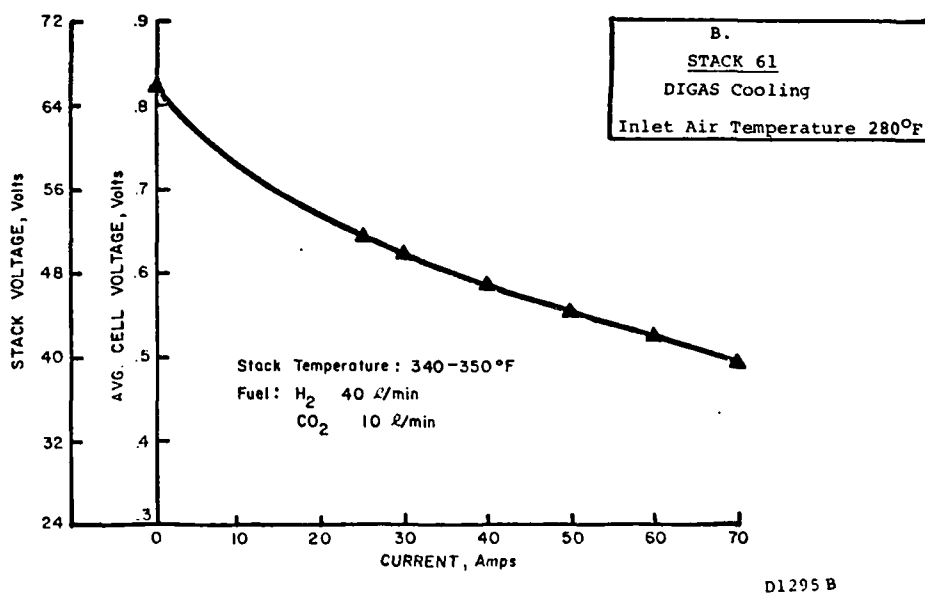
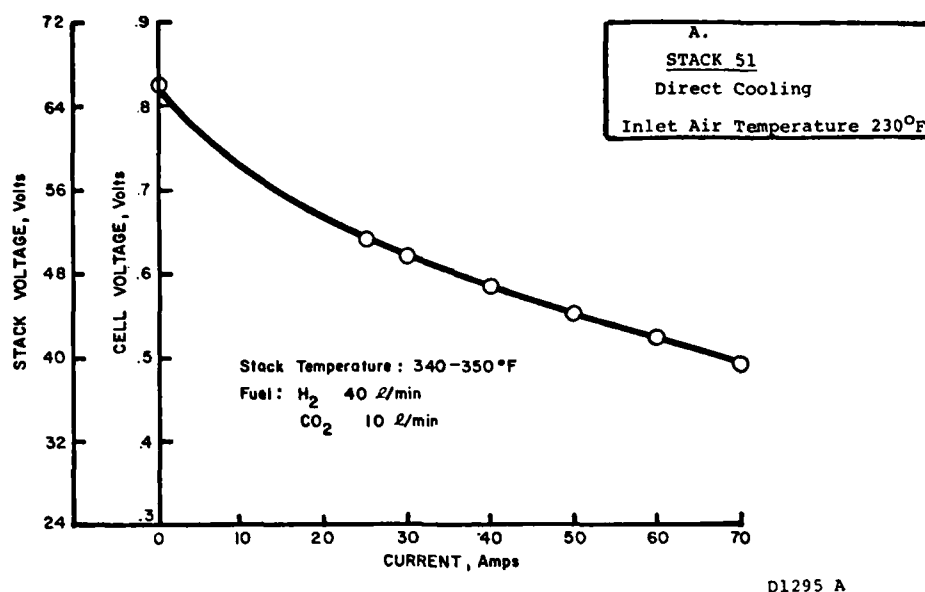


FIGURE 50. EIGHTY-CELL STACK PERFORMANCE

ENERGY RESEARCH CORPORATION

4.5.3 Testing with Methanol Reformer

A methanol reformer was constructed in July of 1979 for the purpose of evaluating stack characteristics with reformed methanol. Construction features of the annular reformer employed are shown in Figure 51, and its major design parameters are listed in Table XXI. The unit was operated at 380 to 460°F with 1.3:1 water-methanol ratio; this operating condition produced fuel having the composition shown in Table XXII. A temperature profile obtained for the reformer with 20 cc/min fuel feed rate is shown in Figure 52.

The test setup used for testing the second 80-cell stack (No. 61) with the methanol reformer is shown in Figure 53. With 75 to 80% fuel utilization, the anticipated drop in stack performance of 15 to 20 mV/cell was observed with reformed methanol compared to hydrogen fuel, as seen from the voltage-current data in Table XXIII.

TABLE XXI
REFORMER CHARACTERISTICS

Construction Material	SS-316
Blower	Rotron Aximax-3
Ignitor	Glow plug
Thermocouples	Chromel-Alumel
Catalyst type	United Catalyst T2130
Catalyst weight	6.2 lbs
Heat transfer area	3.5 ft ²
Height of bed	14 in.
Bed thickness	0.5 in.
Outside diameter	6.25 in.
Inside diameter	5.25 in.
Total weight	25 lbs (approx.)
Design space velocity	2000 hr ⁻¹ (total product)
Fuel input	5.9 lbs/hr
Heat required	2740 BTU/hr
Heat flux	772 BTU/hr/ft ²
Overall heat transfer coefficient	2.15 BTU/hr/°F/ft ²

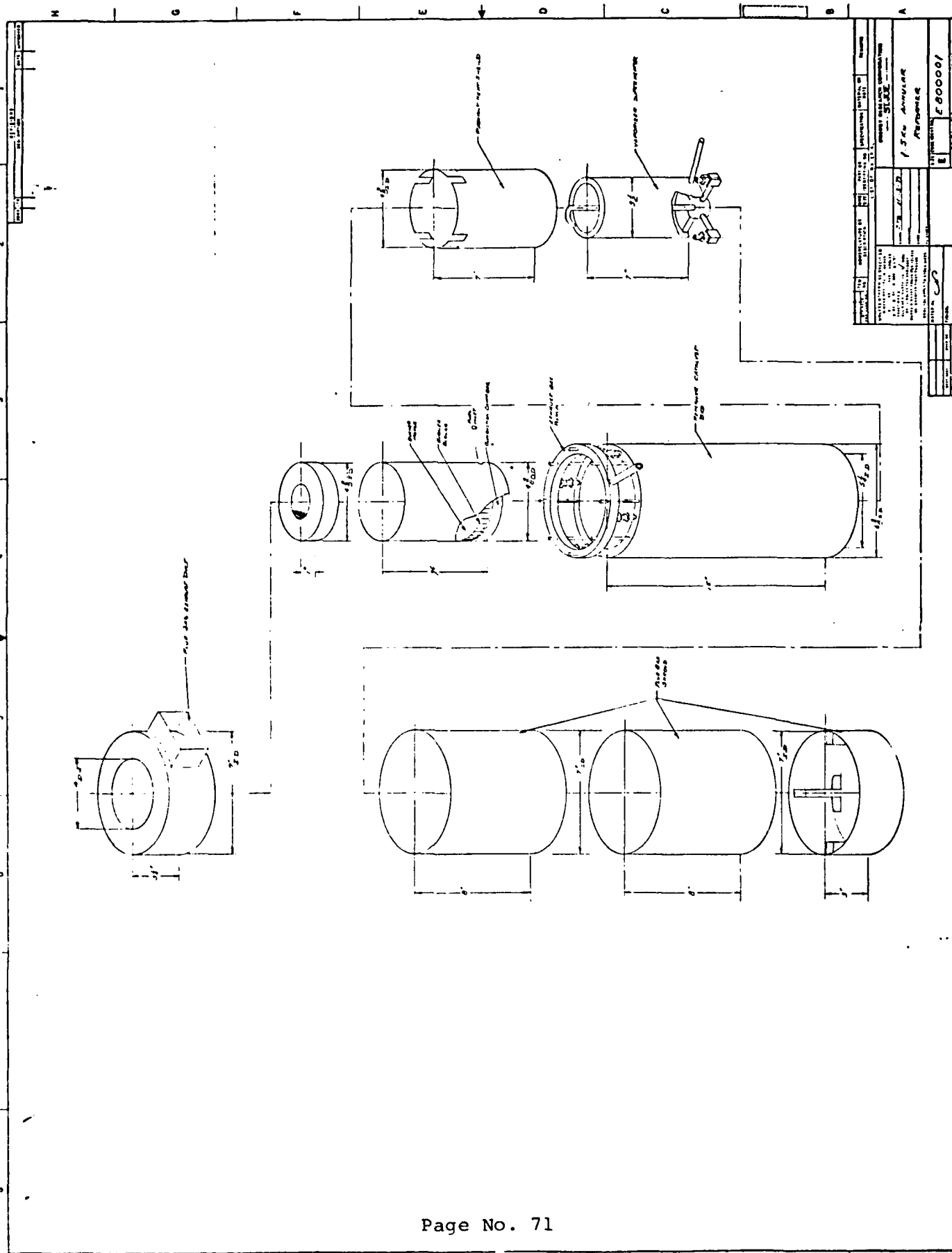


FIGURE 51
MECHANICAL DRAWING

ENERGY RESEARCH CORPORATION

TABLE XXII
REFORMER GAS COMPOSITION (DRY BASIS)

Hydrogen	:	74.7%
Carbon Dioxide	:	24.0%
Carbon Monoxide	:	1.2%
Methanol	:	0.1%
Total:		100.0%

TABLE XXIII
PERFORMANCE OF STACK 61 WITH REFORMED METHANOL

Stack Temperature: 350°F
Fuel Rate : 35 ml/min*

CELL GROUP	LOAD VOLTAGE, V	
	3.35A	3.40A
1 - 10	5.58	5.42
11 - 20	5.11	4.97
21 - 30	5.59	5.47
31 - 40	5.44	5.25
41 - 50	5.38	5.14
51 - 60	5.47	5.35
61 - 70	5.55	5.40
71 - 80	5.65	5.47

* 400 Btu/lb based on 100% CH₃OH conversion and 1.2% H₂ product.

ENERGY RESEARCH CORPORATION

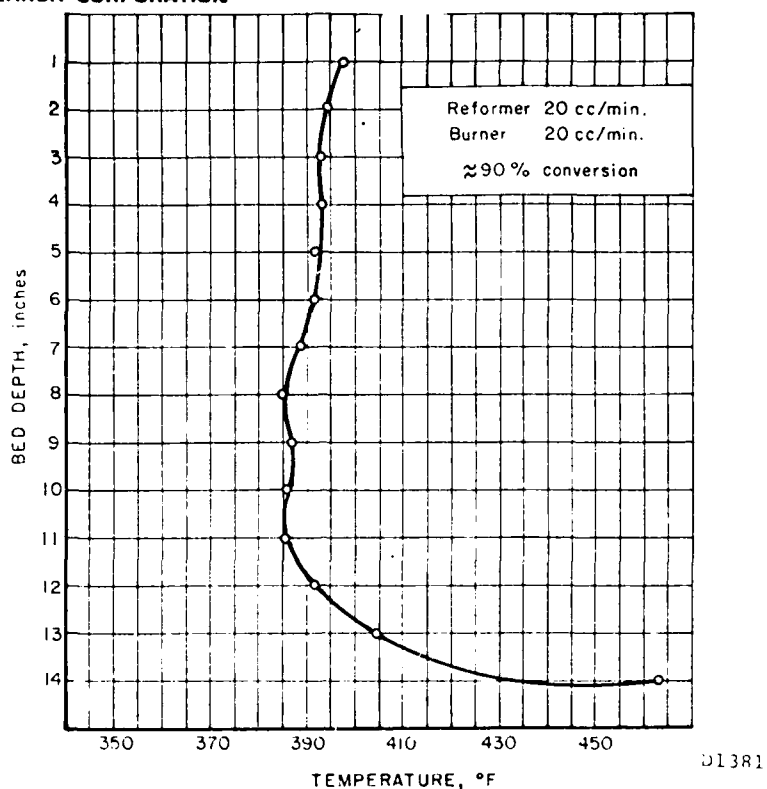


FIGURE 52. TEMPERATURE PROFILE OF 1.5kW REFORMER

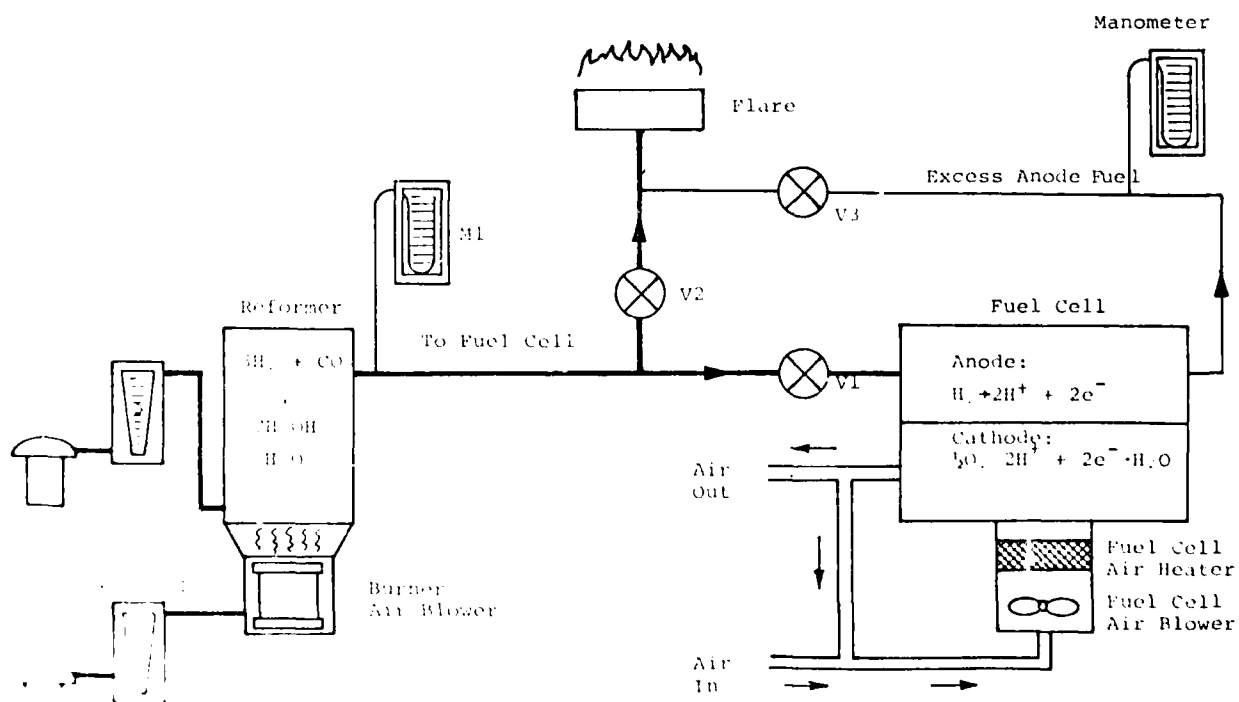


FIGURE 53. FUEL CELL TEST SETUP WITH METHANOL REFORMER

D1380

ENERGY RESEARCH CORPORATION

5.0 CONCLUSIONS

During this program, stack assembly procedures were established which resulted in reliable performance of 10- and 80-cell stacks of the two basic assembly methods, (wet and dry). The wet method appears to be more desirable since reliable performance can be achieved and stack assembly time is considerably reduced. Both 80-cell stacks built on this project were assembled by the dry method, however. Other significant accomplishments were: incorporation of an air-cooled bipolar plate (DIGAS plate) and an improved ERC matrix (Mat-1) into the stack assembly. The latter appears to be the matrix of choice because of its excellent acid retention properties.

This project also resulted in the successful construction and testing of stacks with relatively low platinum catalyst loadings. The loading was reduced from 4g/ft^2 in earlier stacks using platinum black catalyst to as low as 0.75g/ft^2 in the current stacks using supported platinum catalyst. The capability for operating low loaded stacks on methanol reformer product gas was also demonstrated.

AUG 15 1979

DISTRIBUTION LIST

Commander (12)
Defense Documentation Center
Cameron Station, Bldg. 5
ATTN: TISIA
Alexandria, VA 22314

Chief (1)
Research Development & Acquisition
Office, Deputy Chief of Staff
Department of the Army
Washington, DC 20310

Office of the Under Deputy Secretary (1)
of Defense (Research & Advanced Technology)
ATTN: ASST DIR, Electronics & Physical
Sciences
Washington, DC 20301

Director, Technical Information (1)
Advanced Research Projects Agency
1400 Wilson Blvd
Arlington, VA 22209

Commander (1)
US Army Materiel Development
and Readiness Command
ATTN: DRCDE-D
5001 Eisenhower Avenue
Alexandria, VA 22333

Commander (1)
US Army Tank-Automotive R&D Command
Technical Library, DRDTA-UL
Warren, MI 48090

Commander (1)
US Army Electronics R&D Command
ATTN: DELET-PB
Fort Monmouth, NJ 07703

Commander (1)
US Army Transportation Research &
Engineering Command
ATTN: Research Directorate
Fort Eustis, VA 23604

Technical Documents Center (2)
US Army Mobility Equipment R&D Command
ATTN: DRDME-WC
Fort Belvoir, VA 22060

Chief (1)
Naval Ships Engineering Center
Department of the Navy
ATTN: Code 6157D, Mr. Albert Himy
Washington, DC 20362

Director, Power Branch (1)
Office of Naval Research
ATTN: 473
800 Quincy Street
Arlington, VA 22217

Department of the Navy (1)
Office of Naval Research
Ballston Tower #1
800 N. Quincy Street Code: 472, Rm 624
Arlington, VA 22217

Commander (1)
Naval Ordnance Test Station
ATTN: Technical Library
China Lake, CA 93555

Commander (1)
Naval Electronics Laboratory Center
ATTN: Research Library
San Diego, CA 92152

Director (1)
US Naval Research Laboratory
ATTN: Code 2027
Washington, DC 20390

Commander (1)
Aerospace Power Division
ATTN: AFAPL/PO (Mr. J.D. Reams)
Wright-Patterson Air Force Base
Dayton, OH 45443

DISTRIBUTION LIST

Commander (1)
Department of the Air Force (AFSC)
Rome Air Development Center
ATTN: TUGG (Mr. F.J. Mollura, 3068)
Griffiss AFB, NY 13441

Power Information Center (1)
Franklin Research Center
20th and Race Streets
Philadelphia, PA 19130

Director (1)
George Marshall Space Flight Center
ATTN: Mr. J.L. Miller (M-ASTR-E)
Huntsville, AL 38809

Director (1)
Lewis Research Center
National Aeronautics & Space Administration
ATTN: Mr. H.J. Schwartz (M.S. 309-1)
21000 Brookpark Road
Cleveland, OH 44135

Dr. Paul Nelson, Director (1)
Argonne National Laboratory
Bldg 205
9700 South Cass Avenue
Argonne, IL 60439

Mr. Norman Rosenberg (1)
US Department of Transportation
Transportation Systems Center
55 Broadway
Cambridge, MA 02142

US Department of Energy (1)
ATTN: Mr. Gary Voelker
Division of Fossil Fuel Utilization
Mail Station E-178, Germantown
Washington, DC 20545

Mr. Paul Milner (1)
Room 1D-259
Bell Telephone Laboratories
Murray Hill, NJ 07974

Electrochimica Corporation (1)
2485 Charleston Road
ATTN: Technical Library
Mountain View, CA 94040

Engelhard Industries Division (1)
Engelhard Minerals & Chemicals Corp.
ATTN: V.A. Forlenza
Menlo Park, Edison, NJ 08817

Mr. George Ciprios (1)
Exxon Research & Engineering
PO Box 8
Linden, NJ 07036

General Electric Company (1)
50 Fordham Road
ATTN: L.J. Nuttall
Bldg 1A
Wilmington, MA 01887

P.L. Howard Associates, Inc (1)
Millington, MD 21561

Power Systems Division (1)
United Technologies Corporation
ATTN: Al Meyer
PO Box 109
Governor's Highway
South Windsor, CT 06074

Occidental Research Corporation (1)
ATTN: Herbert P. Silverman
PO Box 310, Department 2-K
LaVerne, CA 91750

Union Carbide Corporation (1)
Parma Research Center
PO Box 6166
ATTN: Dr. R. Brodd
Parma, OH 44101

Energy Research Corporation (1)
ATTN: Dr. B.S. Baker
3 Great Pasture Road
Danbury, CT 06810

Dr. S.B. Brummer (1)
Director of Physical Research
EIC, Inc.
55 Chapel Street
Newton, MA 02158

DISTRIBUTION LIST

Electric Power Research Institute (1)
ATTN: A.P. Fickett
PO Box 10412
Palo Alto, CA 94304

Dr. Ralph Roberts (1)
Energy Resources & Environmental Systems
Engineering
The MITRE Corporation
Mail Stop W-389
Westgate Research Park
McLean, VA 22101

Universal Oil Products, Inc. (1)
Ten UOP Plaza
ATTN: Stephen N. Massie
Government Contract Administrator
Des Plains, IL 60016

Technology Center (1)
ESB Incorporated
19 W. College Avenue
ATTN: Dr. D. T. Ferrell, Jr.
Yardley, PA 19067

Dr. Paul Stonehart (1)
Stonehart Associates, Inc.
34 Five Fields Road
Madison, CT 06443

Dr. Jose Giner (1)
Giner, Inc.
14 Spring Street
Waltham, MA 02154

Massachusetts Institute of Technology (1)
ATTN: Professor H.P. Meissner
Cambridge, MA 02138

Dr. Douglas N. Bennion (1)
Energy & Kinetics Department
School of Engineering & Applied Science
5532 Boelter Hall
University of California
Los Angeles, CA 90024

University of Florida (1)
Department of Chemical Engineering
PO Box 3027
ATTN: Professor R.D. Walker
Gainesville, FL 32601

Dr. R.T. Foley (1)
Chemistry Department
The American University
Washington, DC 20016

State University of New York (1)
at Buffalo
ATTN: Professor Stanley Bruckenstein
Chemistry Department
Acheson Hall, SUNY/AB
Buffalo, NY 14214

Hugh J. Barger, Jr. (1)
Box 2232
Davidson, NC 28036

Department of the Air Force (1)
Sacramento Air Logistics Center (AFLC)
ATTN: David C. Hall
2852 ABG/DEE
McClellan AFB, CA 95652

Defense Research Establishment (1)
ATTN: E. Criddle
Ottawa, Ontario, Canada, KIA024

US Army Engineer School (1)
Director of Combat Developments
ATTN: ATZA-CDM (MAJ Mundt)
Fort Belvoir, VA 22060

DOD Project Manager-Mobile Electric Power(1)
ATTN: DRCPM-MEP-TM (Glynn Burchette)
7500 Backlick Road
Springfield, VA 22150

Logistics Evaluation Agency(1)
ATTN: DALO-LEI (Jack Daveau)
New Cumberland Army Depot
New Cumberland, PA 17070

DISTRIBUTION LIST

Dr. John O. Smith (1)
Chief, Engineering Analysis Branch
Control Systems Laboratory
Research Triangle Park, NC 27711

Office Deputy Chief of Staff (1)
Research, Development and Engineering
ATTN: DAMA-CSS (Maj. Hiemann)
Washington, DC 20301

Gas Research Institute (1)
ATTN: Mr. Vincent Fiore
10 West 35th Street
Chicago, IL 60616

Jet Propulsion Laboratory (1)
California Institute of Technology
ATTN: Dr. John Houseman
Fuel Conversion Group
4800 Oak Drive
Pasadena, CA 91103

Gas Research Institute (1)
ATTN:
3424 South State St.
Chicago, IL 60616

Commander (1)
US Army Test & Evaluation Command
ATTN: DRSTE-IN (Mr. Huang)
Aberdeen Proving Ground, MD 21005

Gulton Engineered Magnetics Division (1)
ATTN: Mr. John Rance
13041 Cerise Avenue
Hawthorne, CA 90250

DELTA Electronic Control Corporation (1)
ATTN: Mr. Larry Suelzle
2801 S.E. Main St.
Irvine, CA 92714

Westinghouse R&D Center (1)
ATTN: Mr. D.Q. Hoover
1310 Beulah Road
Pittsburgh, PA 15235

Commander (2)
US Army Training & Doctrine Command
ATTN: ATCD-MC (Major Miller)
Ft. Monroe, VA 23651

Commander (1)
Harry Diamond Laboratories
DELHD-RDD (Benderly)(Batteries)
Adelphi, MD 20783

Globe-Union Inc (1)
ATTN: Corporate Research
5757 North Green Bay Ave.
Milwaukee, WI 53210

Commanding Officer (1)
David Taylor Naval Ship R&D Center
Annapolis Division
Annapolis, MD 21402

Commander ()
US Army Mobility Equipment R&D Command
ATTN: DRDME-EC
Fort Belvoir, VA 22060

Office of Naval Research (1)
Department of Navy
ATTN: Code 425
800 North Quincy Street
Arlington, VA 22217

Commander (1)
US Air Force Security Service
ATTN: DCS/Communications-Electronics
(ESO)
San Antonio, TX 78241

Commander (1)
Marine Corps Development & Education
Center
ATTN: M&L Division (M. Horstkamp)
Quantico, VA 22134

Commanding Officer (1)
US Army Signal Warfare Lab
ATTN: DELSW-CC, Mr. Crabbe
Arlington Hall Station, VA 22212

FILMED
- 8